Intervertebral Articulation and the Evolution of Large Body size in Archosauria

Candice M. Stefanic

Department of Geosciences

Thesis submitted to the faculty of the Virginia Polytechnic Institute and State University in partial fulfillment of the requirements for the degree of

Master of Science
In
Geosciences

Sterling J. Nesbitt, Chair
Michelle R. Stocker
John J. Socha

April 25, 2017
Blacksburg, VA

Keywords: hyposphene-hypantrum, vertebrae, body size, evolutionary biology

Intervertebral Articulation and the Evolution of Large Body Size in Archosauria

Candice M. Stefanic

ABSTRACT

Dinosaurs are the largest animals to ever walk on the continents and some reached body sizes of up to 70 tons. Observation of their closest living relatives, birds and crocodylians, could never allow for prediction of gigantic dinosaurian forms. Therefore, the fossil record is crucial to understanding the evolutionary changes of these animals through time, including body size trends. The reptile group Archosauria encompasses living and extinct birds and crocodylians as well as non-avian dinosaurs and crocodile relatives called pseudosuchians. My research focuses on studying fossils of extinct archosaurs to determine how the morphology of their skeletons allowed for growth to large body sizes. I am specifically interested in how the vertebral column fits together and how the structures that articulate vertebrae change throughout the phylogeny (i.e. family tree) of Archosauria.

Although major body size trends are well known for archosaurs, less research has focused on skeletal features that are associated with the evolution of large body size in that group. I hypothesize that the vertebral column will have these features. To answer the question of how vertebrae morphology is related to body size, I first described eight vertebrae from a large pseudosuchian archosaur *Poposaurus langstoni*. This animal possesses an accessory articulation between the vertebrae in its trunk region (i.e. between the neck and hips) called the hyposphene-hypantrum articulation. I then surveyed vertebrae from across Archosauria and found a close fit of presence of the articulation with large sizes and that it evolves independently in several archosaur groups.

Intervertebral Articulation and the Evolution of Large Body Size in Archosauria

Candice M. Stefanic

GENERAL AUDIENCE ABSTRACT

Dinosaurs are the largest animals to ever live on land and some weighed up to 70 tons. Today, the living relatives of dinosaurs are birds and crocodylians, and observation of these animals could never allow for prediction of gigantic dinosaurian forms. Therefore, paleontologists must study the fossil record to understand the evolutionary changes of these animals through time, including body size trends. Fossils can provide information about the evolution of dinosaurs to enormous sizes and their subsequent shrinking to the small sizes we see today in their living relatives. The reptile group Archosauria encompasses living and extinct birds and crocodylians as well as non-avian dinosaurs and crocodile relatives called pseudosuchians. My research focuses on studying fossils of extinct members of Archosauria, or archosaurs, to determine how changes in their skeletons over millions of years allowed for many species to grow to extremely large body sizes. I am specifically interested in how their vertebrae fit together and how the structures that link together their backbone change throughout the family tree of Archosauria.

For my family:

Thank you for teaching me to love science and exploration for as long as I can remember.

TABLE OF CONTENTS

LIST OF FIGURES

Chapter 1

Chapter 2

LIST OF TABLES

Chapter 1

Chapter 2

ATTRIBUTION

Chapters 1 and 2 was conceived of and designed by CMS and SJN, with input from SJN. All data collection and analysis was conducted by CMS with advisement from SJN. All figures were made by CMS and all chapters were written by CMS, with advisement from SJN.

Chapter 1

THE AXIAL SKELETON OF *POPOSAURUS LANGSTONI* (PSEUDOSUCHIA: POPOSAUROIDEA) AND ITS IMPLICATIONS FOR ACCESSORY INTERVERTEBRAL ARTICULATION EVOLUTION IN PSEUDOSUCHIAN ARCHOSAURS

Candice M. Stefanic, Department of Geosciences, Virginia Polytechnic and State University, cms292@vt.edu

1. Abstract

Dinosaurs and their close relatives grew to sizes larger than any other terrestrial animal in the history of life on Earth, and many enormous dinosaurs (e.g. *Diplodocus*, *Spinosaurus*, *Tyrannosaurus*) have accessory intervertebral articulations that have been suggested to support these large body sizes. Some pseudosuchian archosaurs have been reported to have these articulations as well, but few have been characterized in these taxa because of a lower abundance of complete, three-dimensional pseudosuchian vertebral material in relation to dinosaurs. I describe the axial column of the large (~4-5 meters) poposauroid pseudosuchian *Poposaurus langstoni* from the Upper Triassic of Texas (TMM Locality 31025 of the Otis Chalk localities, Dockum Group). *Poposaurus langstoni* was originally named from pelvic girdle elements and vertebrae; here we describe newly discovered and prepared presacral vertebrae and a presacral rib from the original excavation of the holotype in the 1940s. The well-preserved vertebrae have well-defined vertebral laminae and clear hyposphene-hypantrum intervertebral articulations, character states mentioned in pseudosuchians but rarely described. The new material demonstrates variation present in the hyposphene-hypantrum articulation through the vertebral column. I compared these morphologies to other pseudosuchians with and without the hyposphene-hypantrum articulation. Based on these careful comparisons, I provide an explicit definition for the hyposphene-hypantrum articulation applicable across Archosauria. Within Pseudosuchia, I find the hyposphene-hypantrum evolves independently in the clade more than once, but I also see the loss of these structures in clades that had them plesiomorphically. I find a relationship between large body sizes and the presence of the hyposphene-hypantrum in some pseudosuchian archosaurs because the articulation is absent in taxa with femoral lengths less than ~300 mm.

2. Introduction

The clade Archosauria, which includes extant birds and crocodylians, contains some of the largest land animals ever to exist (i.e. sauropod and theropod dinosaurs, Mazetta et al., 2004; phytosaurs, Stocker and Butler, 2013; rauisuchians, Nesbitt et al., 2013), and to understand the consequence of body size on skeletal morphologies seen only in extinct taxa, we must turn to the fossil record. The appearance of large body sizes in Archosauria during the Mesozoic Era was accompanied by large variation in vertebral morphologies (Gauthier, 1986; Apesteguia, 2005; Wilson et al., 2016). One example of a morphology present in dinosaurs that has been cited as associated with increased body size is an accessory intervertebral articulation known as the hyposphene-hypantrum articulation (Gauthier, 1986; Rauhut, 2003; Apesteguia, 2005). In addition to the centrum faces and zygapophyses, this hyposphene-hypantrum articulation forms a 'lock-and-key' configuration between consecutive vertebrae. More specifically, the hyposphene-hypantrum articulation consists of a ventrally expanded lamina of bone that is present at the junction of the postzygapophyses (= the hyposphene) that fits into a complementary space (= the hypantrum) that separates the prezygapophyses at the midline (Rauhut, 2003; Apesteguia, 2005). In sauropod dinosaurs, the presence of these structures has been hypothesized to be related to increased vertebral column rigidity, thereby decreasing flexibility of locomotion (Apesteguia, 2005).

Among dinosaurs, the hyposphene-hypantrum articulation is present in many clades with exceptionally large-bodied members such as derived sauropodomorphs and theropods (Wilson, 1999; Makovicky and Norell, 2004; Brusatte and Benson, 2008; Benson, 2010; Bandyopadhyay et al., 2010; Pol et al., 2011), and it has been cited as a saurischian synapomorphy (Gauthier,

1986) because the articulation is not present in ornithischian dinosaurs. The hyposphene-hypantrum is also found to vary in shape and size relative to the rest of the neural arch in sauropods (Apesteguia, 2005). The hyposphene-hypantrum articulation, however, is not restricted to saurischian dinosaurs, and descriptions of this vertebral feature have been reported in the close relatives of dinosaurs (*Nyasasaurus parringtoni*, Nesbitt et al., 2013; *Asilisaurus kongwe*, Nesbitt et al., 2010) and in extinct archosaurs more closely related to crocodylians than to birds (Bonaparte, 1981; Azevedo, 1991; Weinbaum, 2013; Weinbaum and Hungerbühler, 2007; Parker, 2008; Nesbitt, 2005; Peyer et al. 2008; Gower and Schoch, 2009; Lautenschlager and Desojo, 2011; Nesbitt et al., 2014). Although the hyposphene-hypantrum articulation is present in some paracrocodylomorphs (e.g., *Poposaurus gracilis*, Weinbaum and Hungerbühler, 2007; *Arizonasaurus babbitti*, Nesbitt, 2005; *Postosuchus kirkpatricki*, *Postosuchus alisonae*, Peyer et al., 2008; *Prestosuchus chiniquensis*, Azevedo, 1991; *Fasolasuchus tenax*, Bonaparte 1981; *Batrachotomus kupferzellensis*, Gower and Schoch, 2009), and in some aetosaurs (*Desmatosuchus spurensis*, Parker, 2008; *Scutarx deltatylus*, Parker, 2016b; *Longosuchus meadei*, TMM 31100-448, TMM 31100-452), it is not present in extant crocodylians (Romer, 1956). Previous work has not provided a comprehensive description of the hyposphene-hypantrum articulation across taxa or explore the possible homologies across archosaurs. Furthermore, the application of the term 'hyposphene-hypantrum' to presacral vertebral morphology is inconsistent because the variation of these structures, if any, is rarely reported.

To explore the morphology of the hyposphene-hypantrum articulation in pseudosuchians, I describe the axial column of the large pseudosuchian *Poposaurus langstoni* from the Late Triassic of Texas. The holotype specimen of this species was collected in the early 1940s near Otis Chalk, Texas, (TMM Locality 31025) from the Dockum Group (Long and Murry, 1995).

The holotype was erected solely based on the right ilium (TMM 31025-12), but additional material comprising four presacral vertebrae (eighth cervical, pathologically fused ninth cervical and first trunk, and third trunk) and a right ischium was also referred to the same species by Long and Murry (1995). Additional presacral vertebrae and most of a rib were collected from the same quarry as the holotype and previously referred material during the original excavation in the early 1940s; we attribute this material to *Poposaurus langstoni* and describe it herein for the first time because it has only been prepared recently. I also describe two vertebrae (TMM 31025-177, TMM 31025-257) in detail for the first time that were previously figured by Long and Murry (1995), but not described in detail with the previously published material. The material of *P. langstoni* I describe here is of interest because it includes a variety of presacral vertebrae (4 cervical, 4 trunk) from throughout the column, and it is preserved in three dimensions so that articulation surfaces are easy to discern. These characteristics are not present in most Triassic pseudosuchian fossils (e.g. *Sillosuchus longicervix*, PVSJ 85; *Ticinosuchus ferox,* PIZ T 2817) because preservation is typically poor in Triassic-aged deposits. These vertebrae possess features that traditionally have been associated with saurischian taxa, including vertebral laminae (Wilson, 1999) and the hyposphene-hypantrum articulation (Apesteguia, 2005), and help act as a benchmark for comparison with other pseudosuchians with similar structures.

Institutional Abbreviations

AMNH – American Museum of Natural History, New York, NY, USA

GPIT – Institut für Geowissenschaften, Universität Tubingen, Germany

GR – Ruth Hall Museum of Paleontology, Ghost Ranch, NM, USA

IVPP – Institute of Vertebrate Paleontology and Paleoanthropology, Beijing, China

MNA – Museum of Northern Arizona, Flagstaff, AZ, USA

MSM – Arizona Museum of Natural History (formerly Mesa Southwest Museum), Mesa, AZ, USA

NMMNH – New Mexico Museum of Natural History and Science, Albuquerque, NM, USA

NMT – National Museum of Tanzania, Dar es Salaam, Tanzania

PEFO – Petrified Forest National Park, Petrified Forest, AZ, USA

PVL – Instituto Miguel Lillo, Tucumán, Argentina

PVSJ – Division of Paleontology of the Museo de Ciencias Naturales de la Universidad Nacional de San Juan, San Juan, Argentina

SAM – Iziko: South African Museum, Cape Town, South Africa

SMNS – Staatliches Museum für Naturkunde, Stuttgart, Germany

TMM – Jackson School of Geosciences Vertebrate Paleontology Laboratory, University of Texas at Austin, Austin, TX, USA

TTU P – Texas Tech University Museum, Lubbock, TX, USA

UCMP – University of California Museum of Paleontology, Berkeley, CA, USA

UFRGS-PV – Instituto de Geociencias, Universidade Federal do Rio Grande do Sul, Porto Allegre, Brazil

UNC – University of North Carolina, Chapel Hill, NC, USA

USNM – National Museum of Natural History, Washington, DC, USA

SYSTEMATIC PALEONTOLOGY

ARCHOSAURIA Cope, 1869 sensu Gauthier, 1986

PSEUDOSUCHIA Zittel, 1887-1890 sensu Gauthier and Padian, 1985

POPOSAUROIDEA Nopcsa, 1923 sensu Nesbitt, 2011

POPOSAURUS LANGSTONI Long and Murry, 1995 sensu Weinbaum and Hungerbühler, 2007

Horizon and Locality: Quarry 1 of the Otis Chalk localities (TMM Locality 31025) Dockum Group, Howard County, Texas, USA. Biostratigraphic and lithostratigraphic correlations indicate the Otis Chalk localities are Upper Triassic (latest Carnian-early Norian) (Stocker et al. 2016)

Holotype: TMM 31025-12, right ilium

Previously Referred Specimens:

TMM 31025-257, right ischium

TMM 31025-259, fused last cervical (9th presacral) and first trunk (10th presacral) vertebrae

TMM 31025-177, presacral vertebra (posterior cervical)

TMM 31025-257, presacral vertebra (anterior trunk)

Newly Referred Specimens:

TMM 31025-1261.5, presacral vertebra (mid-cervical)

TMM 31025-1262, presacral vertebra (mid-cervical)

TMM 31025-1261.3, presacral vertebra (mid- to posterior cervical)

TMM 31025-1261.4, presacral vertebra (anterior to mid-trunk)

TMM 31025-1261.1, presacral vertebra (anterior to mid-trunk)

TMM 31025-1261.2, presacral vertebra (mid- to posterior trunk)

TMM 31025-2160, most of a presacral rib

Justification for Newly Referred Material:

The holotype and the newly referred material were collected from the same quarry (TMM 31025 Quarry 1) during the 1940 and 1941 excavations (unpublished WPA field notes, TMM). The preservation and color of the holotype, referred, and newly referred material are identical. The relative size is also consistent between this new material and the previously referred material and holotype, but appears to represent two individuals (see below).

We assign six presacral vertebrae to *Poposaurus langstoni* based on general morphology of their centra and neural arches, well-defined vertebral laminae, and an accessory rib articulation in the posterior cervical vertebrae (figures 2,3). These newly referred vertebrae share some character states with both of the previously described vertebrae of *Poposaurus langstoni* (Long and Murry, 1995; Weinbaum and Hungerbühler, 2007). The posterior cervical vertebra of the newly referred material (TMM 31025-1261.3) possesses an accessory rib articulation adjacent to the parapophyses and lacks a ridge on the ventral surface of the centum, both features that link this material to previously referred material (TMM 31025-177). This accessory rib articulation is a synapomorphy of the clade Poposauroidea (Nesbitt, 2005; Weinbaum and Hungerbühler, 2007) because it is also present in *Poposaurus gracilis* (TTU P-10419, Weinbaum and Hungerbühler, 2007), and in another member of the clade, *Arizonasaurus babbitti* (MSM 4590, Nesbitt, 2005). These newly referred vertebrae of *Poposaurus langstoni* also possess well-defined vertebral laminae that are also on vertebrae previously assigned to *Poposaurus gracilis*

(TTU P-10419, Weinbaum and Hungerbühler, 2007), as well as on the vertebrae of many saurischian dinosaurs such as *Apatosaurus louisae* and *Allosaurus fragilis* (Wilson, 1999) and other paracrocodylomorphs such as *Arizonasaurus babbitti*, *Postosuchus sp.*, *Fasolasuchus tenax*, *Batrachotomus kupferzellensis*, and *Prestosuchus chiniquensis* (Nesbitt, 2005; Weinbaum, 2013; Bonaparte, 1981; Gower and Schoch, 2009; Azevedo, 1991). The shape and morphologies of the centra and neural arches, including dorsoventrally elongate centrum facets, well-defined and pronounced laminae, and an accessory rib articulation on the cervical vertebrae, of the new material described here is also strikingly similar to that of *Poposaurus gracilis* (TTU P-10419, Weinbaum and Hungerbühler, 2007) and previously referred vertebrae of *Poposaurus langstoni* (TMM 31025-177, TMM 31025-257, TMM 31025-259, Long and Murry, 1995). The presence of these features in these new vertebrae allows us to assign them to the genus *Poposaurus*; however, because the diagnostic characteristics that separate *P. gracilis* and *P. langstoni* are in the ilium and ischium (Long and Murry, 1995; Weinbaum and Hungerbühler, 2007), we can only assign this material to *Poposaurus langstoni* by relying on the information that they were collected from the same quarry during the 1940 and 1941 excavations as the ilium and ischium that erected the species (unpublished WPA field notes, TMM).

We suggest that among the holotype, referred material, and newly referred material there are at least two individuals of *P. langstoni* based on a bimodal distribution of the prezygapophyseal height to centrum height, and it appears at least one of the vertebral positions is duplicated. We refer two of these vertebrae (TMM 31025-177, TMM 31025-257) to the same individual (individual 'A' [Figure 1]) as the previously referred pathologically fused vertebrae of *Poposaurus langstoni* from Quarry 1 (TMM 31025-259) because they most closely resemble that material in size. These vertebrae (TMM 31025-177, TMM 31025-257) were both figured but not

fully described by Long and Murry (1995) along with TMM 31025-259, and those authors attributed these specimens to a novel taxon, *Lythrosuchus langstoni*, because these presacral vertebrae were more compressed and taller than previously described material of *P. gracilis* and possessed an accessory rib articulation. Weinbaum and Hungerbühler (2007) later assigned these vertebrae to the same genus, *Poposaurus*, because a specimen of *P. gracilis* (TTU P-10419) also possessed the accessory rib articulation in a posterior cervical vertebra. The presacral specimens TMM 31025-1261.5, TMM 31025-1262, TMM 31025-1261.3, TMM 31025-1261.4, TMM 31025-1261.1, and TMM 31025-1261.2 we refer to as belonging to individual 'B' (figure 1) because they are slightly larger than those vertebrae we have assigned to individual 'A'.

Poposaurus langstoni is only known from a single locality and other archosauromorphs are known from the locality. The stem archosaur *Trilophosaurus buettneri* and a phytosaur are also known from TMM 31025, Quarry 1. The vertebral morphologies of the three taxa known from the locality are disparate and can easily be distinguished from one another. For example, the centra of *T. buettneri* are much longer anteroposteriorly than they are dorsoventrally tall, whereas the centra of *Poposaurus langstoni* are dorsoventrally taller than they are anteroposteriorly long. The vertebrae of *T. buettneri* (e.g., TMM 31025-140) are also much smaller in overall size than the known material of *P. langstoni* (Long and Murry, 1995), which is sufficient evidence to claim that all material from TMM 31025, Quarry 1 that is much larger than the known *T. buettneri* material is likely *P. langstoni*.

3. Description

a. Vertebrae (General): The axial column of *P. langstoni* consists of eight presacral vertebrae, and all are well preserved and nearly complete although most are missing parts of the

diapophyses, parapophyses, zygapophyses, and some are crushed slightly (figures 2, 3). Each vertebra can be assigned to a presacral position within a range of two or three positions, depending on its general location in the vertebral column and based on comparisons with other archosaurs with more complete vertebral columns. For this specimen of *Poposaurus langstoni*, the positions of all the vertebrae were assigned general positions in the vertebral column mainly based on the position of the diapophyses, as they appear higher on the neural arch further posteriorly in the series as with *Poposaurus gracilis* (TTU-P 10419), *Parringtonia gracilis* (NMT RB426**),** and a number of specimens of *Alligator mississippiensis* (e.g., TMM M-12606).

In *Poposaurus langstoni*, cervical vertebrae were identified by the presence of the parapophyses on the anterior rim of the centrum located anywhere from the base of the centrum to the base of the neural arch just ventral to the location of the neurocentral suture, whereas the parapophyses of trunk vertebrae are only present on the neural arch. The parapophyses migrate dorsally from the base of the centrum posteriorly along the tetrapod vertebral column (such as in *Parringtonia gracilis* and *Alligator mississippiensis*). Because the diapophyses are located on the neural arch in vertebrae posterior to presacral 7 in other paracrocodylomophs (e.g. *Poposaurus gracilis*, *Parringtonia gracilis*, *Alligator mississippiensis*) we can constrain the position of the anteriormost vertebra of *Poposaurus langstoni* (TMM 31025-1261.5) at presacral ~7 or 8. This vertebra also has a very slight ventral keel, which further constrains its position to presacral ~7 or 8 because this is characteristic of the most anteriorly located cervical vertebrae in other paracrocodylomorphs (e.g. *Parringtonia gracilis*).

Using these criteria for assignment of position within the axial column, the known vertebrae of *Poposaurus langstoni* include four cervical vertebrae and four trunk vertebrae (figure 1). All centra are amphicoelous and slightly mediolaterally compressed. All vertebrae

have clearly defined vertebral laminae, and these laminae are identified using the nomenclature of Wilson (1999) and more broadly used for early archosaur taxa (Nesbitt, 2005; Nesbitt, 2007; Nesbitt et al., 2010; Nesbitt, 2011; Nesbitt et al., 2014; Weinbaum, 2013; Lautenschlager and Desojo, 2011; Parker, 2008; Parker, 2016a; Parker, 2016b). All of the trunk vertebrae of this specimen preserve one or both of the accessory articulation structures (i.e., hyposphene, hypantrum) that form the hyposphene-hypantrum articulation. None of the cervical vertebrae however have the hyposphene-hypantrum present, and this is consistent with my observations that the articulation is only present in the trunk region (presacral position 10 to the last presacral before the sacrum) of archosaur vertebral columns.

b. Vertebrae (Cervical): All three of the cervical vertebrae of individual 'A' and the one cervical vertebra of individual 'B' are amphicoelous, but both the posterior and anterior articular surfaces of the centrum are only slightly concave. The lateral and ventral portions of the anterior and posterior articular faces of the centra of the cervical vertebrae of individual 'B' are thickened and rugose, more similar to *Poposaurus gracilis* than to both previously described material from *Poposaurus langstoni* (Weinbaum and Hungerbühler, 2007) and the centrum of the cervical vertebra of individual 'A'. The centra of these vertebrae are shorter anteroposteriorly in comparison to their dorsoventral height.

Both articular facets of the centrum of TMM 31025-1261.5 are slightly elliptical, with the long axis oriented dorsoventrally. The anterior articular facets of the centra of TMM 31025-1262, TMM 31025-1261.3, and TMM 31025-177 are circular, and the posterior articular facets of these centra are slightly elliptical with the elongated axis oriented dorsoventrally. These posterior centrum facets are very similar in shape to those of the anterior cervical vertebrae of

Postosuchus kirkpatricki (UCMP A269/124557, Long and Murry, 1995; TTU-P 9002, Weinbaum, 2013) in that they appear elliptical and elongated dorsoventrally. All of the cervical vertebrae possess deep laterally opening fossae on the centrum on both their left and right sides just dorsal to the parapophyses and about 1 cm ventral the neurocentral sutures.

The two more posterior cervical vertebrae of individual 'B' (TMM 31025-1262 and TMM 31025-1261.3) and the posterior cervical vertebra of individual 'A' (TMM 31025-177) possess a well-preserved accessory rib articulation between the diapophysis and the parapophysis. The accessory rib articulations are dorsoventrally long and thin, projecting laterally from their respective centra. The accessory rib articulation of TMM 31025-1262 is broken at its base on the left lateral side but is intact on the right lateral side, protrudes 0.5 cm from where it attaches to the rest of the centrum, and is located 1 cm dorsal to the parapophyses. The accessory rib articulations of TMM 31025-1261.3 are intact on both sides, protrude 1.5 cm laterally, are located 3.2 cm from the diapophyses, and are located just dorsal to and touching the parapophyses. On the right lateral side of TMM 31025-177, the accessory rib articulation is just dorsal to and separated by 1 cm from the parapophyses. The left lateral side does not preserve this articulation; however, the paradiapophyseal lamina is clearly broken in the place where the articulation would be present. The accessory rib articulations on each cervical vertebra connect to the diapophyses through the paradiapophyseal laminae. This accessory rib articulation is also present in the posterior cervical vertebrae of *Poposaurus gracilis* (TTU P-10419) and *Arizonasaurus babbitti* (MSM 4590), and it is a synapomorphy of the clade Poposauroidea (Nesbitt, 2005; Weinbaum and Hungerbühler, 2007).

Vertebrae (Cervical; individual 'A') –

i. TMM 31025-177

TMM 31025-177 is a posterior cervical vertebra. The positions of the parapophyses and diapophyses place it as likely between presacrals 7 and 9, and the positions of these articulations are very similar to those in TMM 31025-1262. The parapophyses are low on the centrum and well separated from the diapophyses, which are located on the neural arch.

This specimen is mostly intact but is missing the neural spine, which is broken at the base, and the left prezygapophysis is broken. Both postzygapophyses are broken slightly at the edges and the diapophyses are both broken off where they connect to the neural arch and laminae. The neural arch is fused to the centrum, and although the neurocentral suture is nearly obliterated, there is still clear evidence of where it was located because raised areas on the lateral sides with a distinctive texture make the juncture (Brochu, 1996). The neural arch is slightly taller than the height of the centrum, and the neural arch is taller than it is laterally wide. In anterior view, the neural canal is deeply excavated and appears elliptical due to elongation of the dorsoventral axis.

TMM 30125-177 has distinct laminae forming thin, pronounced ridges on its neural arch. These laminae are thinner than those on the cervical vertebrae attributed to individual 'A'. On its lateral sides there are clear posterior and anterior centrodiapopohyseal laminae, which connect the diapophyses to the posterior and anterior portions of the neurocentral junction, respectively. There is a clear paradiapophyseal lamina connecting the parapophyses and diapophyses, and the accessory rib articulation is located on this lamina. This paradiapophyseal lamina extends nearly straight ventrally from the diapophysis, less than 5^{o} from vertical. The postzygapophyseal laminae are thin and well defined and connect the parapophyses and the lateral aspect of the postzygapophyses at about a 10^{o} angle dorsal to the anteroposterior horizontal. The

prezygodiapophyseal laminae are laterally thick and short with the prezygapophyses and diapophyses less than 0.5 cm apart. These laminae are at a ~45^{o} angle dorsal to the anteroposterior horizontal.

Vertebrae (Cervical; individual 'B') –

ii. TMM 30125-1261.5

TMM 30125-1261.5 is the anteriormost vertebra of this newly referred material and can be identified as a posterior cervical vertebra (presacral 7 or 8). It is nearly complete, with only slight breakage and very minor post-depositional compression in some areas including on and just ventral to the prezygapophyses. It also has a very slight ridge along the midline of the ventral surface of the centrum. The parapophyses on the lateral sides of this vertebra are located on the base of the anterior rim of the centrum and are lowest on the centrum relative to the other vertebrae and well separated from the diapophyses. The neural arch is fused to the centrum, and the neurocentral suture is nearly obliterated, but there is a slightly raised area with a distinctive texture on the lateral surface where the suture was originally present (Brochu, 1996). In anterior view, the neural canal is circular and filled with matrix and in posterior view, the canal is obstructed by a large bivalve shell that based on general morphology, can be attributed to the freshwater mussel group Unionidae (Huber, 2010).

The neural spine is tall and laterally compressed in TMM 31025-1261.5. A long depression extends dorsoventrally along the posterior surfaces of the neural spine. The neural spine is virtually identical in preserved morphology to that of TMM 31025-1262, but it is broken off at the dorsal end. In posterior view, the spinopostzygapophyseal laminae are paired and form distinct ridges from the base of the neural spine to nearly the distal end of the neural spine. The

neural spine is flat in anterior view, and no spinoprezygapophyseal laminae are present on that side. The neural spine is much wider at its base, at 2.5 cm just dorsal to the postzygapophyses in posterior view, and tapers to about 0.5 cm thick in anterior and posterior views at its most dorsal point. It does not expand laterally into a 'spine table' as in the mid-trunk vertebrae of *Nundasuchus songeaensis* (NMT RB48), the anterior and posterior trunk vertebrae of *Fasolasuchus tenax* (PVL 3850, PVL 3851), the trunk vertebrae of *Prestosuchus chiniquensis* (UFRGS-PV-0156-T), and anterior trunk vertebrae of *Batrachotomus kupferzellensis* (SMNS 80294). From lateral view, the neural spine of TMM 31025-1261.5 remains relatively consistent in anterior-posterior length at about 2.5 cm.

TMM 31025-1261.5 has distinct laminae that form thin, pronounced ridges on all surfaces of its neural arch and centrum. These laminae are more laterally expanded than the laminae of the posterior cervical vertebra of individual 'B' (TMM 31025-177) and are more similar in terms of lateral expansion to the other cervical vertebrae of individual 'A', TMM 31025-1261.3 and TMM 31025-1262. On the lateral sides of TMM 31025-1261.5, there are clear anterior and posterior centrodiapopohyseal laminae, which connect the diapophyses to their respective portions of the neurocentral junction. The paradiapophyseal lamina connects the parapophysis with the diapophysis, and is angled ~5^{o} from vertical in lateral view. The postzygapophyseal laminae are well defined and connect the parapophyses and the lateral aspect of the postzygapophyses at about a 45^{o} angle dorsal to the anteroposterior horizontal. This specimen is crushed so that the left postzygapophysis is pushed towards the diapophysis and this has compressed the lateral side of the left postzygapophyseal lamina (figure 2). The prezygodiapophyseal laminae are laterally thick and the prezygapophyses and diapophyses are ~3 cm apart. These laminae extend dorsally from the diapophyses at a right angle to the

anteroposterior horizontal with the prezygapophyses being dorsal to the diapophyses. The club-like diapophyses are fully intact where they connect to the neural arch, and the articular facets at their distal ends are elliptical. In posterior view, there are clear embayments present on the lateral sides of the transverse processes. A deep fossa is present on the left transverse process in anterior view (= prezygapophyseal centrodiapophyseal fossa of Wilson et al. [2011]), but a symmetrical counterpart is not present on the right transverse process (figure 2). There are epipophyses on the dorsal portion of the postzygapophyses that form a rugose structure about 0.2 cm from the end of the articular surface. The presence of epipophyses is typically cited as a synapomorphy of Dinosauria (Long and Murry, 1995, Langer and Benton, 2006, Langer et al., 2010, Novas, 1996), but are known to occur within Pseudosuchia (Nesbitt et al., 2010; Gower and Schoch, 2009; Bonaparte, 1981, Nesbitt et al., 2007, PEFO 34561) and are found outside Archosauria among stem members (Nesbitt, 2011; Nesbitt et al., 2015). There are interzygapophyseal laminae on the dorsal portion of the prezygapophyses connecting their lateral edge to the anterior extent of the postzygapophyses, a feature also found in *Azendohsaurus madagaskarensis* (FMNH PR 3823, Nesbitt et al., 2015).

iii. TMM 31025-1262

TMM 31025-1262 is a nearly complete posterior cervical vertebra, with slight breakage and minor post-depositional compression in some areas, including the prezygapophyses being pushed towards the neural spine (Figure 2). This specimen can be attributed to presacral 8 or 9; the parapophyses are low on the centrum, but slightly higher than those of TMM 31025-1261.5, and well separated from the diapophyses, which are located on the neural arch. TMM 31025-1262 also differs from TMM 31025-1261.5 in that it has club-like diapophyses that are more expanded

and flare out at the distal end where the articular facets are located; these articular facets are circular rather than elliptical like those of TMM 31025-1261.5. The neural arch is fused to the centrum and there is some evidence of where a neurocentral suture was present on the right lateral side in the form of a small, raised ridge (Brochu, 1996). There is no keel on the ventral surface of the centrum. In anterior view, the neural canal is circular and filled with matrix, and the postzygapophyses nearly come together at the dorsal portion of the neural canal.

The neural spine is tall and mediolaterally compressed. A long depression extends dorsoventrally along the posterior surfaces of the neural spine. The neural spine is nearly identical to that of TMM 31025-1265.5. In posterior view, the spinoprezygapophyseal laminae are paired and form distinct ridges from the base to nearly the distal end of the neural spine. There are no spinoprezygapophyseal laminae present on the neural spine in anterior view. The neural spine is much wider at its base, at 3 cm dorsal to the postzygapophyses in posterior view, and tapers to about 0.5 cm mediolaterally in anterior and posterior views at its most dorsal point. It does not expand into a spine table as in the mid-trunk vertebrae of *Nundasuchus songeaensis* (NMT RB48), the anterior and posterior trunk vertebrae of *Fasolasuchus tenax* (PVL 3850, PVL 3851), the trunk vertebrae of *Prestosuchus chiniquensis* (UFRGS-PV-0156-T), and anterior trunk vertebrae of *Batrachotomus kupferzellensis* (SMNS 80294). From lateral views, the neural spine remains relatively consistent in thickness mediolaterally at about 2.7 cm. The distal end of the neural spine is also rounded slightly in lateral view and is slightly taller posteriorly.

TMM 30125-1262 has distinct laminae forming thin, pronounced ridges on its neural arch; however, these laminae are more laterally expanded than the laminae of the posterior cervical of individual ‘B’ (TMM 31025-177) and more similar to the anterior cervical vertebrae of individual ‘A’ (TMM 31025-1261.3 and TMM 31025-1261.5). On the lateral sides of the

vertebra, there are clear posterior and anterior centrodiapopohyseal laminae, which connect the diapophyses to the posterior and anterior portions of the neurocentral junction, respectively. There is a clear paradiapophyseal lamina connecting the parapophyses and diapophyses, and the accessory rib articulation is located on this lamina. This paradiapophyseal lamina extends nearly straight down from the diapophysis, ~5^{o} from the vertical. The postzygapophyseal laminae are well defined and connect the parapophyses and the lateral aspect of the postzygapophyses at about a 45^{o} angle dorsal to the anteroposterior horizontal. This lamina is compressed on the left lateral side, because the specimen is crushed so that the left postzygapophysis is pushed towards the diapophysis (figure 2). The prezygodiapophyseal laminae are thick in lateral view and the prezygapophyses and diapophyses are ~3 cm apart. These laminae extend dorsally from the diapophyses at right angles to the anteroposterior horizontal plane, and the prezygapophyses are dorsal to the diapophyses. The diapophyses are intact where they connect to the neural arch, and they are more robust than in TMM 31025-1261.5 and end in circular articular facets. Centroprezygapophyseal laminae extend from the ventral side of the prezygapophyses ventrally along the neural canal to the dorsal edge of the centrum. There are epipophyses on the dorsal portion of the postzygapophyses that form a rugose structure about 0.2 cm from the end of the articular surface.

iv. TMM 31025-1261.3

TMM 31025-1261.3 is a posterior cervical vertebra that can be attributed to presacral 9 or 10. The diapophyses are located on the neural arch and are well separated from the parapophyses. The parapophyses are also more dorsal on the centrum than in both TMM 31025-1261.5 and TMM 31025-1262. Although this specimen's neural arch is detached from the centrum, the two

portions were fused and then broken post-depositionally. There is evidence of where a neurocentral suture was located, because there are some slightly raised areas on the lateral sides of the centrum ventral to the break (Brochu, 1996). There is a rugose projection, which resembles a thickened and pronounced keel on the ventral surface of the centrum (figure 2); however, it is asymmetrical and protrudes substantially anterior of the articular facet in anterior view. This structure seems to be pathologic in origin because it is asymmetrical and no other archosaurs possess this structure in that place.

The detached neural arch of this specimen is broken through the center of the neural canal, and is not a sufficiently close fit with the centrum to be reattached because small bits of bone are missing. The neural canal is deeply excavated; it is circular in anterior view and elliptical with the long axis oriented dorsoventrally in posterior view. The diapophyses are broken off at the point where they begin to extend out from the neural arch. A few laminae are broken and the specimen is slightly post-depositionally compressed in some areas, but otherwise it is intact.

TMM 31025-1261.3 has distinct laminae forming thin, pronounced ridges on its neural arch, and these laminae are more laterally expanded than the laminae of the cervical vertebra of individual 'B' (TMM 31025-177) and more similar to the other cervical vertebrae of individual 'A' (TMM 31025-1262 and TMM 31025-1261.5). On the left lateral side there is a clear posterior centrodiapopohyseal laminae, which connects the diapophysis to the posterior portion of the neurocentral junction, but this lamina is broken off on the right lateral side. There is a clear paradiapophyseal lamina, which connects the parapophyses and diapophyses, but the lamina on this vertebra connects the diapophyses to the accessory rib articulation instead of the parapophyses because the articulation is located just dorsal to the parapophyses and nearly

touching. The paradiapophyseal lamina extends nearly straight down from the diapophysis, ~5° from vertical. The postzygapophyseal laminae are well defined and connect the parapophyses and the lateral aspect of the postzygapophyses at about a 45° angle dorsal to the anteroposterior horizontal. The prezygodiapophyseal laminae are thick in lateral view and the prezygapophyses and diapophyses are ~1.5 centimeters apart. These laminae extend dorsally from the diapophyses at a right angle to the anteroposterior horizontal with the prezygapophyses being dorsal to the diapophyses. The diapophyses are broken off about where they connect to the neural arch, but the left one extends about 0.5 cm laterally before its break. The neural spine is broken off at its base, so spinoprezygopophyseal laminae are unable to be seen.

c. Vertebrae (Trunk): The trunk vertebra of individual 'A' (TMM 31025-257) and all three trunk vertebrae of individual 'B' (TMM 31025-1261.4, TMM 31025-1261.1, TMM 31025-1261.2) are waisted between the articular facets of the centra. The anterior and posterior articular facets of the two anterior most trunk vertebrae (TMM 31025-1261.4 and TMM 31025-1261.1) and the trunk vertebra of individual 'A' (TMM 31025-257) appear narrow mediolaterally in lateral and ventral views. The general shape of these centra in posterior and anterior view is similar to that seen in *Batrachotomus kupferzellensis* (SMNS 80296, Gower and Schoch, 2009), *Poposaurus gracilis* (TTU P-10419, Weinbaum and Hungerbühler, 2007), *Effigia okeeffeae* (AMNH FR 30587, Nesbitt, 2007), and *Postosuchus kirkpatricki* (TTU P-9002, Weinbaum, 2013), and the articular facets of these taxa are elliptical, with a long dorsoventrally oriented axis. The articular facets of the centrum of the most posterior trunk vertebra of individual 'B' (TMM 31025-1261.2) are round and not compressed in any direction, and the anterior and posterior articular facets of the centrum appear thick (~1 cm) in lateral and ventral views. There

are deep fossae on the centra on both the left and right lateral sides about 1 cm ventral to the position of the neurocentral sutures. There is no ridge on the midline on the ventral surfaces of any of the three trunk vertebrae of individual 'B'; however there is a recognizable, but poorly developed ridge along the midline of the ventral surface of the centrum of the trunk vertebra of individual 'A', which suggests that the trunk vertebra of individual 'A' is located more anteriorly in the column than the other trunk vertebrae.

All four of the trunk vertebrae preserve one or both of the accessory articulation structures (i.e., hyposphene, hypantrum) that form the hyposphene-hypantrum articulation. TMM 31025-1261.4 is weathered so that a hyposphene could not be recognized, but a clear and deep hypantrum is visible on the anterior aspect of the neural arch. TMM 31025-1261.1 is weathered so that a hypantrum could not be recognized, but on the posterior aspect of the neural arch there is a hyposphene preserved. TMM 31025-1261.2 and TMM 31025-257 preserve both hyposphenes and hypantra on their neural arches.

Vertebrae (Trunk; individual 'A') –

i. TMM 31025-257

TMM 31025-257 is an anterior mid-trunk vertebra (figure 3). The positions of the parapophyses and diapophyses place it as likely between presacral 12 and 14 (see above). The parapophysis is slightly more dorsally located on the neural arch than TMM 31025-1261.4. Both of the parapophyses and both the diapophyses are broken off at their bases. The neural spine, left and right postzygapophyses, and left prezygapophysis are broken off. The neural arch is firmly attached to the centrum, with a visibly raised evidence of where the neurocentral suture was. In

anterior view, the neural canal is deeply excavated and elliptical as the dorsoventral axis is slightly elongated relative to the mediolateral axis.

The posterior and anterior neural arches of TMM 31025-257 preserve clearly developed hyposphene and hypantrum articulation structures, respectively. In posterior view, the hyposphene is broken, but its shape is identifiable; it is triangular with the ventral edge along the mediolateral horizontal plane and a point of the triangle directed dorsally, to where the articular surfaces of the postzygapophyses meet at ~45^{o} angles dorsal to the horizontal. The sides of the hyposphene each measure 1.2 cm and the base of the triangle is 0.8 cm across, although it is slightly arched as the dorsal boarder of the neural canal. The trunk vertebra of *Postosuchus kirkpatricki* (TTU P-9002, Weinbaum, 2013, Fig. 4), the trunk vertebra of *Prestosuchus chiniquensis* (UFRGS-PV-0156-T), and the posterior trunk vertebra of *Fasolasuchus tenax* (PVL 3850, Bonaparte, 1981, Fig. 10, Fig. 11) have similarly shaped hyposphenes in that they are triangular and connect with the postzygapophyses at the dorsally located point. *Batrachotomus kupferzellensis* (SMNS 80296, Gower and Schoch, 2009, Fig. 2) has a hyposphene structure present on its trunk vertebrae that appears rectangular and dorsoventrally elongate. On TMM 31025-257, the face of the hyposphene is approximately 2 cm from the diapopohyses in lateral view. The hypantrum space between the prezygapophyses is 1 cm across. On the lateral edges of the hypantrum, centroprezygapophyseal laminae project laterally from the ventral side of the prezygapophyses, and they extend ventrally along the neural canal to the dorsal edge of the centrum.

The neural spine is laterally compressed, and roughly the same height as the height of the rest of the vertebra to the base of the neural spine. Grooves extend dorsoventrally along both the posterior and anterior surfaces of the neural spine. The spinoprezygapophyseal laminae are

paired and cease to form distinct ridges about halfway up dorsoventrally from the base of the neural spine. The dorsal edge of the neural spine is rounded and the top centimeter of the neural spine is slightly laterally expanded, although it is not sufficiently wide to form a 'spine table' as in the mid-trunk vertebrae of *Nundasuchus songeaensis* (NMT RB48) and the anterior and posterior trunk vertebrae of *Fasolasuchus tenax* (PVL 3850). The neural spine of TMM 31025-257 is angled on the posterior edge and extends further dorsally on the anterior edge, causing it to be slightly wider at the distal end than at the base in lateral view, unlike the neural spines of the posterior trunk vertebrae of *Postosuchus kirkpatricki* (TTU P-9002) and *Batrachotomus kupferzellensis* (SMNS 52970), which are both more rectangular in lateral view.

TMM 31025-257 has distinct laminae between the prezygapophyses, postzygapophyses, parapophyses, and diapophyses. On the lateral sides, the specimen has paradiapophyseal laminae, which connect the diapophyses with the parapophyses. There are anterior centroparapophyseal laminae, which connect the parapophyses with the anterior portion of the neurocentral junction, and there are also posterior centrodiapophyseal laminae, which connect the diapophyses with the posterior portion of the neurocentral junction, and all of these laminae are at a 45^{o} angle ventral to the anteroposterior horizontal (figure 4). The prezygapophyseal laminae are well defined and connect the parapophyses and the lateral aspect of the prezygapophyses at a 45^{o} angle dorsal to the anteroposterior horizontal. The anterior centroparapophyseal laminae are recognizable but poorly defined, as the parapophyses are almost on the furthest anteroventral portion of the neural arch. The prezygadiapophyseal laminae are laterally thin and pronounced and connect the diapophyses and lateral edge of the prezygapophyses at a $\sim 10^{o}$ angle to the anteroposterior horizontal with the articular surfaces of the prezygapophyses completely ventral to the diapophyses. TMM 31025-257 has

centroprezygapophyseal laminae on each lateral side of the neural arch; they are thinner laterally in relation to the other laminae on this specimen's neural arch, and both are vertically oriented. The postzygodiapophyseal laminae are thick in lateral view and poorly laterally expanded with the postzygapophyses and diapophyses only ~0.5 cm apart. These laminae are at a ~10^{o} angle to the anteroposterior horizontal with the postzygapophyses being dorsal to the diapophyses. There are slight knobs extending along the anterodorsal portions of the postzygapophyses from the neural spine, but they do not appear pronounced enough for us to definitively call them epipophyses.

Vertebrae (Trunk; individual 'B') –

ii. TMM 31025-1261.4

TMM 30125-1261.4 is an anterior to mid-trunk vertebra. It is weathered post-depositionally, and the neural arch is broken horizontally through the mediolateral middle and separate completely from the centrum (figure 3). It is further weathered so that the neural arch cannot be accurately reattached to the centrum in a close fit. Both postzygapophyses are broken off, and the neural spine is broken off near its base. This specimen can be attributed to presacral 11 through 13, as the parapophyses are well separated from the diapophyses, and the parapophyses are located at the junction of the neural arch and the centrum. The neural arch is fused to the centrum, and there is evidence of where a neurocentral suture was, which is slightly raised in some areas (Brochu, 1996).

On the left lateral side, TMM 30125-1261.4 has distinct laminae forming pronounced ridges, the posterior and anterior centrodiapopohyseal laminae, which connect the diapophyses to the posterior and anterior portions of the neurocentral junction, respectively. The anterior

centrodiapophyseal lamina is recognizable but not clearly defined on the right lateral side. On both lateral sides the prezygapophyseal laminae are recognizable and connect the parapophyses and the lateral aspect of the prezygapophyses at a steep angle (>80^{o}) to the anteroposterior horizontal.

The posterior facet of the neural arch is sufficiently weathered so that no hyposphene structure is recognizable, however there is a well-defined hypantrum visible on the anterior facet of the neural arch (figure 3). The hypantrum is 0.5 cm wide at its dorsal edge where it meets the articular faces of the prezygapophyses, and widens out ventrally to 1.1 cm at its ventral edge. The prezygapophyseal articular surfaces are gently curved and concave dorsally. They are positioned at ~45^{o} dorsal to the horizontal. The postzygapophyses are both completely broken off, and it is also unclear as to where they were originally positioned on the neural arch because of the extensive weathering. The neural spine is broken at 1.5 cm from its base. A deep groove extends dorsoventrally along what is preserved of the anterior surfaces of the neural spine. On either side of this groove, the spinoprezygapophyseal laminae are paired and form thin (< 0.5 cm) and distinct ridges and are separated for the preserved length of the neural spine. On the right lateral side of the neural arch, in dorsal view, there is a deep fossa between the base of the neural spine and the prezygapophyseal lamina. The left lateral side is broken in this corresponding place, obstructing any potential lateral fossa.

iii. TMM 31025-1261.1

TMM 31025-1261.1 is an anterior to mid-trunk vertebra that is nearly complete, but is well weathered post-depositionally, more so on the anterior and right lateral portions. The specimen is attributed to presacral 12 through 14, as the parapophyses are well separated from diapophyses,

and both are located on the neural arch. The neural arch is completely fused to the centrum with only a slight textural trace of where the neurocentral suture was located (Brochu, 1996).

The parapophyses are slightly higher on the neural arch than those on the trunk vertebra we attribute to individual 'B' (TMM 31025-257). Both of the parapophyses are broken off at their bases. They are circular in lateral view with a diameter of about 1 cm. The left parapophysis is in the correct anatomical position, but the right parapophysis has broken from its originally position and has shifted about 3-4 centimeters posteriorly. The right diapophysis is broken off at its base, and the left diapophysis is broken off about 1.5 cm from its base. This left diapophysis is dorsoventrally compressed, shaped as a narrow ellipse in lateral view with the long axis along the anteroposterior horizontal. There is a clear paradiapophyseal lamina connecting the parapophysis and the diapophysis on the left side. There is also a posterior centrodiapophyseal lamina connecting the diapophysis with the posterior section of the neurocentral suture junction. The right side is too weathered and broken to see any laminae. No zygapophyses are preserved. The neural canal is filled with sediment but appears to be only slightly laterally compressed (figure 3).

The neural spine of TMM 31025-1261.1 is complete but is broken and offset dorsally by ~25°. The neural spine is tall relative to the rest of the neural arch and laterally compressed and the dorsal edge of the neural spine is sloped at 45°, increasing in height posteriorly, in lateral view. The anteroposterior width of the neural spine is nearly uniform throughout in lateral view. The distal end of the neural spine is slightly rounded. The neural spine is posteriorly shifted in relation to the anteroposterior center of the centrum. The anterior surface of the neural arch is well weathered post-depositionally so that a hypantrum is not recognizable. The posterior surface of the neural arch preserves a clearly defined hyposphene. The shape of the hyposphene is

triangular in posterior view, with a point directed dorsally along the dorsoventral midline, and the ventral side is slightly concave, forming the dorsal border of the neural canal (figure 3). It has a similar shape to the hyposphene of TMM 31025-257, but the structure in TMM 31025-1261.1 extends much further distally from the neural arch. The sides of the hyposphene both measure 1 cm and the ventral edge, straight across from bottom of each side to the other and not along the concave surface, measures 1.2 cm. The connection between the hyposphene and the postzygapophyses cannot be seen, as the neural spine is broken and offset from the point just dorsal to the hyposphene and ventral to the articular surfaces of the postzygapophyses. There are clear spinopostzygapophyseal laminae and spinoprezygapophyseal laminae on the anterior and posterior aspects of the neural spine.

iv. TMM 31025-1261.2

TMM 31025-1261.2 is a posterior trunk vertebra and I attribute it to presacral position somewhere among 14 through 17, as the parapophyses are only separated from the diapophyses by about 1 cm, and both are located on the neural arch. It is well weathered post-depositionally. The neural arch is completely fused to the centrum with slight evidence of where the neurocentral suture was located. The neural canal is deeply excavated and laterally compressed in anterior view, but appears round and less laterally compressed in posterior view (figure 3).

On the lateral sides of this specimen, the diapophyses are broken about 2 cm from where they connect to the neural arch. Both are dorsoventrally compressed and thin out posteriorly from a circle with a diameter ~1 cm across to a flat surface with a thickness of 0.5 cm. Both diapophyses are in tact and both are dorsoventrally compressed so that they are shaped as a narrow elliptical with the long axis along the anteroposterior horizontal. There are clearly

defined paradiapophyseal lamina connecting the parapophysis and the diapophysis on both lateral sides. There are also posterior centrodiapophyseal laminae connecting the diapophyses with the posterior sections of the neurocentral suture junction on both lateral sides.

The left postzygapophysis is broken off at its base, and the right postzygapophysis is broken off about 1.5 cm from its base and there is a subtle but recognizable postzygodiapophyseal lamina connecting the postzygapophysis to the diapophysis on the right lateral side. The right prezygapophysis is broken off at its base, and the left prezygapophysis is only broken slightly at the tip with no more than half a centimeter of missing material. There are clear prezygodiapophyseal laminae connecting the prezygapophyses with the diapophyses on both sides. There are also clear prezygoparapophyseal laminae connecting the prezygapophyses with the parapophyses on both sides.

The neural spine is broken off ~3 cm dorsal to the postzygapophyses, so spinoprezygopophyseal laminae are obstructed from view. However, there are clear spinopostzygopophyseal laminae extending dorsally on the intact portion of the neural spine from the postzygapophyses. There is a distinct hyposphene dorsal to where the bases of the postzygapophyses meet at a point. The shape of the hyposphene is triangular in posterior view, with a point directed dorsally, and the ventral side is slightly concave, curving around the dorsal portion of the neural canal (figure 3). The hyposphene is similarly shaped to the hyposphene of TMM 31025-257; however it appears more dorsoventrally compressed in posterior view, and this does not appear to be related to compression of the fossil post-depositionally, as no other aspects of the vertebra appear more compressed. The sides of the hyposphene both measure 1.2 cm and from the ventral most portion of one lateral side to the other, measures 1.5 cm. Although

the right prezygapophysis is broken off, there is a clear hypantrum visible, and the space would have been ~1 cm between the two prezygapophyses.

d. Rib (TMM 31025-2160): This specimen is broken about 12 centimeters distally from the capitulum. The capitulum, tuberculum, and accessory rib facet are all intact. A thin ridge extends from the dorsal edge of the capitulum along the rib (figure 5). This rib fragment has an accessory articular facet that is located just dorsal to the tuberculum (figure 5). I assign it to the posterior cervical region of the axial skeleton because of the relative locations of the capitulum and tuberculum and the presence of an accessory rib facet, as a corresponding accessory rib articulation is seen on the posterior cervical vertebrae described in this paper (TMM 31025-177, TMM 31025-1262, TMM 31025-1261.3). An accessory rib facet between the capitulum and tuberculum is also present in *Poposaurus gracilis* (Weinbaum and Hungerbühler, 2007) and *Arizonasaurus babbitti* (Nesbitt, 2005), and it matches in position, just dorsal to the parapophysis to the accessory rib articulation structures in the posterior cervical vertebrae described herein. Weinbaum and Hungerbühler (2007) cited this accessory articulation as a synapomorphy of the clade Poposauroidea, which includes *Poposaurus gracilis*, *Poposaurus langstoni*, *Effigia okeeffeae*, and *Arizonasaurus babbitti*.

Variation in the hyposphene-hypantrum articulation in *P. langstoni*

The hyposphene-hypantrum articulation of the trunk vertebrae of *P. langstoni* presents an important opportunity to examine within-vertebral column variation because these vertebrae are preserved in three dimensions so that articulation surfaces and hyposphene-hypantrum are visible and easy to discern. Moving posteriorly along the vertebral column, the hyposphene-hypantrum

articulation is present in the anteriormost trunk vertebrae of the individuals represented by presacral 11 in individual 'A' (TMM 31025-1261.4) and presacral 12 of individual 'B' (TMM 31025-257). The articulation is also present in presacral 12 in individual 'A' (TMM 31025-1261.2). All three of the preserved hyposphenes are triangular in posterior view, and the ventralmost edges of the triangular hyposphenes are oriented horizontally with their apexes pointed dorsally along the midline. The ventrolateral corners of the triangular hyposphenes curve slightly ventrally around the neural canal. The hyposphenes (TMM 31025-1261.1, TMM 31025-1261.2, TMM 31025-257) appear to be more dorsoventrally compressed (i.e. smaller height to width ratio) in individual 'B' than in individual 'A'. This material described herein includes the twelfth presacral from both individuals (TMM 31025-1261.1, TMM 31025-257), so it is likely that this variation is not based on location in the vertebral column. The hypantra (TMM 31025-1261.4, TMM 31025-1261.2, TMM 31025-257) reflect a complementary shape of the hyposphene structures on their respective vertebrae. The horizontal distance between the prezygapophyses is narrower across the structure at the dorsal most edge than at the ventralmost extent, creating a triangular space for articulation. In summary, the hyposphene-hypantrum articulation appears triangular in all vertebrae described herein and therefore does not vary in general shape along the vertebral column of one individual of *Poposaurus langstoni*, but the two recognized individuals of *P. langstoni* have hyposphene structures that are markedly different in terms of height to width ratio (table 1).

4. Discussion

Definition of the hyposphene-hypantrum articulation

The hyposphene-hypantrum articulation appears in many clades within Archosauria and has been defined simply as a vertical wall of bone ventral to the postzygapophyses and a notch between the prezygapophyses (Rauhut, 2003; Apesteguia, 2005; Williston, 1851-1918). Those previous studies included definitions of the hyposphene-hypantrum articulation that were based on the vertebral morphology of saurischian dinosaurs, but they are not comprehensive in incorporating the variation in shape in dinosaurs and pseudosuchians. Furthermore, a number of pseudosuchians also have been reported to bear the hyposphene-hypantrum articulation without an explanation of why it is homologous with those structures in saurischian dinosaurs (Bonaparte, 1981; Weinbaum and Hungerbühler, 2007; Peyer et al., 2008; Gower and Schoch, 2009; Lautenschlager and Desojo, 2011; Weinbaum, 2013). This is important to clarify because the hyposphene-hypantrum has been cited as a synapomorphy of Saurischia (Gauthier, 1986) and of at least one clade of pseudosuchians (*Ticinosuchus* + Paracrocodylomorpha, Nesbitt, 2011). Here I apply an explicit definition of this articulation to facilitate identification and future studies of intervertebral articulation in archosaurs.

I define the hyposphene-hypantrum articulation as a bony projection, the hyposphene, on the posterior portion of the vertebra that fits into a complementary space, the hypantrum, on the anterior portion of the subsequent vertebra within a vertebral series (figure 6). Specifically, the hyposphene is located ventral to the articular surfaces of the postzygapophyses and is connected to these articular surfaces where they converge. It is located dorsal to the neural canal and in posterior view is symmetrical or nearly symmetrical across the midline. There is a distinct angle change (typically between ~45-90^{o}) between the articular surfaces of the postzygapophyses and the lateral surfaces of the hyposphene. The hyposphene projection must be a comparable shape and size to that of the hypantrum space of the subsequent vertebrae because these structures

articulate precisely. The shapes in lateral view of the hyposphenes may appear as circular, square, dorsoventrally-elongate rectangular, triangular, diamond, and quadrilateral, and the most common shapes found in pseudosuchian archosaurs are triangles and dorsoventrally elongate rectangles (figure 7). Though these shapes can vary between taxa, they also can vary within an individual. *Poposaurus langstoni* does not show drastic variation in hyposphene shape, but the proportions do vary along the column and between our two individuals (i.e. ratio of height to width increasing posteriorly in individual 'B' and greater ratio of height to width in individual 'A' than in individual 'B') (table 1). As long as these projections extend posteriorly from the neural arch, their lateral surfaces are confluent with the articular surfaces of the postzygapophyses, and there is a distinct angle change between the articular surfaces of the postzygapophyses and the projection, any of these aforementioned shapes may be considered hyposphenes. Additionally, it is important to note that these structures are currently only known from trunk vertebrae posterior to the first nine presacral vertebrae.

Descriptions of a vertebra with the hyposphene-hypantrum should describe the shape that the hyposphene appears to be in posterior view. In vertebrae without the hyposphene, the articular surfaces of the postzygapophyses may converge but not form a ventrally elongated bony projection, as in *Revueltosaurus callenderi* (PEFO 34561; figure 7), *Erythrosuchus africanus* (SAM 905, figure 7), *Parringtonia gracilis* (NMT RB426), or *Nundasuchus songeaensis* (NMT RB48), or they may not converge at all and appear well separated, as in *Deinosuchus riograndensis* (TMM 43632-1, figure 7) or *Alligator mississippiensis* (Romer, 1956, Fig. 130).

The lateral surfaces of the hyposphene articulate with the medial surfaces of the hypantrum, which is located between and ventral to the prezygapophyses and dorsal to the neural canal (figure 7). The articular surfaces of the prezygapophyses continue ventrally from their

medial surfaces to form the articular surfaces of the hyposphene. As such, there must be a distinct angle change (typically between ~45-90^{o}) between these articular surfaces. In dorsal view, a hypantrum appears as a gap framed by parallel to sub-parallel medial surfaces of the prezygapophyses, which contact the neural arch just dorsal to the neural canal. In vertebrae without a hypantrum articulation (e.g., *Revueltosaurus callenderi*, PEFO 34561; *Parringtonia gracilis*, NMT RB426; *Effigia okeeffeae*, AMNH FR 30587; *Deinosuchus riograndensis*, TMM 43632-1; *Alligator mississippiensis*, Romer, 1956), the medial edges of the prezygapophyses will converge in a "v" shape and will not appear parallel in dorsal view.

Accessory Intervertebral Articulations within Pseudosuchia –

The presence of the hyposphene-hypantrum articulation in *Poposaurus langstoni* allows for comparisons with the presacral vertebrae of other pseudosuchian archosaurs. Other closely related members of Poposauroidea, *Poposaurus gracilis* -the sister taxon to *Poposaurus langstoni*- and the smaller *Effigia okeeffeae*, have also been reported to have a hyposphene-hypantrum between trunk vertebrae (Weinbaum and Hungerbühler, 2007; Nesbitt, 2007).

The presacral vertebrae of the poposauroid *Effigia okeeffeae* (AMNH FR 30587, Nesbitt, 2007: Fig. 30) are only known from four semi-articulated vertebrae, and the anterior aspect of the neural arch is only visible on the anteriormost vertebra of the articulated series. There is not a clearly defined space between the prezygapophyses in this vertebra to satisfy our definition of a hypantrum. There is a slight gap between the medial aspects of the prezygapophyses, of which the articular surfaces are oriented horizontally, however these articular surfaces do not extend ventrally to form a hypantrum in accordance with our definition. No posterior surface of any vertebra of AMNH FR 30587 is clearly visible and intact, so I cannot conclusively state whether

a hyposphene was present in the trunk vertebrae of known material of *Effigia okeeffeae*. Additionally, because I do not see a hypantrum present in this specimen of *Effigia okeeffeae*, I conclude that this taxon probably did not possess the hyposphene-hypantrum. Furthermore, there are no specimens of *Shuvosaurus inexpectatus* (e.g. TTU P-9001), the current sister taxon of *Effigia okeeffeae* (Nesbitt and Norell, 2006; Nesbitt, 2007; 2011), that preserve a neural arch where I could evaluate whether the hyposphene-hypantrum articulation was present or absent. The other known shuvosaurid, *Sillosuchus longicervix* (PVSJ 85), is poorly preserved (Alcober and Parrish, 1997), and therefore it is difficult to determine definitively whether a hyposphene-hypantrum was present in that taxon as well. The sail-backed poposauroid *Lotosaurus aduntus* (IVPP V 4880, IVPP V 48013) has not been reported to have the hyposphene-hypantrum articulation.

Arizonasaurus babbitti is one of the oldest members of Poposauroidea, outside of *Lotosaurus adentus* + Shuvosauridae, and it has been reported to have the hyposphene-hypantrum articulation (MSM 4590, Nesbitt, 2005; 2007). The hyposphene structure of the trunk vertebra of *A. babbitti* (MSM 4590) is rectangular with the long axis oriented dorsoventrally in posterior view and located ventral to the postzygapophyses and dorsal to the neural canal (Nesbitt, 2005: Fig. 19). It does not have the triangular shape as in the trunk vertebrae of *Poposaurus langstoni*. The sister taxon of *Arizonasaurus babbitti* is the earliest diverging poposauroid, *Xilousuchus sapingensis* (IVPP V6026), and it has been cited as having the hyposphene-hypantrum as well (Nesbitt et al., 2011). The ninth presacral vertebra figured by Nesbitt et al. (2011: Fig. 8) has a clearly defined hyposphene, and it is square in posterior view. A hypantrum between the prezygapophyses is clearly seen in anterior view and is of comparable size and shape to the hyposphene of the same vertebra (Nesbitt et al., 2011: Fig. 8). The

identification of this vertebra as the ninth presacral (Nesbitt et al. 2011) may be incorrect given that there are no other taxa with a hyposphene in the first nine presacrals. Alternatively, the presence of a hyposphene in this position may be autapomorphic for this taxon.

Several Triassic loricatan paracrocodylomorphs and their closest relatives possess the hyposphene-hypantrum articulation, and this structure varies in shape and structure between taxa and even within an individual. *Stagonosuchus nyassicus* (GPIT/RE/3831, von Huene, 1938; Gebauer, 2004; Lautenschlager and Desojo, 2011) is reported to have the hyposphene-hypantrum in the trunk vertebrae. The anterior trunk vertebra of *S. nyassicus* (GPIT/RE/3831 – 9, von Huene, 1938; Gebauer, 2004; Lautenschlager and Desojo, 2011: Fig. 7) has a clearly defined hyposphene that is rectangular, but it is only slightly elongated dorsoventrally. The posterior trunk vertebra of *S. nyassicus* (GPIT/RE/3831-14, von Huene, 1938; Gebauer, 2004; Lautenschlager and Desojo, 2011: Fig. 7) has a hyposphene that is narrower mediolaterally and more elongated dorsoventrally than the hyposphene of its anterior trunk vertebra. This shape is distinctly different from the triangular hyposphenes of *Poposaurus langstoni* (figure 3). In anterior view, there is a clear space between the prezygapophyses to form a hypantrum in *S. nyassicus*. *Ticinosuchus ferox* is a close relative to *Stagonosuchus nyassicus* (Lautenschlager and Desojo, 2011), but the presence of the hyposphene-hypantrum articulation in that taxon is ambiguous because the known material (PIZ T 2817) is preserved in a flattened slab, and the vertebral column is mostly articulated so that the anterior and posterior aspects of the vertebrae cannot clearly be seen.

Fasolasuchus tenax (PVL 3850, Bonaparte, 1981: Fig. 10, Fig. 11), *Batrachotomus kupferzellensis* (SMNS 80296, Gower and Schoch, 2009: Fig. 2), *Prestosuchus chiniquensis* (UFRGS-PV-0156-T, Azevedo, 1991: Fig. 11), and *Saurosuchus galilei* (PVSJ 32, Trotteyn et

al., 2011: Fig. 7) have hyposphene-hypantrum articulations present in their trunk vertebrae. *Fasolasuchus tenax* has a hyposphene structure that appears rectangular in posterior view in the anterior trunk vertebra figured by Bonaparte (1981: Fig. 10). In the posterior trunk vertebra of *Fasolasuchus tenax* (figure 7), the hyposphene structure is triangular in posterior view with the midline apex directed dorsally and the ventrolateral corners curved slightly ventrally around the neural canal, similar to that of *Poposaurus langstoni* and *Postosuchus kirkpatricki* (TTU P-9002). The trunk vertebra of *Batrachotomus kupferzellensis* figured in lateral view by Gower and Schoch (2009: Fig. 2) (SMNS 80296) has a clearly defined hyposphene that is rectangular and elongated dorsoventrally in posterior view (figure 7); in anterior view there is a clear space between the prezygapophyses to form a hypantrum in this specimen. The posterior trunk vertebra of *Prestosuchus chiniquensis* that was figured in posterior view by Azevedo (1991: Fig. 11) has a well-defined hyposphene that is rectangular with the long axis oriented dorsoventrally in posterior view. The shape of this hyposphene most closely resembles the hyposphene shapes in *Batrachotomus kupferzellensis* (SMNS 80296) and *Postosuchus kirkpatricki* (TTU P-9002) (figure 7). *Saurosuchus galilei* (PVSJ 32) has a hyposphene-hypantrum articulation present on at least one of its posterior trunk vertebrae (Trotteyn et al., 2011), but it is difficult to tell the shape because of poor preservation of the specimen.

A large member of the paracrocodylomorph clade Rauisuchidae, *Postosuchus kirkpatricki* has been reported to have the hyposphene-hypantrum articulation present on its middle and posterior trunk vertebrae (TTU P-9002; Weinbaum, 2013). The figured anterior trunk vertebra and posterior trunk vertebra of TTU P-9002 have clearly defined hyposphene structures that appear triangular in posterior view, with the ventralmost aspect as a horizontal surface and the dorsalmost aspect as a midline apex (TTU P-9002; Weinbaum, 2013: Fig. 4, Fig. 5). The

ventrolateral corners of the triangular hyposphene also slightly curve around the neural canal at its dorsal margin. This shape is nearly identical to those hyposphenes of *Poposaurus langstoni* in the anterior trunk vertebrae TMM-31025-1261.1 and TMM-31025-1261.2. The hypantrum of the anterior portion of the neural arch of the anterior (Weinbaum, 2013: Fig. 4) and posterior (Weinbaum, 2013: Fig. 5) trunk vertebrae of *Postosuchus kirkpatricki* (TTU P-9002) also appear triangular in anterior view with a shape and size complementary to the hyposphene of the same vertebra. The hyposphene structure of the mid-trunk vertebra of *Postosuchus kirkpatricki* (TTU P-9002, Weinbaum, 2013: Fig. 4) appears rectangular in posterior view with the long axis oriented dorsoventrally. The one known trunk vertebra of *Postosuchus alisonae* (UNC 15575) has clear hyposphene and hypantrum structures (figure 7). The hyposphene appears triangular in posterior view, similar to those of the anterior and posterior trunk vertebrae of *Postosuchus kirkpatricki* (TTU P-9002), with the midline apex directed dorsally and the ventrolateral corners curved slightly around the dorsal edge of the neural arch (Peyer et al., 2008: Fig. 4). The hypantrum of *Postosuchus alisonae* is of complementary shape and size to the hyposphene.

Just outside of Paracrocodylomorpha, *Nundasuchus songeaensis* (NMT RB48, Nesbitt et al., 2014) was reported to possess the hyposphene-hypantrum articulation on its mid-trunk vertebrae. Evidence for a hypantrum was cited as a small gap between the anterior portion of the prezygapophyses, and the hyposphene was cited as a thin, ventrally directed lamina of bone between the postzygapophyses. However, this proposed hyposphene was not clearly defined, and appears simply as the postzygapophyses converging at the midline, without an extension of a bony process ventral to them (NMT RB48, Nesbitt et al., 2014: Fig. 4). There is a slight gap between the medial aspects of the prezygapophyses; however, articular surfaces do not extend ventrally from the prezygapophyses to form a hypantrum in accordance with our refined

definition. This morphology in *Nundasuchus songeaensis* is similar to that in *Effigia okeeffeae*, which I have concluded does not have the hyposphene-hypantrum articulation.

Hyposphene-hypantrum articulations have been reported in some members of Aetosauria, a group of quadrupeds with an extensive osteoderm carapace (Parker, 2008; Desojo et al., 2012; Parker, 2016b). The largest known aetosaur, *Desmatosuchus spurensis* (MNA V9300; Parker, 2008), has hyposphene-hypantrum articulations between its trunk vertebrae. The hyposphene structures of the anterior and mid-trunk vertebrae are rectangular in posterior view and more elongated dorsoventrally relative to the hyposphene structures of the posterior trunk vertebrae (figure 7). The rectangular hyposphenes of the anterior and mid-trunk vertebrae of *D. spurensis* appear more similar to those structures of *Batrachotomus kupferzellensis*, *Fasolasuchus tenax*, and *Prestosuchus chiniquensis* than to taxa with triangular hyposphenes (e.g. *Poposaurus langstoni*). The posterior trunk vertebrae of *D. spurensis* have hyposphenes that have a width and height nearly equal to each other and have a greater surface area in posterior view in comparison to the rest of the neural spine visible from that view in comparison to those of the anterior vertebrae. These hyposphenes also curve around the neural canal and appear triangular in posterior view (MNA V9300; Parker, 2008, Fig. 9). These triangular hyposphenes of the posterior trunk vertebrae appear more similar to the structures of the anterior trunk vertebrae of *Poposaurus langstoni* and *Postosuchus kirkpatricki* than to taxa with rectangular hyposphenes.

Several other aetosaurs besides *Desmatosuchus spurensis* have been reported to have the hyposphene-hypantrum articulation including *Scutarx deltatylus* (PEFO 34045; Parker, 2016b), possibly *Longosuchus meadei* (TMM 31100-448, TMM 31100-452), and *Aetobarbakinoides brasiliensis* (CPE 2 168; Desojo et al., 2012). However, a hyposphene structure is difficult to infer on most of the vertebrae of *A. brasiliensis* (CPE 2186; Desojo et al., 2012: Fig. 5, figure 7)

because much of the holotype is articulated or broken on the neural arch. Desojo et al. (2012) described *A. brasiliensis* as having hyposphenes that are "Y-shaped" where the elongated hyposphene structure forms the "trunk" of the "Y" and the postzygapophyses connected and dorsal to it form the top two dorsolaterally projecting "branches" of the "Y" in posterior view. On our close inspection of the well-preserved and non-articulated vertebrae of *A. brasiliensis*, there does not appear to be a distinct angle change between the articular surfaces of the postzygapophyses to the bony projection ventral to and between them (figure 7). Therefore I conclude that *A. brasiliensis* does not have a hyposphene-hypantrum according to my definition. However, the aetosaur *Scutarx deltatylus* does have a hyposphene-hypantrum according to my definition. It has two different shape varieties of hyposphene structures present in its trunk vertebrae: one that is circular in posterior view and tapers to a point distally from the body of the vertebra (PEFO 34045 FF-22, Parker, 2016b: Fig. 13, figure 7) and a second that is triangular with a dorsally-oriented point extending along the dorsoventral margin of the neural arch (PEFO 34045 FF-51, Parker, 2016b: Fig. 12). *Scutarx deltatylus* also preserves hypantrum structures of complementary size and shapes on the anterior aspects of its neural arches.

The aetosaur *Longosuchus meadei* (TMM 31100-448, TMM 31100-452) may have a hyposphene-hypantrum articulation in its trunk vertebrae, but this is ambiguous because of the poor preservation of known material. The trunk vertebra of *Longosuchus meadei*, TMM 31100-448 appears to have a hyposphene that is square in posterior view; however, the postzygapophyses and surrounding portions of the neural arch are broken and compressed, making it difficult to definitively discern a hyposphene structure according to our definition (figure 7). Neither *Typothorax coccinarium* (NMMNH P-12964, Heckert et al., 2010: Fig. 4A) nor *Paratypothorax andressorum* (PEFO 3004; Lucas et al., 2006, Hunt and Lucas, 1992: Fig. 4)

was reported to have the hyposphene-hypantrum, and I concur with this through our observations of the published figures of those materials and through direct observation. The small aetosaur *Coahomasuchus kahleorum* (TMM 31100-437, Parker, 2016a) does not appear to have the hyposphene-hypantrum in its trunk vertebrae; however, the known vertebral material is mostly articulated, poorly preserved, and portions of the neural arches are broken or obscured (TMM 31100-437).

Although it is present in a few aetosaurs, the hyposphene-hypantrum articulation is not present in the sister taxon to Aetosauria, *Revueltosaurus callenderi* (PEFO 34561, figure 7). It is also not present in *Parringtonia gracilis* (NMT RB426), the sister taxon of *Revueltosaurus callenderi* (PEFO 34561) + Aetosauria (Nesbitt et al., in review). The postzygapophyses of the vertebrae of *Parringtonia gracilis* converge at the midline but they do not extend into a projection ventrally. The articular surfaces of the postzygapophyses of the few known anterior trunk vertebrae of *Revueltosaurus callenderi* that are intact and not obscured by sediment (PEFO 34561-DVf, PEFO 34561-DVh) do converge; however, they do not have a bony and dorsoventrally elongated process that could definitively be a hyposphene. The cervical vertebrae (PEFO 34561-CV) of this specimen definitively do not have the hyposphene-hypantrum articulation. Therefore, both *Revueltosaurus callenderi* and *Parringtonia gracilis* are small pseudosuchian archosaurs that lack the hyposphene-hypantrum.

Relationship of the hyposphene-hypantrum articulation with body size

The articulation structures of the hyposphene-hypantrum are widespread in the clade Pseudosuchia, but are noticeably absent in the living members of the group, Crocodylia and their more inclusive group Crocodylomorpha (i.e. *Sphenosuchus acutus,* UCMP 129740; *Deinosuchus*

riograndensis, TMM 43632-1; *Alligator mississippiensis*, TMM M-12606) (figure 8). Most early members of Crocodylomorpha are markedly smaller (i.e. shorter femoral lengths) (Turner and Nesbitt, 2013) than their Triassic relatives (figure 9), such as the poposaurids (i.e. *Poposaurus langstoni*; *Poposaurus gracilis*, Weinbaum and Hungerbühler, 2007, TTU P-10419), the rauisuchid *Postosuchus kirkpatricki* (TTU-P 9002, Weinbaum, 2013), other pseudosuchians (i.e. *Prestosuchus chiniquensis*, UFRGS-PV-0156-T, Azevedo, 1991; *Fasolasuchus tenax*, PVL 3850, Bonaparte, 1981; *Stagonosuchus nyassicus*, GPIT/RE/3831, Lautenschlager and Desojo, 2011; *Mandasuchus tanyauchen*, NHMUK PV R6792, Butler et al., 2017), and the largest aetosaur *Desmatosuchus spurensis* (MNA V9300, Parker, 2008). Because the hyposphene-hypantrum articulation is in many large bodied taxa and not in smaller ones (figure 9), I explored this potential correlation with body size by assigning each taxon I examined to either presence or absence of the hyposphene-hypantrum, and then plotted these two groups by their femoral length as a proxy for body size (Turner and Nesbitt, 2013). I found a relationship between larger body sizes and the presence of the hyposphene-hypantrum articulation, but larger body size does not always correlate perfectly with the presence of the hyposphene-hypantrum (figure 7). Some pseudosuchians with femoral lengths above the threshold where the hyposphene-hypantrum is typically present (~210-300 mm) lack the hyposphene-hypantrum. These taxa include *Effigia okeeffeae* and *Shuvosaurus inexpectatus*, which are sister taxa of one another and have femoral lengths of 301 mm and 255 mm, respectively. These body sizes are within the threshold range for presence of the hyposphene-hypantrum in pseudosuchians. Therefore, within the range (210-300 mm) the articulation may or may not be seen, but based on my observations, taxa with femoral lengths above 300 mm almost always possess it.

Another exception to the body size relationship is phytosaurs, which are either the earliest diverging pseudosuchians (Gauthier, 1986; Benton and Clark, 1988; Sereno, 1991; Benton, 1999; Ezcurra, 2016) or the sister group of Archosauria (Nesbitt, 2011). All taxa in this clade lack the hyposphene-hypantrum articulation but some have femoral lengths greater than many pseudosuchians that possess the articulation (e.g. *Smilosuchus gregorii*, 545mm; *Machaeroprosopus pristinus*, 444mm) (figure 9). The absence of the hyposphene-hypantrum in phytosaurs may be related to their inferred semi-aquatic ecology, (Parrish, 1986), which differs from the fully terrestrial pseudosuchians. This could mean that femoral length cannot explain the presence or absence of the hyposphene-hypantrum in aquatic forms.

In summary, our observations of pseudosuchian archosaurs both with and without the hyposphene-hypantrum articulation showed a relationship between larger body sizes (osteological correlate = greater femoral lengths) and the presence of the hyposphene-hypantrum articulation in trunk vertebrae. Because of this close fit, this character may be controlled by body size and not by phylogenetic inheritance. If so, the character of hyposphene-hypantrum presence or absence would have limited use in matrixes for determining relationships between archosaurian taxa although many phylogenetic analyses have used it (Gauthier, 1986; Nesbitt, 2011). The relationship between body size and the hyposphene-hypantrum articulation should be investigated further in Archosuaria, including on the avemetatarsalian line to determine if this trend holds true across the clade.

5. Acknowledgements

I thank the University of Texas at Austin and the Vertebrae Paleontology Laboratory for the loan of *Poposaurus langstoni*, and K. Bader for preparing the *Poposaurus langstoni* material

described here. I thank the Virginia Tech Paleobiology and Geobiology Research Group (M. Stocker, C. Griffin, C. Colleary, K. Formoso, K. Koeller, M. Riegler) and J. Socha for discussion. The Department of Geosciences' Eula and Aubrey Orange Award allowed CMS to travel to museum collections. I thank W. Parker for access to Petrified Forest National Park's collection and for personal discussion, The University of California Museum of Paleontology Doris O. and Samuel P. Welles Research Fund, and K. Padian for access to their collection and for personal discussion, C. Mehling at the American Museum of Natural History for access and assistance in the FARB collection, A. Henrici at the Carnegie Museum for access and assistance in the vertebrate paleontology collection, and J. Desojo for photographs of aetosaur specimens.

6. References

Alcober, O. A., Parrish, J. M. 1997 A new poposaurid from the Upper Triassic of Argentina. *Journal of Vertebrate Paleontology*. **17**, 548-556.

Apesteguia, S. 2005 Evolution of the hyposphene-hypantrum complex within Sauropoda. In *Thunder-Lizards: The Sauropodomorph Dinosaurs*. (eds. pp. 248-267: Indiana University Press.

Azevedo, S. A. K. 1991 *Prestosuchus chiniquensis* Huene 1942 (Reptilia, Archosauria, Rauisuchidae), da Formacao Santa Maria, Triassico do Estado do Rio Grande do Sul, Brasil. *Univeridade Federal Do Rio Grande Do Sul Curso De Pos-Graduacao Em Geociencias*. Bandyopadhyay, S., Gillette, D. D., Ray, S., Sengupta, D. P. 2010 Osteology of *Barapasaurus tagorei* (Dinosauria: Sauropoda) from the Early Jurassic of India. *Palaeontology*. **53**, 533-569. Benson, R. B. J. 2010 A description of *Megalosaurus*

bucklandii (Dinosauria: Theropoda) from the Bathonian of the UK and the relationships of Middle Jurassic theropods. *Zoological Journal of the Linnean Society*. **158**, 882-935.

Bonaparte, J. F. 1981 Descripcion de *Fasolasuchus tenax* y su significado en la sistematica y evolucion de los thecodontia. *Paleontologia*. **111**, 55-101.

Brochu, C. 1996 Closure of neurocentral sutures during crocodilian ontogeny: Implications for maturity assessment in fossil archosaurs. *Journal of Vertebrate Paleontology*. **16**, 49-62.

Brusatte, S. L., Benson, R. B. J. 2008 The systematics of Late Jurassic tyrannosauroid theropods from Europe and North America. *Acta Palaeontologica Polonica*. **58**, 47-54.

Butler, R. J., Nesbitt, S. J., Charig, A. J., Gower, D. J., Barrett, P. M. 2017 *Mandasuchus tanyauchen* gen. et sp. nov., a pseudosuchian archosaur from the Manda Beds of Tanzania. In *Vertebrate and climatic evolution in the Triassic rift basins of Tanzania and Zambia*. (eds. C. A. Sidor, S. J. Nesbitt), Society of Vertebrate Paleontology Memoir 17: Journal of Vertebrate Paleontology.

Desojo, J. B., Ezcurra, M. D., Kischlat, E. E. 2012 A new aetosaur genus (Archosauria: Pseudosuchia) from the early Late Triassic of southern Brazil. *Zootaxa*. **3166**, 1-33.

Gauthier, J. A. 1986 Saurischian monophyly and the origin of birds. *Memoirs of the California Academy of Sciences*. **8**, 1-55.

Gauthier, J. A., Padian, K. 1985 Phylogenetic, funtional, and aerodynamic analyses of the origin of birds and their flight. In *The beginning of birds*. (eds. pp. 185-197

Gebauer, E. V. I. 2004 Neubeschreibung von *Stagonosuchus nyassicus* V. HUENE, 1938 (Thecodontia, Rauisuchia) aus der Manda-Formation (Mittlere Trias) von Südwest-Tansania. [Redescription of *Stagonosuchus nyassicus* V. HUENE, 1938 (Thecodontia, Rauisuchia) from the Manda Formation (Middle Triassic) of Southwest Tanzania]. *Neues Jahrbuch fur Geologie und Palaontologie-Abhandlungen* **213**, 1-35.

Gower, D. J., Schoch, R. R. 2009 Postcranial anatomy of the rauisuchian archosaur *Batrachotomus kupferzellensis*. *Journal of Vertebrate Paleontology*. **29**, 103-122.

Heckert, A. B., Lucas, S. G., Rinehart, L. F., Celeskey, M. D., Spielmann, J. A., Hunt, A. P. 2010 Articulated skeletons of the aetosaur *Typothorax coccinarum* Cope (Archosauria: Stagonolepididae) from the Upper Triassic Bull Canyon Formation (Revueltian: Early-Mid Norian), eastern New Mexico, USA. *Journal of Vertebrate Paleontology*. **30**, 619-642.

Huber, M. 2010 *Compendium of Bivalves: A Full-color Guide to 3,300 of the World's Marine Bivalves. A Status on Bivalvia after 250 Years of Research.*: ConchBooks.

Hunt, A. P., Lucas, S. G. 1992 The first occurence of the aetosaur *Paratypothorax andressi* (Reptilia, Aetosauria) in the western United States and its biochronological significance. *Palaontologische Zeitschrift*. **66**, 147-157.

Krebs, B. 1965 Die Triasfauna der Tessiner Kalkalpen. XIX. *Ticinosuchus ferox*, nov. gen. nov. sp. Ein neuer Pseudosuchier aus der Trias des Monte San Georgio. *Schweizersiche Palaontologische, Abhandlungen*. **81**, 1-140.

Langer, M. C., Benton, M. J. 2006 Early dinosaurs: A phylogenetic study. *Journal of Systematic Paleontology*. **4**, 309-358.

Langer, M. C., Ezcurra, M. D., Bittencourt, J. S. 2010 The origin and early evolution of dinosaurs. *Biological Reviews*. **85**, 55-110.

Lautenschlager, S., Desojo, J. B. 2011 Reassessment of the Middle Triassic rauisuchian archosaurs *Ticinosuchus ferox* and *Stagnosuchus nyassicus*. *Palaontologische Zeitschrift*. **85**, 357-381.

Long, R. A., Murry, P. A. 1995 Late Triassic (Carnian and Norian) tetrapods from the southwestern United States. *Bulletin of the New Mexico Museum of Natural History and Science*. **4**, 1-254.

Lucas, S. G., Heckert, A. B., Rinehart, L. F. 2006 The Late Triassic aetosaur *Paratypothorax*. *New Mexico Museum of Natural History and Science Bulletin*. **37**, 575-580.

Makovicky, P. J., Norell, M. A. 2004 Troodontidae. In *The Dinosauria, second ed.* (eds. D. B. Weishampel, P. Dodson, O. Halszka), pp. 184-195. University of Calfornia Press, Berkeley

Mazetta, G. V., Christiansen, P., Farina, R. A. 2004 Giants and bizarres: Body size of some southern South American Cretaceous dinosaurs. *Historical Biology*. 1-13.

Nesbitt, S. J. 2005 Osteology of the Middle Triassic pseudosuchian archosaur *Arizonasaurus babbitti*. *Historical Biology*. **17**, 19-47.

Nesbitt, S. J. 2007 The anatomy of *Effigia okeeffeae* (Archosauria: Suchia), theropod-like convergence, and the distribution of related taxa. *Bulletin of the American Museum of Natural History*. **302**, 1-84.

Nesbitt, S. J. 2011 The early evolution of archosaurs: Relationships and the origin of major clades. *Bulletin of the American Museum of Natural History*. **352**, 1-292.

Nesbitt, S. J., Barrett, P. M., Werning, S., Sidor, C. A., Charig, A. J. 2013 The oldest dinosaur? A Middle Triassic dinosauriform from Tanzania. *Biology Letters*. **9**, 1-5.

Nesbitt, S. J., Desojo, J. B., Irmis, R. B. 2013 Anatomy, phylogeny and palaeobiology of early archosaurs and their kin. *Geological Society, London, Special Publications*. **379**, 1-7.

Nesbitt, S. J., Flynn, J. J., Pritchard, A. C., Parrish, J. M., Ranivoharimanana, L., Wyss, A. R. 2015 Postcranial osteology of *Azendohsaurus madagaskarensis* (?Middle to Upper Triassic,

Isalo Group, Madagascar) and its systematic position among stem archosaur reptiles. *Bulletin of the American Museum of Natural History*. **398**, 1-126.

Nesbitt, S. J., Liu, J., Li, C. 2010 A sail-backed suchian from the Heshanggou Formation (Early Triassic: Olenekian) of China. *Earth and Environmental Science Transactions of the Royal Society of Edinburgh*. **101**, 271-284.

Nesbitt, S. J., Norell, M. A. 2006 Extreme convergence in the body plans of an early suchian (Archosauria) and ornithomimid dinosaurs (Theropoda). *Proceedings of the Royal Society B*. **273**, 1045-1048.

Nesbitt, S. J., Sidor, C. A., Angielczyk, K. D., Smith, R. M. H., Tsuji, L. A. 2014 A new archosaur from the Manda Beds (Anisian, Middle Triassic) of southern Tanzania and its implications for character state optimizations at Archosauria and Pseudosuchia. *Journal of Vertebrate Paleontology*. **34**, 1357-1382.

Nesbitt, S. J., Sidor, C. A., Irmis, R. B., Angielczyk, K. D., Smith, R. M. H., Tsuji, L. A. 2010 Ecologically distinct dinosaurian sister group shows early diversification of Ornithodira. *Nature*. **464**, 95-98.

Nopsca, F. v. 1923 Die Familien der Reptilien. *Fortschritte der Geologie und Palaontologie*. **2**, 1-210.

Novas, F. E. 1996 Dinosaur monophyly. *Journal of Vertebrate Paleontology*. **16**, 723-741.

Parker, W. G. 2008 Description of new material of the aetosaur *Desmatosuchus spurensis* (Archosauria: Suchia) from the Chinle Formation of Arizona and a revision of the genus *Desmatosuchus*. *PaleoBios*. **28**, 1-40.

Parker, W. G. 2016 Revised phylogenetic analysis the Aetosauria (Archosauria: Pseudouchia); assessing the effects of incongruent morphological character sets. *PeerJ*. (4:e1583; DOI 10.7717/peerj.1583)

Parker, W. G. 2016 Osteology of the Late Triassic aetosaur *Scutarx deltatylus* (Archosauria: Pseudosuchia). *PeerJ*. **4**, e2411. (10.7717/peerj.2411)

Peyer, K., Carter, J. G., Sues, H.-D., Novak, S. E., Olsen, P. E. 2008 A new suchian archosaur from the Upper Triassic of North Carolina. *Journal of Vertebrate Paleontology*. **28**, 363-381.

Pol, D., Garrido, A., Cerda, I. A. 2011 A new sauropodomorph dinosaur from the Early Jurassic of Patagonia and the origin and evolution of the sauropod-type sacrum. *PLoS ONE*. **6**, (10.1371/journal.pone.0014572)

Rauhut, O. W. M. 2003 The interrelationships and evolution of basal theropod dinosaurs. *Special Papers in Palaeontology*. **69**, 1-213.

Romer, A. S. 1956 *Osteology of the Reptiles*. Chicago: University of Chicago Press.

Stocker, M. R., Butler, R. J. 2013 Phytosauria. *Geological Society, London, Special Publications*. **379**, 91-117.

Trotteyn, M. J., Desojo, J. B., Alcober, O. A. 2011 Nuevo material postcraneano de *Saurosuchus galilei* reig (Archosauria: Crurotarsi) del Triásico Superior del Centro-Oeste de Argentina. *Ameghiniana*. **48**, 13-27.

Turner, A. H., Nesbitt, S. J. 2013 Body size evolution during the Triassic archosauriform radiation. *Geological Society, London, Special Publications*. **379**, 573-597.

Weinbaum, J. C. 2013 Postcranial skeleton of *Postosuchus kirkpatricki* (Archosauria: Paracrocodylomorpha), from the Upper Triassic of the United States. *Geological Society, London, Special Publications*. **379**, 525-553.

Weinbaum, J. C., Hungerbühler, A. 2007 A revision of *Poposaurus gracilis* (Archosauria: Suchia) based on two new specimens from the Late Triassic of the southwestern U.S.A. *Palaontologische Zeitschrift*. **81**, 131-145.

Williston, S. W. 1851-1918 *Williston's osteology of the reptiles*. Society for the Study of Amphibians and Reptiles.

Wilson, J. A. 1999 A nomenclature for vertebral laminae in sauropods and other saurischian dinosaurs. *Journal of Vertebrate Paleontology*. **19**, 639-653.

Wilson, J. A., D'Emic, M. D., Ikejiri, T., Moacdieh, E. M., Whitlock, J. A. 2011 A nomenclature for vertebral fossae in sauropods and other saurischian dinosaurs. *PLoS ONE*. **6**, (10.1371/journal.pone.0017114)

Wilson, J. P., Woodruff, D. C., Gardner, J. D., Flora, H. M., Horner, J. R., Organ, C. L. 2016 Vertebral adaptations to large body size in theropod dinosaurs. *PLoS ONE*. **11**, 1-15.

Zittel, K. A. v. 1887-1890 *Handbuch der Palaeontologie*. Munchen and Leipzig.

7. FIGURES

Figure 1. The reconstructed vertebral columns of both individuals of *Poposaurus langstoni* from the holotype locality TMM 31025, *(a)* individual ‘A’ and *(b)* individual ‘B’. Grey portions represent missing material. Numbers refer to presacral position within the vertebral column. Arrow indicates anterior direction.

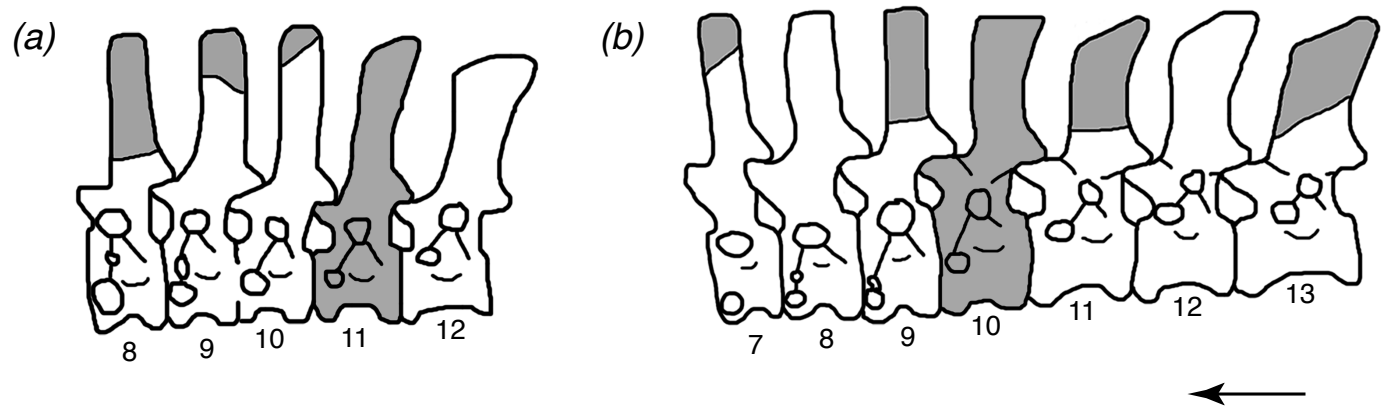
(a)
8
9
10
11
12
(b)
7
8
9
10
11
12
13

Figure 2. Cervical vertebrae of *Poposaurus langstoni* in anterior (left) and posterior (right) views. *(a)* TMM 31025-1261.5, presacral 7; *(b)* TMM 31025-1262, presacral 8; *(c)* TMM 31025-1261.3, presacral 9; *(d)* TMM 31025-177, presacral 8. **Abbreviations: ara**, accessory rib articulation; **bs**, bivalve shell; **c**, centrum; **dp**, diapophysis; **nc**, neural canal; **ns**, neural spine; **poz**, postzygapophysis; **pp**, parapophysis; **prz**, prezygapophysis. Scales = 5 cm.

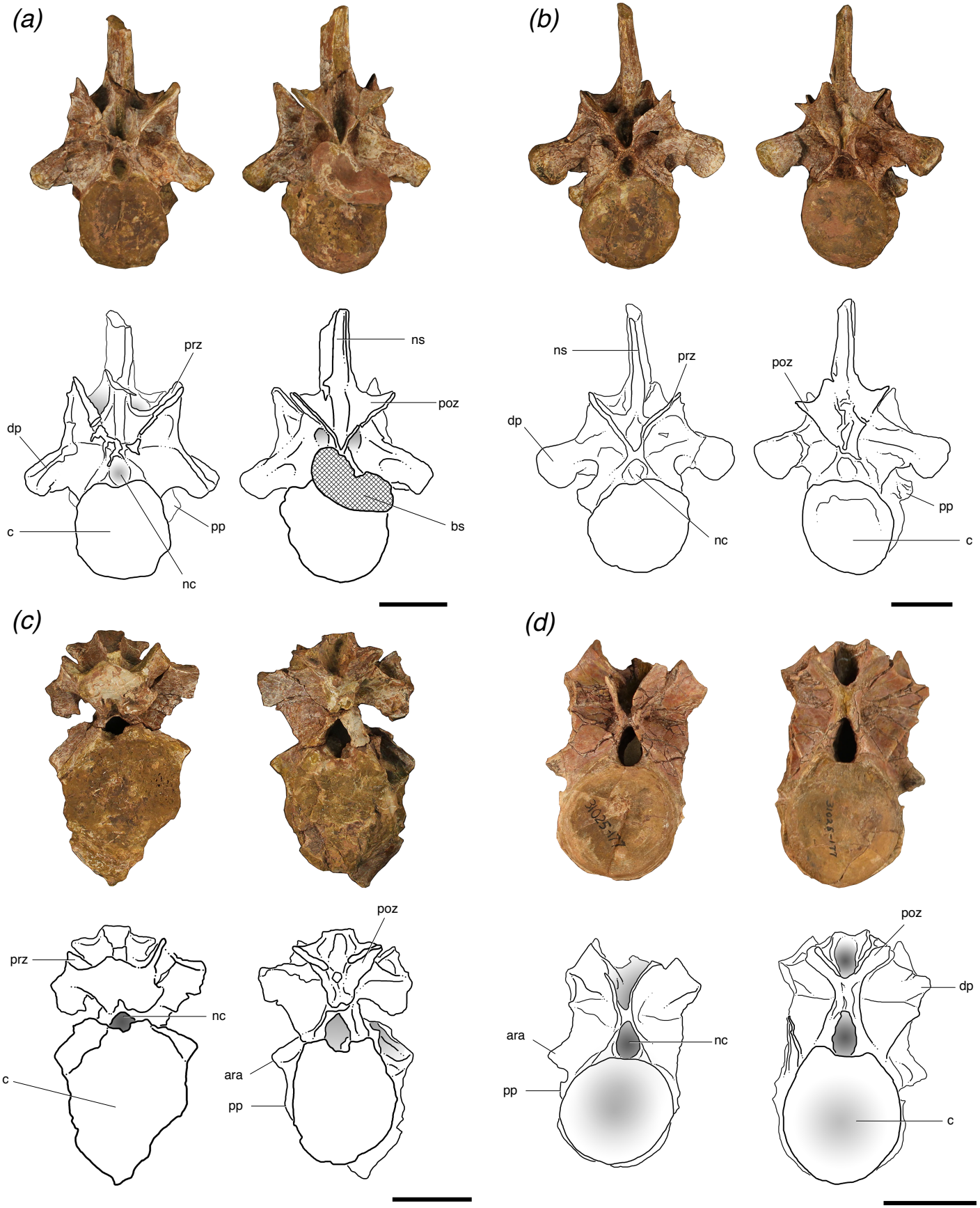
(a)
prz
dp
pp
c
nc
ns
poz
bs
(b)
ns
prz
dp
nc
poz
pp
c
(c)
prz
nc
c
poz
ara
pp
(d)
ara
nc
pp
poz
dp
c

Figure 3. Trunk vertebrae of *Poposaurus langstoni* in anterior (left) and posterior (right) views. *(a)* TMM 31025-1261.4, presacral 11; *(b)* TMM 31025-1261.1, presacral 12; *(c)* TMM 31025-1261.2, presacral 13; *(d)* TMM 31025-257, presacral 12. **Abbreviations: c**, centrum; **dp**, diapophysis; **ha**, hypantrum; **ho**, hyposphene; **nc**, neural canal; **ns**, neural spine; **poz**, postzygapophysis; **pp**, parapophysis; **prz**, prezygapophysis. Scales = 5 cm.

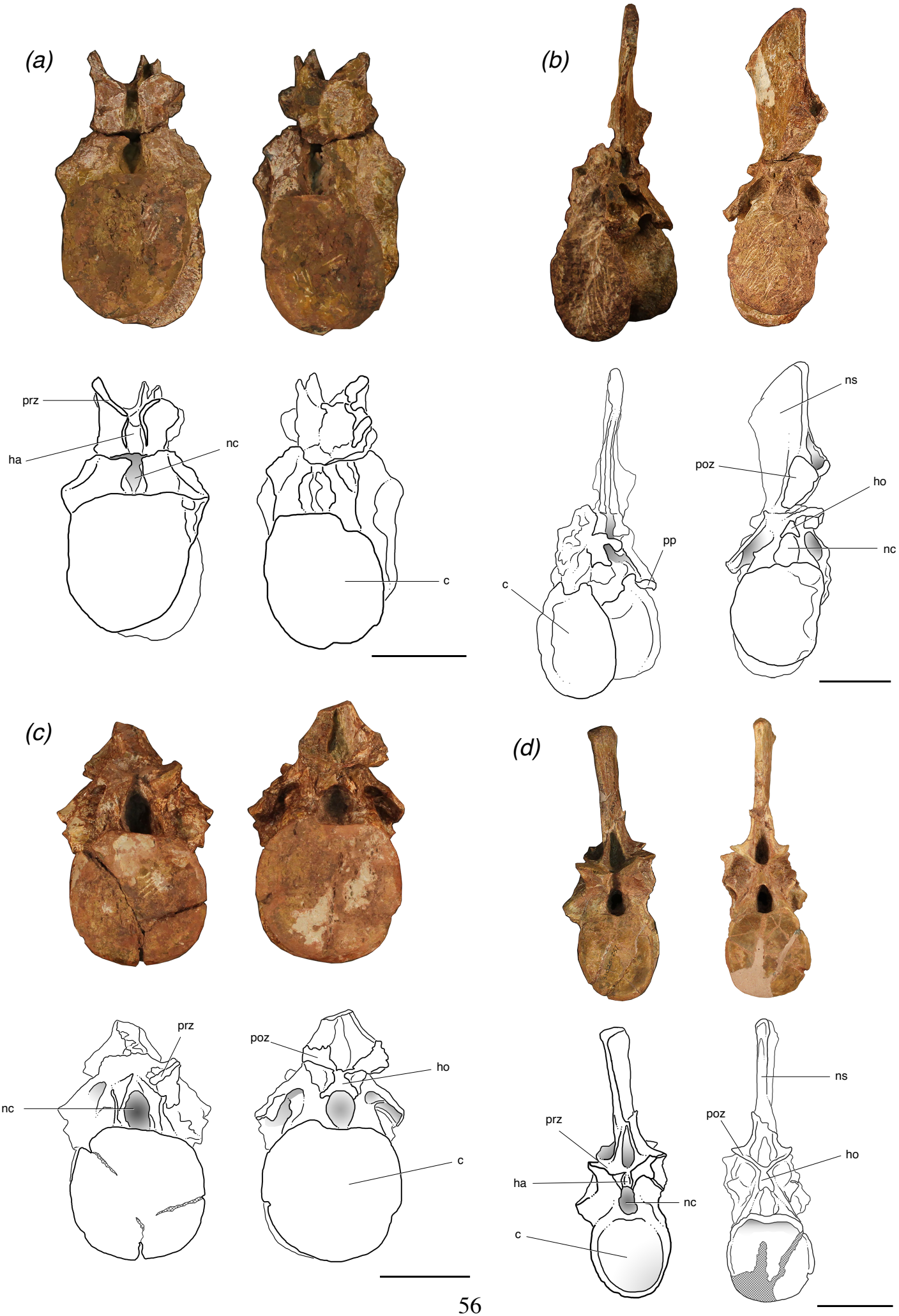
(a)
(b)
(c)
(d)
prz
ha
nc
c
pp
ns
poz
ho
nc
c
prz
nc
poz
ho
c
prz
ha
nc
c
ns
poz
ho

Figure 4. Lateral views of *(a)* one posterior cervical (TMM 31025-1262, presacral 8) and *(b)* one trunk (TMM 31025-257, presacral 12) from individuals 'B' and 'A', respectively, of *Poposaurus langstoni*. **Abbreviations: acpl**, anterior centroparapophyseal lamina; **ara**, accessory rib articulation; **ep**, epipophysis; **dp**, diapophysis; **lf**, lateral fossa; **pcdl**, posterior centrodiapophyseal lamina; **poz**, postzygapophyses; **pp**, parapophysis; **ppdl**, paradiapophyseal lamina; **prdl**, prezygodiapophyseal lamina; **prz**, prezygapophysis. Scales = 5 cm.

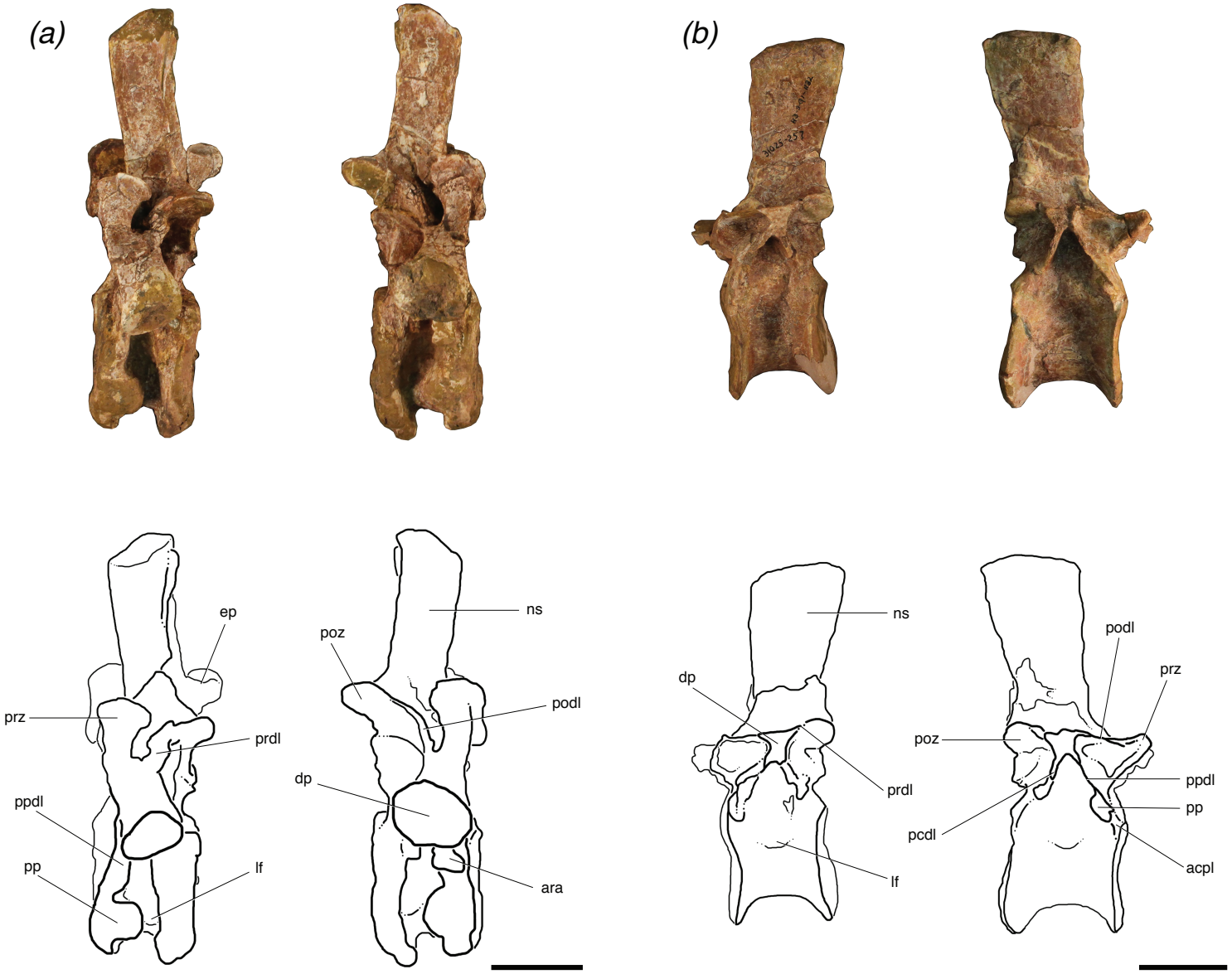
(a)
(b)
ep
prz
prdl
ppdl
pp
lf
ns
poz
podl
dp
ara
ns
dp
prdl
lf
podl
prz
poz
ppdl
pp
pcdl
acpl

Figure 5. Presacral rib of *Poposaurus langstoni* (TMM 31025-2160) in *(a)(b)* lateral views, *(c)* proximal view, and *(d)* dorsal view. **Abbreviations: arf**, accessory rib facet; **cp**, capitulum; **r**, ridge; **tb**, tuberculum. Scales = 5 cm.

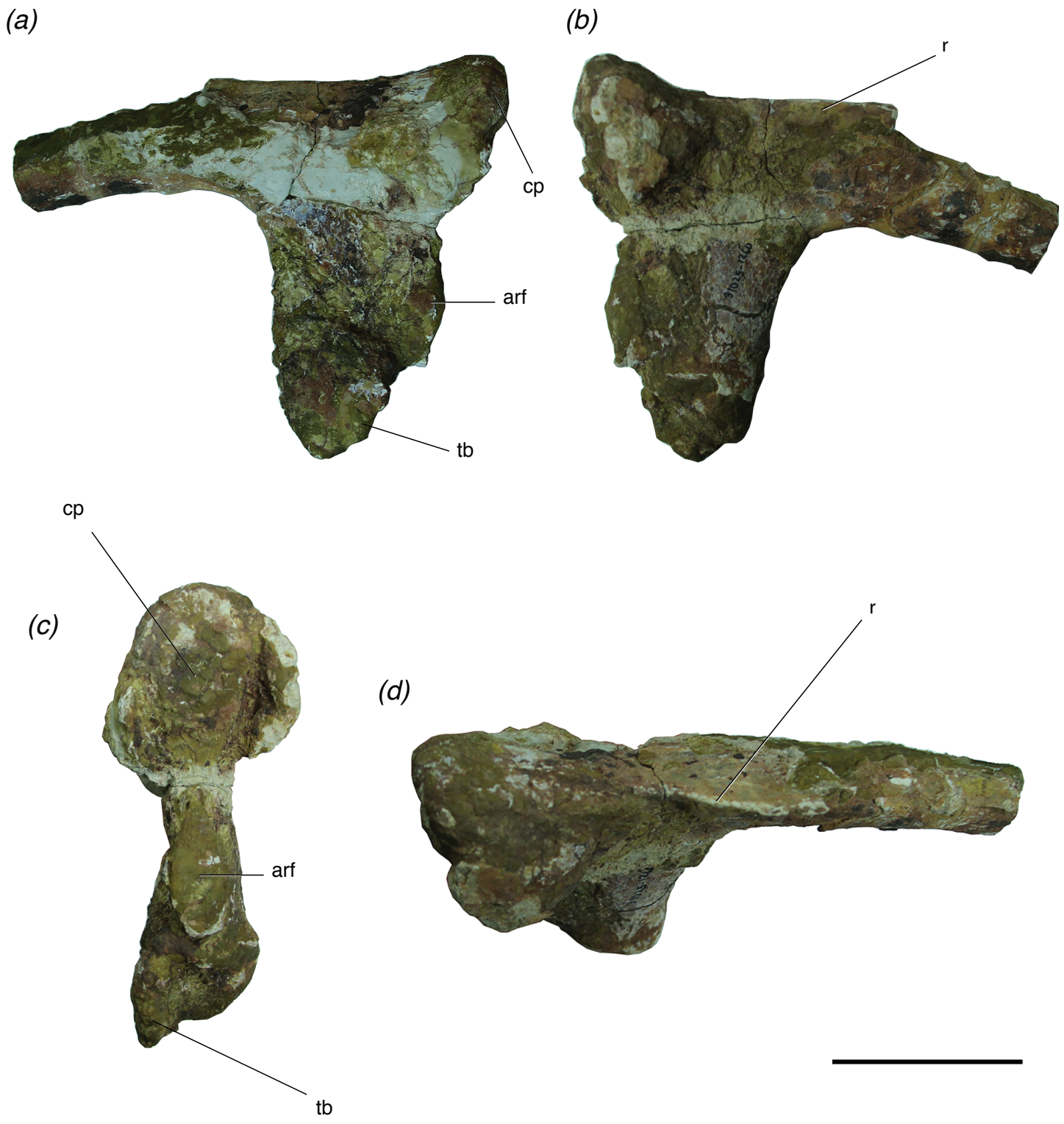
(a)
cp
arf
tb
(b)
r
(c)
cp
arf
tb
(d)
r

Figure 6. The distribution of the hyposphene-hypantrum articulation in Pseudosuchia and close relatives. Relationships from Nesbitt et al. (2011) and Nesbitt et al. (2014). Hyposphene-hypantrum present = orange; Hyposphene-hypantrum absent = blue.

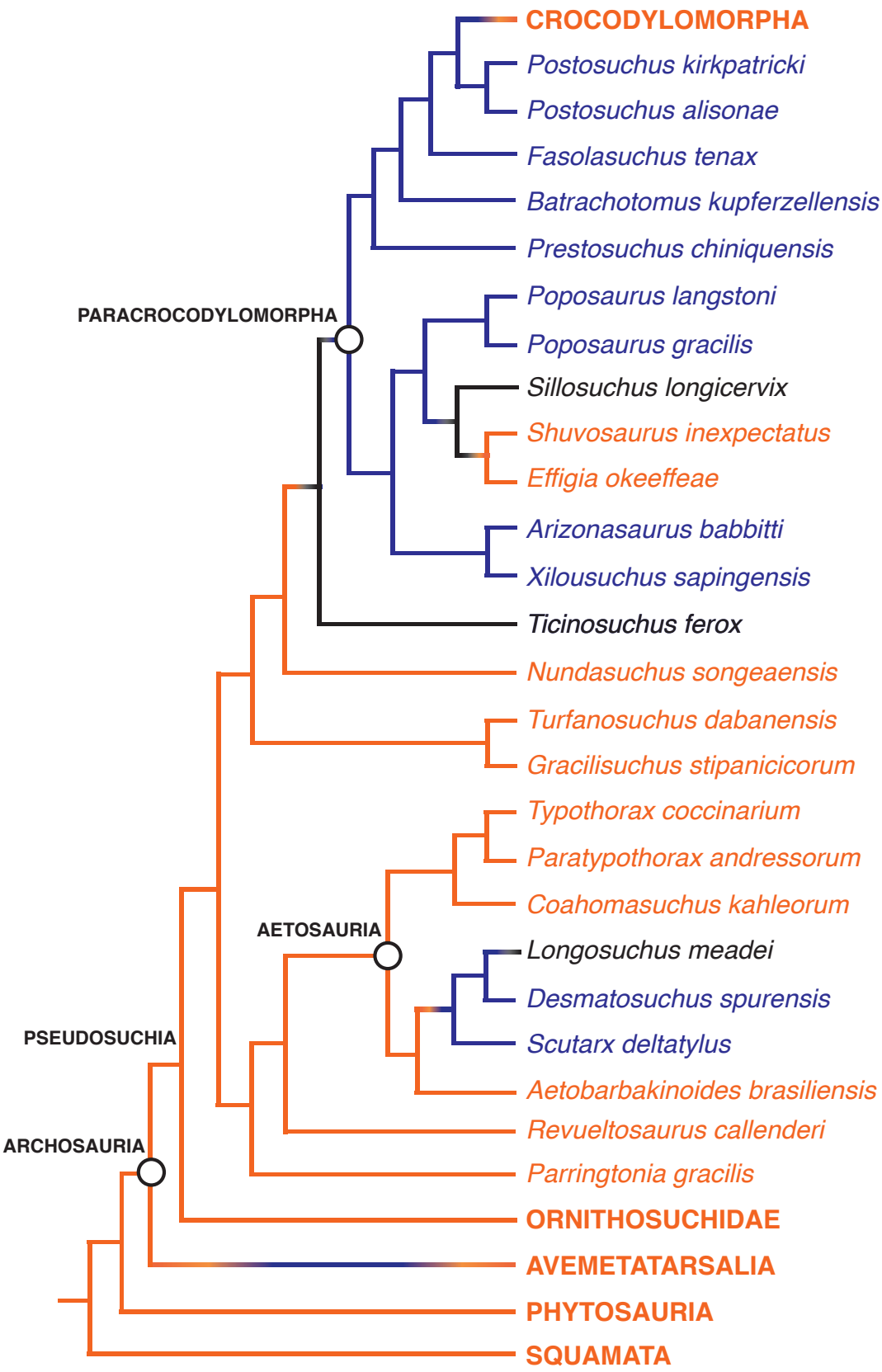
CROCODYLOMORPHA
Postosuchus kirkpatricki
Postosuchus alisonae
Fasolasuchus tenax
Batrachotomus kupferzellensis
Prestosuchus chiniquensis
PARACROCODYLOMORPHA
Poposaurus langstoni
Poposaurus gracilis
Sillosuchus longicervix
Shuvosaurus inexpectatus
Effigia okeeffeae
Arizonasaurus babbitti
Xilousuchus sapingensis
Ticinosuchus ferox
Nundasuchus songeaensis
Turfanosuchus dabanensis
Gracilisuchus stipanicicorum
Typothorax coccinarium
Paratypothorax andressorum
Coahomasuchus kahleorum
AETOSAURIA
Longosuchus meadei
Desmatosuchus spurensis
PSEUDOSUCHIA
Scutarx deltatylus
Aetobarbakinoides brasiliensis
Revueltosaurus callenderi
ARCHOSAURIA
Parringtonia gracilis
ORNITHOSUCHIDAE
AVEMETATARSALIA
PHYTOSAURIA
SQUAMATA

Figure 7. Plot showing femoral length (from Turner and Nesbitt, 2013) versus hyposphene-hypantrum presence or absence with pseudosuchian archosaurs as data points. Black data points represent an ambiguous taxon (*Sillosuchus longicervix*) regarding presence or absence of the hyposphene-hypantrum because of preservation of the single known specimen and two phytosaurs (*Machaeroprosopus*, *Smilosuchus*) due to their large size, absence of the hyposphene-hypantrum, and phylogenetic position as the sister lineage to Archosauria.

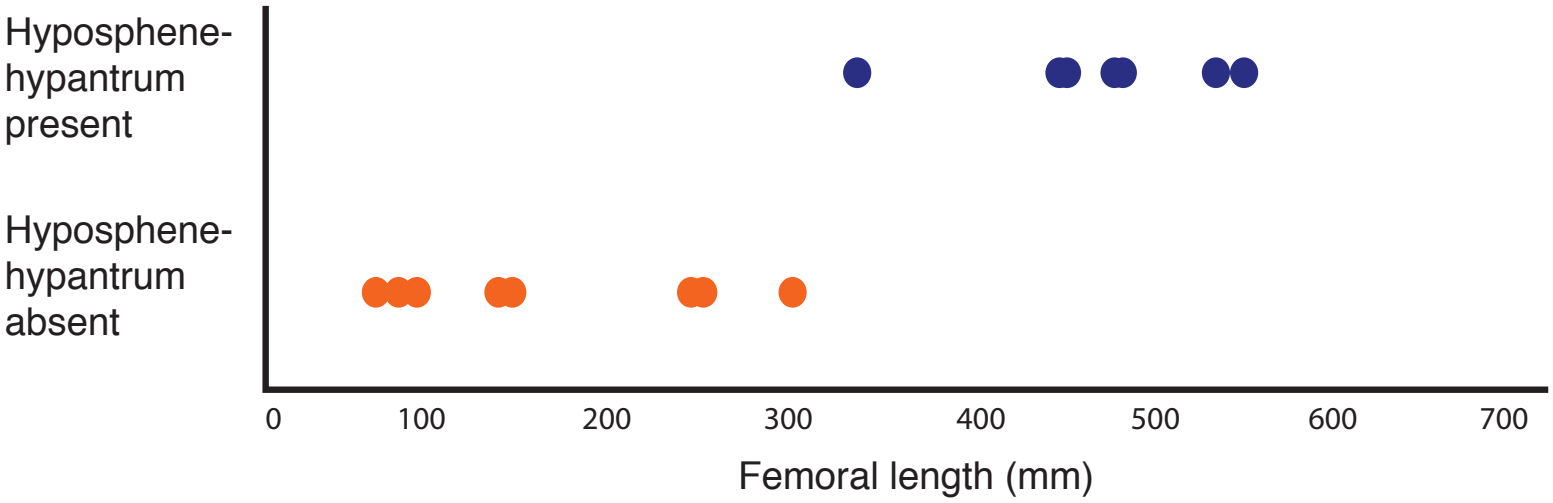
Hyposphene-
hypantrum
present
Hyposphene-
hypantrum
absent
0
100
200
300
400
500
600
700
Femoral length (mm)

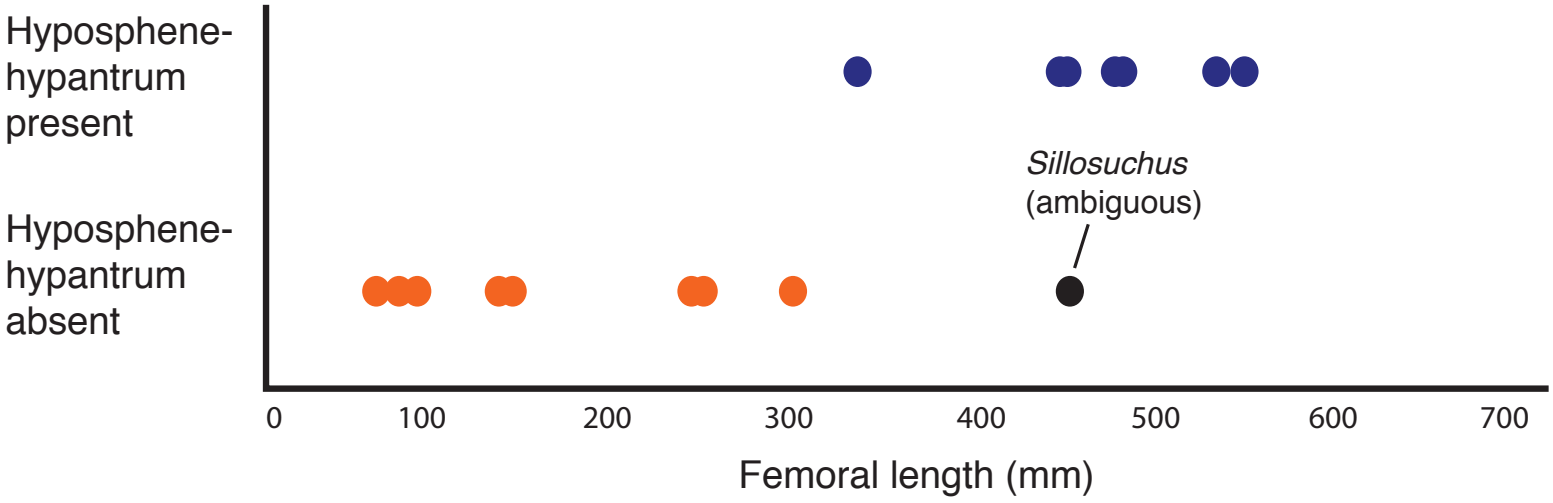
Hyposphene-
hypantrum
present
Hyposphene-
hypantrum
absent
Sillosuchus
(ambiguous)
0
100
200
300
400
500
600
700
Femoral length (mm)

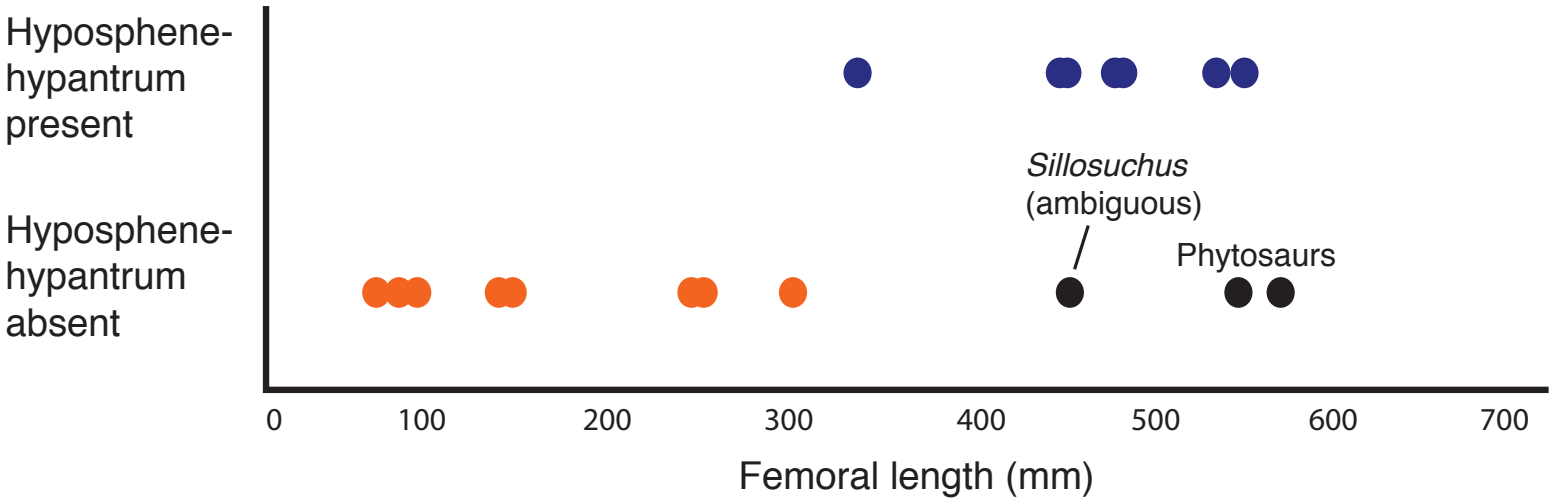
Hyposphene-
hypantrum
present
Hyposphene-
hypantrum
absent
Sillosuchus
(ambiguous)
Phytosaurs
0
100
200
300
400
500
600
700
Femoral length (mm)

Figure 8. Schematic of two idealized archosaur vertebrae both with *(a)(b)* modeled on *Poposaurus langstoni,* TMM 31025-257, and without *(c)(d)* modeled on an unnamed phytosaur trunk vertebra*,* PEFO 26695 the hyposphene-hypantrum articulation in anterior *(a)(c)* and posterior *(b)(d)*) views.

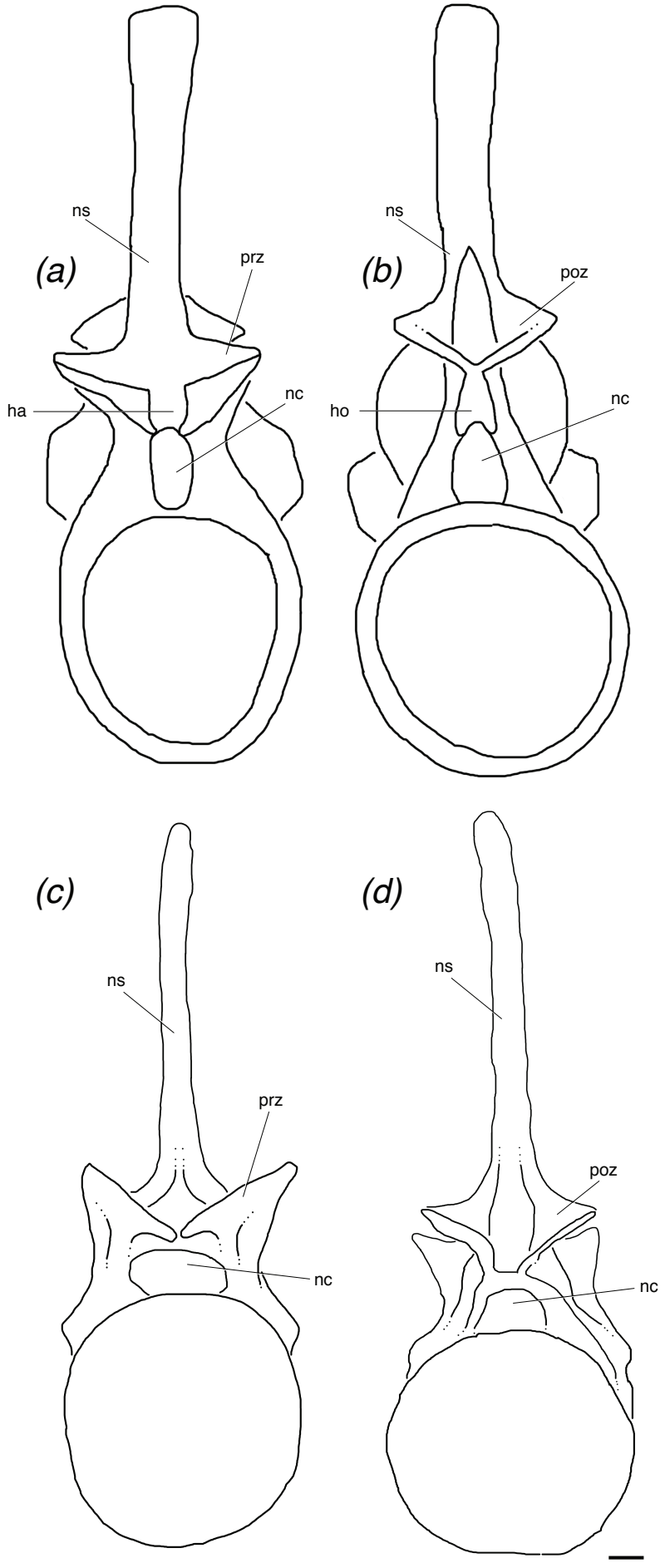
(a)
ns
prz
ha
nc
(b)
ns
poz
ho
nc
(c)
ns
prz
nc
(d)
ns
poz
nc

Figure 9. Trunk vertebrae of pseudosuchian archosaurs and closely related taxa in posterior view, showing examples of vertebrae with a hyposphene *(a) Postosuchus alisonae*, UNC 15575; *(b) Fasolasuchus tenax*, PVL 3850; *(c) Batrachotomus kupferzellensis*, SMNS 80296; *(d) Desmatosuchus spurensis*, MNA V9300; *(e) Scutarx deltatylus*, PEFO 31217; *(f) Aetobarbakinoides brasiliensis*, CPE2 168; *(g) Longosuchus meadei*,TMM 31100-148; *(h) Stagonosuchus nyassicus*, GPIT/RE/3832 and without a hyposphene *(i) Deinosuchus riograndensis*, TMM 43632-1; *(j) Erythrosuchus africanus*; *(k) Revueltosaurus callenderi*, PEFO 34561. Scales = 1 cm

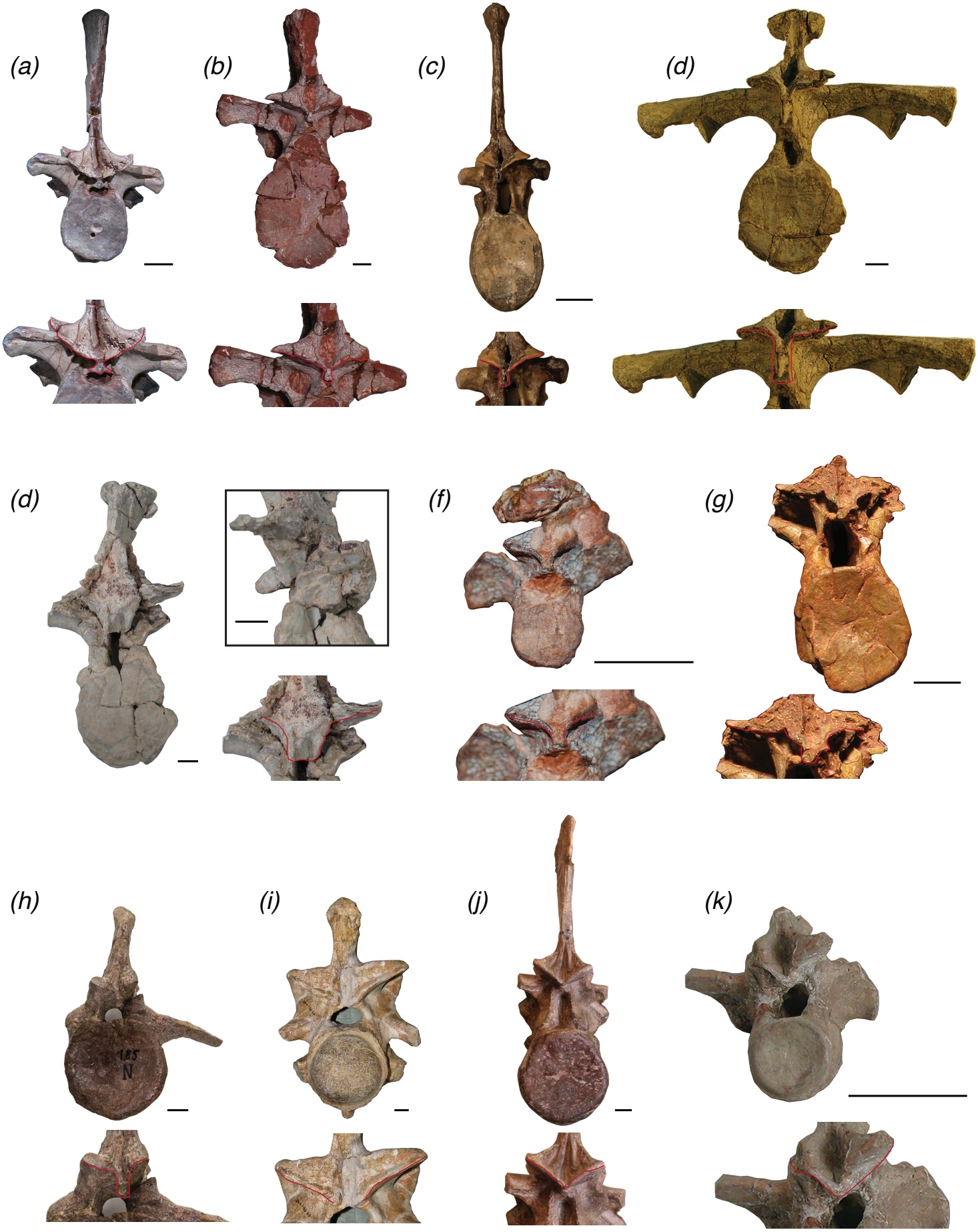
(a)
(b)
(c)
(d)
(d)
(f)
(g)
(h)
(i)
(j)
(k)

8. TABLES

Table 1. Height and width of each of the hyposphenes preserved in this material

		Hyposphene dimensions		
Specimen #	**Individual**	**Height (mm)**	**Width (mm)**	**Height: Width**
TMM 31025-257	A	11	7	1.571
TMM 31025-1261.1	B	10	12	0.833
TMM 31025-1261.2	B	10	11	0.909

Chapter 2

THE EVOLUTION OF THE HYPOSPHENE-HYPANTRUM ARTICULATION IN ARCHOSAURIA AND ITS ROLE IN THE EVOLUTION OF LARGE BODY SIZE

Candice M. Stefanic, Department of Geosciences, Virginia Polytechnic and State University, cms292@vt.edu

1. Abstract

Crocodiles and birds are each other's closest living relatives and both groups exhibit skeletal morphologies and ecologies that are markedly disparate from one another. They are the living members of the reptile clade Archosauria and have a huge range of body sizes, but moreover, the fossil record shows that many extinct members of this clade reached body sizes greater than any other terrestrial vertebrate (e.g. 70 ton titanosaurs, 20 ton theropods) to ever live. Although the major body size transitions in archosaurs are well documented, osteological changes associated with growth to enormous sizes remain less studied. I hypothesize that modification of the intervertebral articulations in extinct archosaurs (e.g. non-avian dinosaurs, pseudosuchians), specifically the addition of the hyposphene-hypantrum articulation, allowed for larger bodies in those lineages. I surveyed the phylogenetic distribution of the hyposphene-hypantrum and measured the articulation surfaces between vertebrae of extinct and extant archosaur taxa to test the relationship between intervertebral articulation and the evolution of large body size. These data demonstrate a relationship between large body size (osteological correlate = femoral length) and presence of the hyposphene-hypantrum. I interpret that this structure facilitated the evolution of large body sizes in extinct archosaurs because it increased complexity of intervertebral articulation. Because of this morphological change in their vertebrae, dinosaurs and pseudosuchians could link together consecutive vertebrae without increasing the mass of their zygapophyses in proportion to their overall vertebra size. The hyposphene-hypantrum evolved convergently in several extinct archosaurian lineages (e.g., paracrocodylomorphs, aetosaurs, saurischian dinosaurs) appearing in the evolution of those groups as taxa reach bigger sizes. Additionally, it is lost in the crown groups (i.e., crocodylians and birds) as they undergo

miniaturization toward much smaller body sizes and occupy ecological morphospace that is widely disparate from each other and their extinct relatives (e.g. semi-aquatic, volant).

2. Introduction

Living vertebrates display a wide array of body sizes from miniscule amphibians to enormous elephants, but the fossil record shows that the disparity of body sizes in terrestrial vertebrates has been much greater, with some animals reaching over 70 tons in estimated body mass (e.g. non-avian dinosaurs) (Mazzetta et al., 2004). Recently, many studies have focused on reconstructing the evolution of body size (Farnia et al., 1998; Carrano, 2006; Turner et al., 2007; Smith et al., 2010; Sookias et al., 2012; O'Gorman and Hone, 2012; Turner and Nesbitt, 2013) and larger trends of body size evolution through time. However, few, if any, studies have focused on skeletal features associated with body size changes during major changes in body size across lineages. The skeletal structures of vertebrates clearly change with increases or decreases in body size, but it has been challenging pin pointing which skeletal morphology modifications correlate with body size changes. With size increases in some dinosaurs, there are substantial changes in limbs through columniation (Bonnan, 2003), joint articulations (Holliday et al., 2010), vertebral morphology (Wilson et al., 2016), and growth rates (Erickson et al., 2009). Out of these skeletal changes, the evolution of vertebrae and body size has been increasingly of interest in recent studies, with correlates with large body size hypothesized to be increased pneumatization (Wedel, 2003), the addition of neural spine projections (Wilson et al., 2016), and complex neurocentral sutures (Fronimos and Wilson, 2017). The evolution of the how vertebrae are constructed and interlock with each other has been immensely important to the evolutionary history of vertebrate life. During the transition from aquatic environments to the terrestrial realm,

vertebrates shifted from simple non-tetrapodomorph osteichthyian vertebrae that only articulate via their centrum facets (Shaeffer, 1967), to more complex vertebrae with interlocking articulation structures (e.g. pre- and postzygapophyses) (Coates, 1996; Danto et al., 2016) and elongate transverse processes (Carrier, 1987).

To address the relationship between body size and intervertebral articulation structures, I studied taxa of the reptilian clade Archosauria, which includes crocodiles, birds and their extinct relatives, because many of the extinct taxa reached body sizes greater than any other terrestrial vertebrate (e.g. 70 ton titanosaurs, 20 ton theropods) (Mazzetta et al., 2004). Although it is difficult to attribute skeletal morphologies to body size evolution, studies of dinosaur vertebral morphology have presented metaplastic projections on neural spines (Wilson et al., 2016) and complex neurocentral sutures (Fronimos and Wilson, 2017) as potential osteological correlates with large body size.

Although not in living taxa, many extinct members of Archosauria had an accessory intervertebral articulation, the hyposphene-hypantrum articulation, ventral to the zygapophyses on the neural arch (Rauhut, 2003; Apesteguia, 2005; Stefanic, Chapter 1). I hypothesize that the presence of the hyposphene-hypantrum articulation between vertebrae in archosaurs is associated with large body sizes. To test this question, I examined the vertebral morphologies of fossils and extant skeletons of archosaurs in both closely and distantly related clades across the phylogeny. I also measured the pre- and postzygapophyseal intervertebral articulations from both extant and extinct groups, both with and without the hyposphene-hypantrum to understand how they vary with body size and throughout the archosaur phylogeny.

3. Materials and Methods

a. Recognition of the Hyposphene-hypantrum Articulation

The hyposphene-hypantrum articulation is defined as a two-part complex consisting of a bony projection, the hyposphene, on the posterior portion of the vertebra that fits into a complementary space, the hypantrum, on the anterior portion of the subsequent vertebra within a vertebral series (Stefanic, Chapter 1). Specifically, the hyposphene is orientated dorsoventrally and is symmetrical across the midline in posterior view. The hyposphene is located ventral to the articular surfaces of the postzygapophyses, which face dorsally and are positioned at between 0 and 45 degrees dorsally from the horizontal in posterior view. The hyposphene is a continuation of the articular surfaces of the postzygapophyses where they converge, and is dorsal to the neural canal. The hyposphene is also of comparable shape and size to that of the hypantrum space of the subsequent vertebrae because these structures articulate precisely. The lateral surfaces of the hyposphene articulate with the medial surfaces of the hypantrum, which is located between and ventral to the prezygapophyses and dorsal to the neural canal (Stefanic, Chapter 1). The articular surfaces of the prezygapophyses continue ventrally from their medial surfaces to form the articular surfaces of the hyposphene. In dorsal view, a hypantrum appears as a gap framed by parallel to sub-parallel medial surfaces of the prezygapophyses, which contact the neural arch just dorsal to the neural canal.

Based on these criteria for recognizing the presence of the hyposphene-hypantrum articulation in fossils, I performed both in-person observations and searched for figured material in literature of fossil trunk vertebrae. I surveyed 97 taxa from nearly every major clade within Archosauria (e.g. Theropoda, Sauropodomorpha, Ornithischia, Paracrocodylomorpha), including a few proximate outgroups (e.g. *Euparkeria capensis*, *Vancleavea campi*, *Erythrosuchus*

africanus). For each taxon I recorded the presence or absence of the hyposphene-hypantrum articulation.

b. Body Size Correlation

For all taxa scored for the presence or absence of the hyposphene-hypantrum articulation, I also collected body size information. I used femoral length as a correlate for body size (Farina et al., 1998; Christiansen and Farina, 2004; Farlow et al., 2005; Carrano, 2006; Turner et al., 2007; Sookias et al., 2012; O'Gorman and Hone, 2012; Turner and Nesbitt, 2013), and I used the largest-recorded length in the published literature (table 1). I then plotted these data for Pseudosuchia (figure 1a) and Avemetatarsalia (figure 1b) within Archosauria.

c. Phylogenetic survey

In order to place my analysis of the relationship between body size and the presence or absence of the hyposphene-hypantrum articulation in a phylogenetic context, I created a phylogenetic tree for each of the two major branches of archosaurs (Pseudosuchia, Avemetatarsalia). I made my trees by combining by hand previously published phylogenies (Erickson and Brochu, 1999; Sereno et al., 2001; Chiappe et al., 2002; Butler et al., 2008; Wilson, 2005; Carrano, 2006; Turner et al., 2007; Novas et al., 2009; Nesbitt, 2011; Irmis et al., 2013; Lee et al., 2014; Nesbitt et al., 2017). I then mapped the presence and absence of the hyposphene-hypantrum articulation onto those trees (figure 2; figure 3) and using ACCTRAN optimization by hand determined positions of acquisition and loss of the articulation.

To understand how body size maps onto the phylogeny, I used ancestral reconstruction data of femoral lengths across Pseudosuchia from Turner and Nesbitt (2013), who used an

extensive phylogenetic analysis from Nesbitt (2011) (figure 4; figure 7), and across Neotetanure by converting Log_{10} femoral reconstruction from Lee et al. (2014) (figure 8). I mapped these reconstructed femoral lengths on to some major nodes (e.g. Paracrocodylomorpha, Aetosauria, Sauropodomorpha, Theropoda) of my phylogenies, which target where the hyposphene-hypantrum is either lost or gained (figure 4; figure 7; figure 8).

d. Measurements

I surveyed 17 taxa from across Archosauria from both fossil collections and extant osteology collections to measure the articular processes (the postzygapophyses in all taxa and hyposphene structures when applicable) on the posterior aspects of trunk vertebrae for relative surface area provided by intervertebral articulation. To obtain a unit-less metric independent of body size, I also measured centrum height for each vertebra surveyed. The metric I used in my analysis of relative articular surface area was centrum height divided by the length (long-axis) of one postzygapophysis for each vertebra observed. I took measurements from 214 total vertebrae from extant and extinct archosaurs as well as some stem archosaurs.

From crown group crocodylians, I measured complete presacral vertebral columns of *Alligator mississippiensis* (TMM M-12606) and *Crocodylus acutus* (USNM 247943) and from crown group birds I measured complete presacral vertebral columns of *Dromaius novaehollandiae* (NMNH 345221), *Apteryx australis* (NMNH 500629), *Rhea americana* (NMNH 20286), *Struthio camelus* (NMNH 291160), *Gallus gallus* (NMNH 560790), and *Chauna chavaria* (NMNH 18996). From all taxa I measured the long-axis of the left postzygapophysis (measurement "A" in figure 5) and the centrum height to normalize for

vertebra size. All of the measurements of extant taxa were done in-person and recorded in millimeters (table 2).

Extinct archosaur taxa I measured in-person include a pseudosuchian (*Parringtonia gracilis*, NMT RB426), a theropod dinosaur (*Dilophosaurus wetherilli*, UCMP 37302; Welles, 1984), a phytosaur (*"Machaeroprosopus" zunii*, UCMP 27036; Camp, 1930), and the early avemetatarsalian *Asilisaurus kongwe* (NMT RB120, Nesbitt et al., 2010). The fossil vertebral columns were not complete, but location could be approximated within 1 position in either direction in the column for each vertebra based on the location of the para- and diapophyses on the centrum using an extant and complete vertebral column from *Alligator mississippiensis* (TMM M-12606) and nearly complete fossil vertebral column from *Allosaurus fragilis* (Madsen, 1976) as models.

In order to expand my dataset of extinct archosaurs to include more major groups and specimens, I used an extensive set of photographs previously taken by myself, specifically targeting morphology of trunk vertebrae. The photographs used were taken in posterior view as close to perpendicular (between the posterior plane and the camera lens) as possible, with a 5 cm scale bar. Using these photographs, I was able to take measurements of important features using the ruler tool in Photoshop CC 2015 (table 3). These measurements were (1) length of 1 cm (on the scale bar included in the photograph), (2) the centrum height, and (3) the length of the left prezygapophysis (or the right if the left was not preserved or postdepositionally altered to change its shape in any way) along its longest axis, from most proximal to most medial aspect along the articular surface (measurement "B" in figure 5). Using the 1 cm measurement, I could convert the zygapophyseal length and centrum height to millimeters in order to include them with my measurements taken in person. To make sure that the photographic measurements were

comparable with my in-person measurements, I took both measurements "A" and "B" (figure 5) on the same vertebrae to determine a conversion factor between the zygapophyseal lengths. Using multiple in-person and photograph measurements from vertebrae of *Alligator mississippiensis* (TMM M-12606), I determined that measurement "B" (Photoshop) / measurement "A" (in-person) was about 1.1 for three samples from varying positions along the presacral region of the *Alligator* vertebral column (i.e. the in-person measurement is 1.1 times greater than the measurement taken from a photograph of the same vertebra in Photoshop CC 2015). My assumption in using this conversion factor for all of the fossils surveyed using this method is that the angle of the postzygapophyses in relation to the neural arch is similar across all archosaur taxa. However, I am aware that compression due to fossilization may warp these angles in extinct taxa surveyed.

To understand how the articular surface of the zygapophyses varies within the vertebral column of a single animal as well as between taxa, I plotted each vertebra measured as a separate data point. For each point, the x-axis value was the position in the vertebral column (estimated for the extinct taxa based on the location of the para- and diapophyses on the centrum) and the y-axis value was the vertebra's centrum height divided by the zygapophyseal measurement (measurement "A" for in-person measured taxa and measurement "B" x 1.1 for the Photoshop measured taxa) (figure 6a). I plotted only trunk vertebrae (presacral position 10 to the last presacral before the sacrum) because this is the only portion of the vertebral column that has the hyposphene-hypantrum articulations (Stefanic, Chapter 1). These data illustrate how the size of the zygapophyses, relative to the vertebra size, change along the trunk series of an individual and in different extinct and extant clades.

e. Statistical Analyses

To determine statistical significance of the relationship seen between the presence of the hyposphene-hypantrum articulation and large body size (see above), I performed logistic regression analyses in R (see Supplemental Materials for code and outputs) because my data of presence or absence was discrete (i.e. 0 or 1 in table 1). The logistic regression will inform on how well body size (represented by femoral length) can explain whether any given data point will plot as a 0 or 1 on the y-axis. This test can only be used when there is a dichotomous variable on the y-axis, meaning there are only two independent possibilities for an outcome. This test will also indicate the probability that any given x-axis value (femoral length) will plot with either discrete y-axis value.

4. Results

In my assessment of the presence or absence of the hyposphene-hypantrum articulation versus body size (femoral length as a comparative estimate), I discovered gain of the articulation during body size increases and loss of the structure during miniaturization in archosaurs. However, the thresholds of these relationships differ among the two major branches of Archosauria and each threshold was represented by a range. Ranges for where the hyposphene-hypantrum appears in the phylogeny were bounded on the low end by the minimum femoral length where a taxon possesses the articulation. A femoral length of about 212-300 mm (table 1; figure 1a) is the threshold of size where the hyposphene-hypantrum appears in pseudosuchian archosaurs (figure 2). Pseudosuchians, with the exceptions of crocodylomorphs and a few others (see below), with a femoral length greater than 300 mm almost always had hyposphene-hypantrum articulations present in the trunk vertebrae. The pseudosuchian taxon possessing the

hyposphene-hypantrum with the shortest femoral length is *Mandasuchus tanyauchen* (femoral length = 212 mm, Butler et al., 2017); however among the three known individuals of *Mandasuchus tanyauchen*, the one from which a complete femur is known (NHMUK PV R6792) is not the largest reported of the taxon (Butler et al., 2017), so this is a conservative estimate for minimum body size with presence of the hyposphene-hypantrum.

To determine statistical significance and fit of my data, I performed a logistic regression statistical test in the statistical program R. This test will not output true R-squared values, but instead, our analyses output pseudo R-squared values that can be interpreted as how closely the presence or absence of the hyposphene-hypantrum can be explained by body size (represented by femoral length). The curves in my logistic regression plots (figure 1) represent the probability that any given x-value will fall in one of the two discrete data categories (presence or absence). I used two of the most widely used pseudo R-squared values for this study. For pseudosuchian archosaurs, the pseudo R-squared values showed a close relationship between large body size and presence of the hyposphene-hypantrum articulation with values close to 1 (Nagelkerke R-squared: 0.796, McFadden's R-squared: 0.660), and these data were significant (p-value: <0.001) (figure 1a).

In avemetatarsalian archosaurs, the threshold femoral length where the hyposphene-hypantrum is gained is restricted between 130-170 mm (table 1; figure 1b) in the phylogeny (figure 3). The taxa possessing the hyposphene-hypantrum with the shortest femoral lengths are *Asilisaurus kongwe* (femoral length = 130 mm, Nesbitt et al., 2010) and *Teleocrater rhadinus* (femoral length = 170 mm, Nesbitt et al., 2017), and these are two of the earliest diverging branches within Avemetatarsalia. Avemetarsalians with a femoral length greater than about 170 mm almost always had hyposphene-hypantrum articulations present in the trunk vertebrae, with

the exception of ornithischians and some titanosaurs (see below). My logistic regression showed a close relationship between large body size and presence of the hyposphene-hypantrum articulation (Nagelkerke R-squared: 0.789, McFadden's R-squared: 0.741), and these data were significant (p-value: <0.001) (figure 1b).

Besides the crown groups, in which the hyposphene-hypantrum is absent, it is also lost in a number of extinct archosaur clades, including some closely related poposauroids within the pseudosuchian clade Paracrocodylomorpha. It is definitively lost in the clade containing *Effigia okeeffeae* and *Shuvosaurus inexpectatus*, which are sister taxa of one another and have femoral lengths of 301 mm and 255 mm, respectively. These body sizes are within the threshold range for presence of the hyposphene-hypantrum in pseudosuchians of 212-300 mm. The presence or absence of the hyposphene-hypantrum in the sister taxon to *Effigia* + *Shuvosaurus*, *Sillosuchus longicervix* (PVSJ 85) is ambiguous because of poor preservation of the only known specimen (Alcober and Parrish, 1997).

A confounding scenario in the distribution of the hyposphene-hypantrum in archosaurs is the reported loss of those structures in titanosaurs, taxa well above the threshold (figure 3) (Apesteguia, 2005). These are the largest of all of the dinosaurs (Mazzetta et al., 2004), and the hyposphene-hypantrum articulation is lost near the base of the clade (figure 3). The earliest diverging members of Titanosauria, *Andesaurus delgadoi* (Mannion and Calvo, 2011) and *Phuwiangosaurus sirindhornae* (SM K11-0038, Suteethorn et al., 2009: Fig. 13), both clearly possess the articulation, but Apesteguia (2005) demonstrated that later diverging lineages of titanosaurs lack a clear hyposphene-hypantrum. I have observed one titanosaur vertebra myself in-person, *Alamosaurus sanjuanensis* (TMM 41891-1) and conclude that it does not have the hyposphene-hypantrum articulation; however, one vertebra out of the trunk series of an

individual may not be indicative of the presence or absence for that genus. Apesteguia (2005) cited the late diverging titanosaurs *Argentinosaurus huinculensis* and *Epachthosaurus sciuttoi* as possessing "hyposphenal bars" but not hyposphene-hypantrum articulations based on the definition I have provided. However, the original publication of *Argentinosaurus huinculensis* (Bonaparte and Coria, 1993) figures a trunk vertebra with a clearly defined and labeled hyposphene that does fit my definition. Furthermore, although the structure in most titanosaurs does not fit my definition, the condition in some titanosaurs might be a highly derived modification of the hyposphene-hypantrum. For this study, I consider the presence of a hyposphene-hypantrum in titanosaurs to be ambiguous because of this discrepancy, but consider this absence noteworthy.

Because of the ambiguity of the presence or absence of the hyposphene-hypantrum in *Sillosuchus longicervix* and in the gigantic titanosaurs, I eliminated these taxa from my body size logistic regressions for pseudosuchians and avemetatarsalians, respectively. I also exclude all ornithischian dinosaurs from my analyses because they are a major dinosaur clade that never possesses the hyposphene-hypantrum articulation, based on the specimens currently known, and therefore the absence of the articulation in later diverging, large taxa may be constrained by phylogeny (table 1). Vertebral morphologies for larger body size in ornithischians should be investigated further; however, I do not address this in this study. Therefore, I removed all ornithischian dinosaurs, such as the ornithopods *Thescelosaurus* (Galton, 1974), *Shantungosaurus* (Xing et al., 2014), *Zhuchengosaurus* (Xing et al., 2014), *Huaxiaosaurus*, and (Xing et al., 2014), *Edmontosaurus* (Xing et al., 2014), and the ceratopsians *Titanoceratops* (Longrich, 2011), *Utahceratops* (Sampson et al., 2010), *Kosmoceratops* (Sampson et al., 2010), and *Torosaurus* (Hunt and Lehman, 2008) from the avemetatarsalian logistic regression,

however their femoral lengths are included in table 1 herein. Many of the taxa eliminated from my logistic regression analysis have been manually placed as open circles onto the R plot and labeled to show their relationship to the included taxa in terms of body size (figure 1a; figure 1b).

My analysis of relative surface area provided by the zygapophyses in archosaurs and their close relatives could demonstrate potential variance in the metric of centrum height divided by the length (long-axis) of one postzygapophysis within an individual and across taxa. This metric did not show any signal based on whether the taxon was a member of the pseudosuchian or avemetatarsalian line of Archosauria or whether it was inside crown Archosauria or outside (figure 6a). However, I did see a slight relationship between body size and relative articular surface area, in that taxa with greater femoral lengths generally showed smaller zygapophyses in relation to their centrum height as illustrated by figure 6b. This is merely a visual relationship however, as I did not run statistical tests on this dataset. When changing the y-axis metric for taxa with the hyposphene-hypantrum to centrum height/(postzygapophyseal measurement + hyposphene lateral side measurement) (figure 6c), I saw an increase in relative articular surface for those taxa that possess the hyposphene-hypantrum articulation. With this change, figure 6b shows larger taxa (red) with the articulation (outlined) plotting among the smaller-bodied taxa (green and orange) that lack the hyposphene-hypantrum (no outline).

5. Discussion

a. The appearance of the hyposphene-hypantrum articulation

The hyposphene-hypantrum articulation evolves convergently within Archosauria at least six times and is lost independently at least five times (figures 2-4; figure 7; figure 8). This distribution of the hyposphene-hypantrum within a phylogenetic context is especially intriguing

because the presence or absence of the articulation appears to be highly correlated with increases and decreases in body size rather than controlled by inheritance.

Outside of Archosauria, the hyposphene-hypantrum articulation is almost always absent, regardless of body size. The one clear exception is the presence of the accessory articulation structures in the stem archosaur *Azendohsaurus madagaskarensis* (FMNH PR 2779, Femoral length = 205 mm, Nesbitt et al., 2015). This condition differs from all archosaurs, however, because the hyposphene-hypantrum articulation is only present in one vertebra in the anterior trunk and not present throughout the trunk (Nesbitt et al., 2015).

Although many stem archosaurs without the hyposphene-hypantrum are small-bodied and fall below the threshold found in all of Archosauria (e.g. *Vancleavea campi*, PEFO 2427, GR 138; *Euparkeria capensis*, SAM 5867, SAM 6047B; *Tropidosuchus romeri*, PVL 4601; *Trilophosaurus buettneri*, TMM 31025-140), many other stem archosaur taxa without the hyposphene-hypantrum are markedly larger with femoral lengths above the 130-170 mm threshold range such as phytosaurs, (e.g. *Smilosuchus gregorii*, Femoral length = 545 mm, USNM 18313; *Machaeroprosopus pristinus*, Femoral length = 444 mm, UCMP 27235) and their close relatives (e.g. *Erythrosuchus africanus*, Femoral length = 466 mm, SAM 905). These are comparable to some of the largest pseudosuchian archosaurs that possess the hyposphene-hypantrum articulation. However, if Phytosauria is included in Archosauria, within Pseudosuchia, as suggested by Ezcurra (2016) that would be an example of an archosaur clade that never evolves the hyposphene-hypantrum. For this study, I refer to them as Archosauriformes and sister to Archosauria, as in the phylogenetic analyses of (Nesbitt, 2011; Stocker, 2012). Therefore, from my observations, it is clear that the hyposphene-hypantrum articulation is present within most of the trunk vertebrae Archosauria only. This suggests that the

common ancestor of Archosauria may have had the ability to form the structure given the wide distribution of the feature in both major branches of the clade.

Based on femoral length data, I can infer a minimum threshold of body size (Femoral length = 230 mm in pseudosuchians, Femoral length = 130 mm in avemetatarsalians) below which the hyposphene-hypantrum is not present (figure 1) and a maximum threshold (Femoral length = 300 mm in pseudosuchians, Femoral length = 170 mm in avemetatarsalians) above which the hyposphene-hypantrum is present. Using reconstructed femoral lengths at important nodes within Archosauria (Turner and Nesbitt, 2013; Lee et al., 2014), I was able to make further predictions about the presence or absence of the hyposphene-hypantrum throughout Archosauria. My observations show that the hyposphene-hypantrum articulation is observed in both pseudosuchian and avemetatarsalian members of Archosauria at body sizes with femoral lengths above 212 and 130 respectively; however, the reconstructed ancestral state femoral length for Archosauria is 109 mm and this is below the minimum threshold for hyposphene-hypantrum presence for both pseudosuchians and avemetatarsalians. Because no known archosaurs with femoral lengths below 130 mm possess the hyposphene-hypantrum, I interpret the gain of the articulation in Pseudosuchia and Avemetatarsalia as convergent.

The hyposphene-hypantrum is definitively present in several members of Poposauroidea, a clade within and near the base of Paracrocodylomorpha (figure 2) (e.g. *Arizonasaurus babbitti*, MSM 4590, Nesbitt, 2005; *Xilousuchus sapingensis*, IVPP V6026, Nesbitt, 2011; *Poposaurus langstoni*, TMM 31025-257, TMM 31025-1261.1, Long and Murry, 1995, Weinbaum and Hungerbühler, 2007, Stefanic, Chapter 1; *Poposaurus gracilis*, TTU P-10419, Weinbaum and Hungerbühler, 2007), but its presence is ambiguous in *Sillosuchus longicervix* (Alcober and Parrish, 1997) because the only known specimen (PVSJ 85) is broken so that the articulation

structures are not preserved. Another pseudosuchian taxon for which the hyposphene-hypantrum articulation is ambiguous is the sister taxon to Paracrocodylomorpha, *Ticinosuchus ferox* (PIZ T 2817, Krebs, 1965, Lautenschlager and Desojo, 2011). That specimen is preserved on a flattened slab with the compressed vertebrae that remain in articulation, and therefore it is difficult to confirm the presence of a hyposphene on the posterior aspects of the vertebrae.

Many Triassic loricatan paracrocodylomorphs possess the hyposphene-hypantrum articulation (e.g. *Fasolasuchus tenax*, PVL 3850, Bonaparte, 1981; *Batrachotomus kupferzellensis*, SMNS 80296, Gower and Schoch, 2009; *Prestosuchus chiniquensis*, UFRGS-PV-0156-T, Azevedo, 1991; *Saurosuchus galilee*, PVSJ 32, Trotteyn et al., 2011). All of these taxa have femoral lengths greater than 400 mm (see Stefanic, Chapter 1).

Within the pseudosuchian clade Aetosauria, the hyposphene-hypantrum is present only in taxa with a largest reported femoral length above the threshold range (230-300 mm) for pseudosuchians. The largest aetosaurs (e.g. *Desmatosuchus spurensis*, Parker, 2008, MNA V9300; *Scutarx deltatylus*, Parker, 2016, PEFO 34045; *Longosuchus meadei*, TMM 31100-448, TMM 31100-452) have distinct hyposphene-hypantrum structures in their trunk vertebrae. The articulation is absent in the closest relatives of aetosaurs (e.g. *Revueltosaurus callenderi* and *Parringtonia gracilis*) and the smallest aetosaur taxa (e.g. *Coahomasuchus*, Parker, 2016, TMM 31100-437; *Aetobarbakinoides*, Desojo et al., 2012) (figure 2). This supports the hypothesis that the appearance of the hyposphene-hypantrum articulation is related to increased body size and is present in most pseudosuchian clades (see below) that increase body size over the 300 mm femoral length threshold.

Within Avemetatarsalia and outside Dinosauria, three taxa evolve the hyposphene-hypantrum articulation, and they represent the smallest body sizes to possess the articulation in

all of Archosauria. These taxa are the early avemetatarsalian *Teleocrater rhadinus* (femoral length = 170 mm, Nesbitt et al., 2017), and the silesaurs *Asilisaurus kongwe* (femoral length = 130 mm, Nesbitt et al., 2010) and *Silesaurus opolensis* (femoral length = 200 mm, Piechowski and Dzik, 2010) (figure 3). The early diverging theropod *Tawa hallae* (femoral length = 174 mm, Nesbitt et al., 2009) also possesses the hyposphene-hypantrum at a similar body size, just above our threshold femoral length for Avemetatarsalia (figure 3). Between the three major clades of dinosaurs, Ornithischia, Sauropodomorpha, and Theropoda, the hyposphene-hypantrum articulation is only present in Sauropodomorpha and Theropoda; it is absent in all ornithischians, regardless of body size (figure 3, table 1). The ancestral femoral length reconstruction for Saurischia is 156 mm (Turner and Nesbitt, 2013), which is above but close to the minimum femoral length at which the hyposphene-hypantrum as seen in avemetatarsalians (130 mm), so we cannot say with confidence whether the presence of the articulation is plesiomorphic for Saurischia or if it evolved convergently in both sauropodomorphs and theropods.

b. Losses of Hyposphene-hypantrum in crown Archosauria

The absence of the hyposphene-hypantrum in both crown groups of Archosauria, Crocodylia and Aves is surprising because some extinct and extant members have femoral lengths that are higher (e.g., *Deinosuchus riograndensis, Dinornis novaezelandiae*) than threshold size for presence of the hyposphene-hypantrum. The absence of the hyposphene-hypantrum in the Crocodylia and Aves can be traced well outside the crown to members of the stem lineages. The earliest diverging members of Crocodylomorpha reduced their body size in the Triassic Period below the threshold body size for the presence of hyposphene-hypantrum (212-300 mm) (e.g. *Sphenosuchus acutus*, Haughton, 1915; *Hesperosuchus agilis*, Colbert, 1952;

Terrestrisuchus gracilis, Crush, 1984) (figure 7). This small body size is retained through the origin of Crocodyliformes (Turner and Nesbitt, 2013).

Not only did crocodylomorphs reduce their body sizes, but they also shifted their ecologies from fully terrestrial to fully and semi-aquatic at those smaller sizes. In addition to changing their ecology, crocodylomorphs also modify their vertebral morphology after the loss of the hyposphene-hypantrum and once the group has undergone miniaturization. It is difficult to tell the order in which changes in ecology and changes in morphology occurred. One notable shift in vertebral morphology crocodylomorphs is the evolution of procoelous centra articulations. The crocodylomorph *Shamosuchus djadochtaensis* (Pol et al., 2009; Fig. 22) possesses at least two procoelous vertebrae (last cervical and first dorsal), which differs from the non-crocodylomorph pseudosuchian condition of amphicoely. This is the first appearance of procoelous vertebrae in the lineage, as the earlier diverging but closely related taxa *Goniopholis simus* and *Bernissartia fagesii* have only amphicoelous vertebrae (Pol et al., 2009). After the transition from terrestrial to aquatic and the evolution of procoely, some members of Crocodylomorpha reached large body sizes higher than pseudosuchian threshold for hyposphene-hypantrum presence (e.g. *Deinosuchus riograndensis*: femoral length = 530, TMM 43632-1; *Sarcosuchus imperator*, Sereno et al., 2001) (table 1), without having the articulation. The absence of the hyposphene-hypantrum articulation in these large crown group crocodylians may be related to either their difference in ecology or vertebral morphology, or a combination of the two. For example, they may not have needed a complex articulation between vertebrae because their aquatic life habit does not require them to hold their bodies up against gravity, similar to how whales and marine reptiles reduced their articulations (Uhen, 2007; Massare, 1994).

In Avemetarsalians, the hyposphene-hypantrum articulation is lost well within the clade Theropoda, which includes crown birds and their relatives. The early diverging theropod *Tawa hallae* has the hyposphene-hypantrum at a small body size (femoral length = 174 mm, Nesbitt et al., 2009), just above the threshold femoral length range (130-170 mm) for presence of the articulation for avemetatarsalians. After the definitive acquisition of the hyposphene-hypantrum at the base of Theropoda, some maniraptorans have body sizes close to but above the threshold femoral length range and retain the accessory articulation (e.g., *Ornitholestes hermanni*: femoral length = 210 mm, Carpenter et al., 2005; *Velociraptor mongoliensis*: femoral length = 238 mm, Norell and Makovicky, 1999).

There is a clear loss of the hyposphene-hypantrum in theropod clades that have secondarily smaller members. The hyposphene-hypantrum is definitively present in large members of Oviraptoridae (*Avimimus portentosus*: femoral length = 180 mm, Vickers-Rich et al., 2002) but absent in smaller members within the clade (*Microvenator celer*: femoral length = 124 mm, Makovicky and Sues, 1998). In Alvarezsauridae, the early diverging members of the clade (e.g., *Patagonykus puertai*: femoral length = 285 mm, Novas, 1997; *Haplocheirus sollers*: femoral length = 214, Choiniere et al., 2010) clearly have the hyposphene-hypantrum whereas the later members decrease their femoral lengths below the 130-170 mm threshold. This is clearly present in the small alvarezsaur *Mononykus olecranus* (femoral length = 150, Chiappe et al., 2002) (figure 8).

In Aves, or crown group birds, the hyposphene-hypantrum articulation is completely absent in all taxa even though some extinct (e.g. *Dinornis novaezelandiae*) and extant (e.g. *Struthio camelus*) have femoral lengths above the avemetatarsalian femoral length threshold of 170 mm. The loss of the articulation occurs outside of Aves clearly at the base of Avialae (e.g.,

Archaeopteryx lithographica: femoral length = 52.6 mm, Wellnhofer, 2009) (figure 8) and I am not aware of any avialan that has the hyposphene-hypantrum articulation. However, it is not clear if the hyposphene-hypantrum in more inclusive clades. As evidence, the reconstructed femoral length at Paraves (130 mm, Lee et al., 2014) is at the absolute minimum of the threshold (130-170 mm) for the presence of the feature, but members of Paraves (e.g., the dromaeosaurid *Velociraptor mongoliensis*: femoral length = 238 mm, Norell and Makovicky, 1999) do have the articulation. Therefore, it is not clear if the common ancestor of Paraves had the hyposphene-hypantrum and it was lost in avialans or that it was absent and gained independently in dromaeosaurids or other non-avialan paraves (figure 8).

Whereas paravians had small body sizes in relation to their non-paravian theropod relatives, avialians were even smaller, with a reconstructed femoral length at Avialae of (83.4 mm). Although it is uncertain where exactly in the paravian phylogeny the hyposphene-hypantrum was lost, it does correspond with a general shrinking in body size. Immediately following this decrease in body size, avialians change their ecology to volant (e.g., *Archaeopteryx lithographica*) (Feduccia and Tordoff, 1979; Olson and Feduccia, 1979; Rubin, 1991; Burgers and Chiappe, 1999). In closely related but later diverging non-avian avialians, there are vertebral modifications that differ markedly from the ancestral non-avian theropod condition including the evolution of heterocoelous centra articulations. Hetercoely appears just outside of the clade Ornithurae in *Patagopteryx deferrariisi* (Chiappe, 2002). *Patagopteryx deferrariisi* is a small (femoral length = 99 mm, Chiappe, 2002) avialian and although it was flightless (Chiappe, 2002), this loss of flight was secondary, and the shift to heterocoelous vertebrae (the condition seen of all living birds) can be placed phylogenetically after the evolution of powered flight.

In all living members of Archosauria, the hyposphene-hypantrum articulation is absent. However, the fossil record shows that it was once widespread and closely constrained by body size in extinct relatives of crocodylians and birds. The lack of the hyposphene-hypantrum in living archosaurs appears to be a combination of the reduction of size below the body size threshold where the articulation is present and then changes in morphology at those smaller sizes. In addition, becoming either semi-aquatic or volant appears to play a role in crown archosaurs not regaining the articulation after those ecological shifts, perhaps because of potential biomechanical restrictions of the hyposphene-hypantrum. In crocodylomorphs the hyposphene-hypantrum is lost in early diverging, small members before changes in ecology or vertebral morphology occur in that group, however it is difficult to discern the order in which the ecological or morphological changes happened in crocodylomorphs. In paravians, miniaturization and the loss of the hyposphene-hypantrum occur near the common ancestor of that clade, but it is difficult to determine the order in which these events occurred. However, it is clear that the ecological shift from terrestrial to volant happened before morphological changes to the vertebrae. In summary, after miniaturization, ecological change, and vertebral morphology changes, the hyposphene-hypantrum articulation is not regained in archosaurs, regardless of body size.

c. Biomechanical Implications

The location of the hyposphene-hypantrum articulation is confined to the trunk of the vertebral column in extinct archosaurs, and this position is concurrent with where the study by Fronimos and Wilson (2017) found the most complex neurocentral sutures. They interpret those complex interdigitating sutures as providing resistance to shear stress, therefore my observation

of the hyposphene-hypantrum articulation only in trunk vertebrae further supports the hypothesis that the most stress on the vertebral column is concentrated in the trunk relative to the neck or tail regions. The data from this study agree with the hypothesis that the addition of the hyposphene-hypantrum as a way of articulating vertebrae may increase rigidity of the vertebral column (Apestiguia, 2005).

Although the hyposphene-hypantrum articulation may have increased rigidity and reduced flexion in the vertebral column, this cannot be confirmed without three-dimensional modeling. A study of snake vertebral articulation determined that even in cases in which mechanical function appears to be narrowly constrained by morphology, specific functions should not be inferred solely from structural analyses (Moon, 1999). The author tested the hypothesis that the zygosphene-zygantrum articulation completely restricts torsion in snake vertebral columns and found that snake vertebral columns can undergo much more twisting than previously thought and are capable of torsion up to 2.89° per joint (Moon, 1999). I also hypothesize that due to the increase in moment arm with elongation of the hyposphene and deepening of the hypantrum in tandem, there would be a decrease in flexibility in the lateral plane. This increase in rigidity could have provided the support necessary for growth to larger body sizes, which would explain the correlation that I found with large body size and the presence of the hyposphene-hypantrum articulation (figure 1).

Bone is metabolically expensive for vertebrates to make because it is twice as dense (~2 gm/cm^3 vs. 1 gm/cm^3) as other body soft tissue (Martin, 2007). In terms of bone structure, modifications in a skeletal element's design that reduce the amount of material necessary to construct it without compromising on function and maintaining an "optimal strain environment" should always be favored (Rubin, 1984). Total body weight is determined by musculoskeletal

weight because physiologic organs will increase in size with larger skeletons in order to deal with required energy and waste products, therefore, it is beneficial for organisms to develop a system to minimize skeletal mass in relation to their functional requirements (Martin, 2007). In order to use less bone but still achieve a large body size while still maintaining a structurally sound skeleton, some taxa build their bodies in novel way, including adding rugose projections on their neural spines or increasing the complex interdigitation of neurocentral sutures (Wilson et al., 2016; Fronimos and Wilson, 2017). The presence of the hyposphene-hypantrum in the vertebrae of big taxa increases articulation complexity (i.e. contact between consecutive vertebrae) without increasing the overall volume of bone. Without the hyposphene-hypantrum or other comparable morphological change in articulation, large taxa would have potentially need to increase the size of their pre- and postzygapophyses linearly with vertebra size, and doing so could have been detrimental to the structural integrity of the vertebral column due to an excess mass of bone. This study provides data-driven evidence that the addition of the hyposphene-hypantrum articulation is a key morphological change that allowed some extinct archosaurs to grow larger than any other terrestrial vertebrate ever to live and it is the only skeletal morphology reported to be significantly correlated with body size and not constrained by phylogenetic history.

6. Acknowledgements

I thank the collections managers and scientists at the following institutions for access to their collections and permission to take photographs for analysis: American Museum of Natural History, the Carnegie Museum, the Vertebrate Paleontology Lab at the University of Texas at Austin, the University of California Museum of Paleontology, Petrified Forest National Park,

and the Museum of Northern Arizona. I also thank my advisor, Dr. Sterling J. Nesbitt and my Masters committee member for discussion and assistance in editing my manuscript and the rest of the Virginia Tech Paleobiology and Geobiology Research Group (S. Zhao, C. Griffin, C. Colleary, K. Formoso, K. Koeller, M. Riegler) for useful discussion, C. Griffin for assistance in statistical methods, and my Masters committee member J. Socha for discussion of biomechanical implications.

7. References

Alcober, O. A., Parrish, J. M. 1997 A new poposaurid from the Upper Triassic of Argentina. *Journal of Vertebrate Paleontology*. **17**, 548-556.

Apesteguia, S. 2005 Evolution of the hyposphene-hypantrum complex within Sauropoda. In *Thunder-Lizards: The Sauropodomorph Dinosaurs*. (eds. V. Tidwell, K. Carpenter), pp. 248-267: Indiana University Press.

Azevedo, S. A. K. 1991 *Prestosuchus chiniquensis* Huene 1942 (Reptilia, Archosauria, Rauisuchidae), da Formacao Santa Maria, Triassico do Estado do Rio Grande do Sul, Brasil. *Univeridade Federal Do Rio Grande Do Sul Curso De Pos-Graduacao Em Geociencias*.

Bonaparte, J. F. 1981 Descripcion de *Fasolasuchus tenax* y su significado en la sistematica y evolucion de los thecodontia. *Paleontologia*. **111**, 55-101.

Bonaparte, J. F., Coria, R. A. 1993 Un neuvo y gigantesco sauropp\odo titanosaurio de la Formacion Rio Limay (Albiense-Cenomaniense) de la Provincia del Neuquen, Argentina. *Ameghiniana*. **30**, 271-282.

Bonnan, M. F. 2003 The evolution of manus shape in sauropod dinosaurs: implications for functional morphology, forelimb orientation, and phylogeny. *Journal of Vertebrate Paleontology*. **23**, 595-

613.

Burgers, P., Chiappe, L. M. 1999 The wing of *Archaeopteryx* as a primary thrust generator. *Nature*. **399**, 60-62.

Butler, R. J., Galton, P. M., Porro, L. B., Chiappe, L. M., Henderson, D. M., Erickson, G. M. 2010 Lower limits of ornithischian dinosaur body size inferred from a new Upper Jurassic heterodontosaurid from North America. *Proceedings of the Royal Society B: Biological Sciences*. **277**, 375-381. (10.1098/rspb.2009.1494)

Butler, R. J., Upchurch, P., Norman, D. B. 2008 The phylogeny of the ornithischian dinosaurs. *Journal of Systematic Paleontology*. **6**, 1-40.

Butler, R. J., Nesbitt, S. J., Charig, A. J., Gower, D. J., Barrett, P. M. 2017 *Mandasuchus tanyauchen* gen. et sp. nov., a pseudosuchian archosaur from the Manda Beds of Tanzania. In *Vertebrate and climatic evolution in the Triassic rift basins of Tanzania and Zambia*. (eds. C. A. Sidor, S. J. Nesbitt), Society of Vertebrate Paleontology Memoir 17: Journal of Vertebrate Paleontology.

Bybee, P. J., Lee, A. H., Lamm, E.-T. 2006 Sizing the Jurassic theropod dinosaur *Allosaurus*: Assessing growth strategy and evolution of ontogenetic scaling of limbs. *Journal of Morphology*. **267**, 347-359. (10.1002/jmor.10406)

Camp, C. L. 1930 A study of the phytosaurs: with description of new material from western North America. University of Calif. Press.**10**, 1-61.

Carpenter, K., Miles, C., Ostrom, J. H., Cloward, K. 2005 Redescription of the small maniraptoran theropods *Ornitholestes* and *Coelurus* from the Upper Jurassic Morrison Formation of Wyoming. In *The Carnivorous Dinosaurs*. (eds. K. Carpenter), pp. 49-71: Indiana University Press.

Carrano, M. T. 2006 Body-size evolution in the Dinosauria. In *Amniote Paleobiology: Perspectives on the Evolution of Mammals, Birds, and Reptiles*. (eds. M. T. Carrano), pp. 225-256: University of

Chicago Press.

Carrier, D. R. 1987 The evolution of locomotor stamina in tetrapods: Circumventing a mechanical constraint. *Paleobiology*. **13**, 326-341.

Chiappe, L. M., Norell, M. A., Clark, J. M. 2002 The Cretaceous, short-armed Alvarezsauridae *Mononykus* and its kin. In *Mesozoic Birds: Above the Heads of Dinosaurs*. (eds. L. M. Chiappe, L. M. Witmer), pp.87-120: University of California Press.

Chiappe, L. M. 2002 Osteology of the Flightless *Patagopteryx deferrariisi* from the Late Cretaceous of Patagonia (Argentina). In *Mesozoic Birds: Above the Heads of Dinosaurs*. (eds. L. M. Chiappe, L. M. Witmer), pp. 281-316: University of California Press.

Choiniere, J. N., Xu, X., Clark, J. M., Forster, C. A., Guo, Y., Han, F. 2010 A basal alvarezsauroid theropod from the early Late Jurassic of Xinjiang, China. *Science*. **327**, 571-574.

Christiansen, P., Farina, R. A. 2004 Mass prediction in theropod dinosaurs. *Historical Biology*. **16**, 85-92.

Coates, M. I. 1996 The Devonian tetrapod *Acanthostega gunnari* Jarvik: Postcranial anatomy, basal tetrapod interrelationships and patterns of skeletal evolution. *Transactions of the Royal Society of Edinburgh: Earth Sciences*. **87**, 363-421.

Colbert, E. H. 1952 A pseudosuchian reptile from Arizona. *Bulletin of the American Museum of Natural History*. **99**, 561-592.

Crush, P. 1984 A late Upper Triassic sphenosuchid crocodilian from Wales. *Palaeontology*. **27**, 131-157.

Danto, M., Witzmann, F., Frobisch, N. B. 2016 Vertebral development in Paleozoic and Mesozoic tetrapods revealed by paleohistological data. *PloS ONE*. **11**, (10.137/journal.pone.0152586)

Desojo, J. B., Ezcurra, M. D., Kischlat, E. E. 2012 A new aetosaur genus (Archosauria: Pseudosuchia)

from the early Late Triassic of southern Brazil. *Zootaxa*. **3166**, 1-33.

Erickson, G. M., Brochu, C. A. 1999 How the 'terror crocodile' grew so big. *Nature*. **398**, 205-206.

Erickson, G. M., Rauhut, O. W. M., Zhou, Z., Turner, A. H., Inouye, B. D., Hu, D., Norell, M. A. 2009 Was dinosaurian physiology inherited by birds? Reconciling slow growth in *Archaeopteryx*. *PLoS One*. **4**, e7390.

Ezcurra, M. D. 2016 The phylogenetic relationships of basal archosauromorphs, with an emphasis on the systematics of proterosuchian archosauriforms. *PeerJ*. **4**, 1-385.

Fariña, R. A., Vizcaíno, S. F., Bargo, M. S. 1998 Body mass estimations in Lujanian (late Pleistocene-early Holocene of South America) mammal megafauna. *Mastozoología Neotropical*. **5**, 87-108.

Farlow, J. O., Hurlburt, G. R., Elsey, R. M., Britton, A. R. C., Langston Jr., W. 2005 Femoral dimensions and body size of *Alligator mississippiensis*: estimating the size of extinct mesoeucrocodylians. *Journal of Vertebrate Paleontology*. **25**, 354-369.

Feduccia, A., Tordoff, H. B. 1979 Feathers of *Archaeopteryx*: asymmetric vanes indicate aerodynamic function. *Science*. **203**, 1021-1022.

Forster, C. A., Sampson, S. D., Chiappe, L. M., Krause, D. W. 1998 The theropod ancestry of birds: new evidence from the Late Cretaceous of Madagascar. *Science*. **279**, 1915-1919.

Fowler, D. W., Sullivan, R. M. 2011 The first giant titanosaurian sauropod from the Upper Cretaceous of North America. *Acta Palaeontologica Polonica*. **56**, 685-690.

Fronimos, J. A., Wilson, J. A. 2017 Neurocentral suture complexity and stress distribution in the vertebral column of a sauropod dinosaur. *Ameghiniana*. **54**, 36-49.

Galton, P. M. 1974 Notes on *Thescelosaurus*, a conservative ornithopod dinosaur from the Upper Cretaceous of North America, with comments on ornithopod classification. *Journal of Paleontology*. **48**, 1048-1067.

Gaudin, T. J., Biewener, A. A. 1992 The functional morphology of xenarthrous vertebrae in the armadillo *Dasypus novemcinctus* (Mammalia, Xenarthra). *Journal of Morphology*. **214**, 63-81.

Gianechini, F. A., Apesteguia, S. 2011 Unenlagiinae revisited: dromaeosaurid theropods from South America. *Anais da Academia Brasileira de Ciências*. **83**, 163-195.

Gower, D. J., Schoch, R. R. 2009 Postcranial anatomy of the rauisuchian archosaur *Batrachotomus kupferzellensis*. *Journal of Vertebrate Paleontology*. **29**, 103-122.

Haughton, S. H. 1915 A new thecodont from the Stormberg beds. *Annals of the South African Museum*. **12**, 98-105.

Holliday, C. M., Ridgely, R. C., Sedlmayr, J. C., Witmer, L. M. 2010 Cartilaginous epiphyses in extant archosaurs and their implications for reconstructing limb function in dinosaurs. *PLoS One*. **5**, e13120.

Hunt, R. K., Lehman, T. M. 2008 Attributes of the ceratopsian dinosaur *Torosaurus*, and new material from the Javelina Formation (Maastrichtian) of Texas. *Journal of Paleontology*. **82**, 1127-1138.

Hwang, S. H., Norell, M. A., Qiang, J., Keqin, G. 2002 New specimens of *Microraptor zhaoianus* (Theropoda: Dromaeosauridae) from northeastern China. *American Museum Novitates*. 1-44.

Irmis, R. B., Nesbitt, S. J., Sues, H.-D. 2013 Early crocodylomorpha. *Geological Society, London, Special Publications*. **379**, 275-302.

Krebs, B. 1965 Die Triasfauna der Tessiner Kalkalpen. XIX. *Ticinosuchus ferox*, nov. gen. nov. sp. Ein neuer Pseudosuchier aus der Trias des Monte San Georgio. . *Schweizersiche Palaontologische, Abhandlungen*. **81**, 1-140.

Lautenschlager, S., Desojo, J. B. 2011 Reassessment of the Middle Triassic rauisuchian archosaurs *Ticinosuchus ferox* and *Stagnosuchus nyassicus*. *Palaontologische Zeitschrift*. **85**, 357-381.

Lee, Y.-N., Barsbold, R., Currie, P. J., Kobayashi, Y., Lee, H.-J., Godefroit, P., Escuillié, F., Chinzorig,

T. 2014 Resolving the long-standing enigmas of a giant ornithomimosaur *Deinocheirus mirificus*. *Nature*. **515**, 257-260.

Lee, M. S. Y., Cau, A., Naish, D., Dyke, G. J. 2014 Sustained miniaturization and anatomical innovation in the dinosaurian ancestors of birds. *Science*. **345**, 562-566.

Long, R. A., Murry, P. A. 1995 Late Triassic (Carnian and Norian) tetrapods from the southwestern United States. *Bulletin of the New Mexico Museum of Natural History and Science*. **4**, 1-254.

Longrich, N. R. 2011 *Titanoceratops ouranos*, a giant horned dinosaur from the late Campanian of New Mexico. *Cretaceous Research*. **32**, 264-276. (http://dx.doi.org/10.1016/j.cretres.2010.12.007)

Madsen Jr., J. H. 1976 *Allosaurus fragilis*: a revised osteology. **109**, 1-163.

Makovicky, P. J., Apesteguia, S., Agnolin, F. L. 2005 The earliest dromaeosaurid theropod from South America. *Nature*. **437**, 1007-1011.

Makovicky, P. J., Sues, H.-D. 1998 Anatomy and phylogenetic relationships of the theropod dinosaur *Microvenator celer* from the Lower Cretaceous of Montana. *American Museum Novitates*. 1-26.

Mannion, P. D., Calvo, J. O. 2011 Anatomy of the basal titanosaur (Dinosauria, Sauropoda) *Andesaurus delgadoi* from the mid-Cretaceous (Albian-early Cenomanian) Rio Limay Formation, Neuquen Province, Argentina: implications for titanosaur systematics. *Zoological Journal of the Linnean Society*. **163**, 155-181. (10.1111/j.1096-3642.2011.00699.x)

Marsh, A. D. 2013 The Osteology of *Sarahsaurus aurifontanalis* and Geochemical Observations of the Dinosaurs from the Type Quarry of *Sarahsaurus* (Kayenta Formation), Coconino County, Arizona: University of Texas at Austin.

Martin, R. B. 2007 The importance of mechanical loading in bone biology and medicine. *Journal of Musculoskeletal and Neuronal Interactions*. **7**, 48-53.

Massare, J. A. 1994 Swimming capabilities of Mesozoic marine reptiles: a review. In *The Mechanics*

and Physiology of Animal Swimming. (eds. L. Maddock, Q. Bone, J. M. V. Rayner), pp.: Cambridge University Press.

Mazzetta, G. V., Christiansen, P., Farina, R. A. 2004 Giants and bizarres: Body size of some southern South American Cretaceous dinosaurs. *Historical Biology*. 1-13.

McIntosh, J. S. 2005 The genus *Barosaurus* Marsh (Sauropoda, Diplocidae). In *Thunder-Lizards: The Sauropodomorph Dinosaurs*. (eds. V. Tidwell, K. Carpenter), pp. 38-77: Indiana University Press.

Moon, B. R. 1999 Testing an inference of function from structure: snake vertebrae do the twist. *Journal of Morphology*. **241**, 217-225.

Nesbitt, S. J. 2005 Osteology of the Middle Triassic pseudosuchian archosaur *Arizonasaurus babbitti*. *Historical Biology*. **17**, 19-47.

Nesbitt, S. J. 2011 The early evolution of archosaurs: Relationships and the origin of major clades. *Bulletin of the American Museum of Natural History*. **352**, 1-292.

Nesbitt, S. J., Flynn, J. J., Pritchard, A. C., Parrish, J. M., Ranivoharimanana, L., Wyss, A. R. 2015 Postcranial osteology of *Azendohsaurus madagaskarensis* (?Middle to Upper Triassic, Isalo Group, Madagascar) and its systematic position among stem archosaur reptiles. *Bulletin of the American Museum of Natural History*. **398**, 1-126.

Nesbitt, S. J., Sidor, C. A., Irmis, R. B., Angielczyk, K. D., Smith, R. M. H., Tsuji, L. A. 2010 Ecologically distinct dinosaurian sister group shows early diversification of Ornithodira. *Nature*. **464**, 95-98.

Nesbitt, S. J., Smith, N. D., Irmis, R. B., Turner, A. H., Downs, A., Norell, M. A. 2009 A complete skeleton of a Late Triassic saurischian and the early evolution of dinosaurs. *Science*. **326**, 1530-1533.

Nesbitt, S. J., Butler, R. J., Ezcurra, M. D., Barrett, P. M., Stocker, M. R., Angielczyk, K. D., Smith, R.

M. H., Sidor, C. A., Niedźwiedzki, G., Sennikov, A. G. 2017 The earliest bird-line archosaurs and the assembly of the dinosaur body plan. *Nature*. **544**, 484-487.

Norell, M. A., Makovicky, P. J. 1999 Important features of the dromaeosaurid skeleton. II: Information from newly collected specimens of *Velociraptor mongoliensis*. *The American Museum Novitates*. **3282**, 1-45.

Norell, M. A., Makovicky, P. J., Bever, G. B., Balanoff, A. M., Clark, J. M., Barsbold, R., Rowe, T. 2009 A review of the Mongolian Cretaceous dinosaur *Saurornithoides* (Troodontidae: Theropoda). *American Museum Novitates*. **3654**, 1-63.

Novas, F. E. 1997 Anatomy of *Patagonykus puertai* (Theropoda, Avialae, Alvarezsauridae), from the Late Cretaceous of Patagonia. *Journal of Vertebrate Paleontology*. **17**, 137-166.

Novas, F. E., Pol, D., Canale, J. I., Porfiri, J. D., Calvo, J. O. 2009 A bizarre Cretaceous theropod dinosaur from Patagonia and the evolution of Gondwanan dromaeosaurids. *Proceedings of the Royal Society of London B: Biological Sciences*. **276**, 1101-1107.

O'Gorman, E. J., Hone, D. W. E. 2012 Body size distribution of the dinosaurs. *PLoS One*. **7**, e51925.

Olson, S. L., Feduccia, A. 1979 Flight capability and the pectoral girdle of *Archaeopteryx*. *Nature*. **278**, 247-248.

Ostrom, J. H. 1969 *Osteology of Deinonychus antirrhopus, an unusual theropod from the Lower Cretaceous of Montana*. Peabody Museum of Natural History, Yale University.

Parker, W. G. 2008 Description of new material of the aetosaur *Desmatosuchus spurensis* (Archosauria: Suchia) from the Chinle Formation of Arizona and a revision of the genus *Desmatosuchus*. *PaleoBios*. **28**, 1-40.

Parker, W. G. 2016 Osteology of the Late Triassic aetosaur *Scutarx deltatylus* (Archosauria: Pseudosuchia). *PeerJ*. **4**, e2411. (10.7717/peerj.2411)

Parker, W. G. 2016 Revised phylogenetic analysis of the Aetosauria (Archosauria: Pseudouchia); assessing the effects of incongruent morphological character sets. *PeerJ*. (4:e1583; DOI 10.7717/peerj.1583)

Piechowski, R., Dzik, J. 2010 The axial skeleton of *Silesaurus opolensis*. *Journal of Vertebrate Paleontology*. **30**, 1127-1141.

Pol, D., Turner, A. H., Norell, M. A. 2009 Morphology of the Late Cretaceous crocodylomorph *Shamosuchus djadochtaensis* and a discussion of neosuchian phylogeny as related to the origin of Eusuchia. *Bulletin of the American Museum of Natural History*. **324**, 1-103.

Rauhut, O. W. M. 2003 The interrelationships and evolution of basal theropod dinosaurs. *Special Papers in Paleontology*. **69**, 1-213.

Rubin, C. T. 1984 Skeletal strain and the functional significance of bone architecture. *Calcified Tissue International*. **36**, S11-S18.

Sampson, S. D., Loewen, M. A., Farke, A. A., Roberts, E. M., Forster, C. A., Smith, J. A., Titus, A. L. 2010 New horned dinosaurs from Utah provide evidence for intracontinental dinosaur endemism. *PLOS ONE*. **5**, e12292. (10.1371/journal.pone.0012292)

Sereno, P. C., Larsson, H. C. E., Sidor, C. A., Gado, B. 2001 The giant crocodyliform *Sarchosuchus* from the Cretaceous of Africa. *Science*. **294**, 1516-1519.

Schaeffer, B. 1967 Osteichthyan vertebrae. *Zoological Journal of the Linnean Society*. **47**, 185-195.

Smith, F. A., Boyer, A. G., Brown, J. H., Costa, D. P., Dayan, T., Ernest, S. K. M., Evans, A. R., Fortelius, M., Gittleman, J. L., Hamilton, M. J. 2010 The evolution of maximum body size of terrestrial mammals. *Science*. **330**, 1216-1219.

Sookias, R. B., Butler, R. J., Benson, R. B. J. 2012 Rise of dinosaurs reveals major body-size transitions are driven by passive processes of trait evolution. *Proceedings of the Royal Society of London B:*

Biological Sciences. **279**, 2180-2187.

Stocker, M. R. 2012 A new phytosaur (Archosauriformes, Phytosauria) from the Lot's Wife beds (Sonsela Member) within the Chinle Formation (Upper Triassic) of Petrified Forest National Park, Arizona. *Journal of Vertebrate Paleontology*. **32**, 573-586.

Suteethorn, S., Le Loeuff, J., Buffetaut, E., Suteethorn, V., Talubmook, C., Chonglakmani, C. 2009 A new skeleton of *Phuwiangosaurus sirindhornae* (Dinosauria, Sauropoda) from NE Thailand. *Geological Society, London, Special Publications*. **315**, 189-215.

Trotteyn, M. J., Desojo, J. B., Alcober, O. A. 2011 Nuevo material postcraneano de *Saurosuchus galilei* reig (Archosauria:Crurotarsi) del Triásico Superior del Centro-Oeste de Argentina. *Ameghiniana*. **48**, 13-27.

Turner, A. H., Hwang, S. H., Norell, M. A. 2007 A small derived theropod from Öösh, Early Cretaceous, Baykhangor Mongolia. *American Museum Novitates*. 1-27.

Turner, A. H., Makovicky, P. J., Norell, M. A. 2012 A review of dromaeosaurid systematics and paravian phylogeny. *Bulletin of the American Museum ofNatural History*. 1-206.

Turner, A. H., Nesbitt, S. J. 2013 Body size evolution during the Triassic archosauriform radiation. *Geological Society, London, Special Publications*. **379**,

Turner, A. H., Pol, D., Clarke, J. A., Erickson, G. M., Norell, M. A. 2007 A basal dromaeosaurid and size evolution preceding avian flight. *Science*. **317**, 1378-1381.

Turner, A. H., Pol, D., Norell, M. A. 2011 Anatomy of *Mahakala omnogovae* (Theropoda: Dromaeosauridae), Tögrögiin Shiree, Mongolia. *American Museum Novitates*. 1-66.

Uhen, M. D. 2007 Evolution of the marine mammals: Back to the sea after 300 million years. *The Anatomical Record*. **290**, 514-522.

Vickers-Rich, P., Chiappe, L. M., Kurzanov, S. 2002 The enigmatic birdlike dinosaur *Avimimus*

portentosus. In *Mesozoic Birds: Above the Heads of Dinosaurs*. (eds. L. M. Chiappe, L. M. Witmer), pp.65-86: University of California Press.

Wedel, M. J. 2003 Vertebral pneumaticity, air sacs, and the physiology of sauropod dinosaurs. *Paleobiology*. **29**, 243-255.

Weinbaum, J. C. 2013 Postcranial skeleton of *Postosuchus kirkpatricki* (Archosauria: Paracrocodylomorpha), from the Upper Triassic of the United States. *Geological Society, London, Special Publications*. **379**, 525-553.

Weinbaum, J. C., Hungerbühler, A. 2007 A revision of *Poposaurus gracilis* (Archosauria: Suchia) based on two new specimens from the Late Triassic of the southwestern U.S.A. *Palaontologische Zeitschrift*. **81**, 131-145.

Welles, S. P. 1984 *Dilophosaurus wetherilli* (Dinosauria, Theropoda) osteology and comparisons. *Palaeontographica*. **185**, 85-180.

Wellnhofer, P. 2009 *Archaeopteryx: The Icon of Evolution*. Verlag Dr. Friedrich Pfeil.

Wilson, J. A. 2005 Overview of sauropod phylogeny and evolution. In *The Sauropods: Evolution and Paleobiology*. (eds. K. C. Rogers, J. A. Wilson), pp. 15-49: University of California Press.

Wilson, J. P., Woodruff, D. C., Gardner, J. D., Flora, H. M., Horner, J. R., Organ, C. L. 2016 Vertebral adaptations to large body size in theropod dinosaurs. *PloS One*. **11**, e0158962.

Xing, H., Zhao, X., Wang, K., Li, D., Chen, S., Mallon, J. C., Zhang, Y., Xu, X. 2014 Comparative osteology and phylogenetic relationship of *Edmontosaurus* and *Shantungosaurus* (Dinosauria: Hadrosauridae) from the Upper Cretaceous of North America and East Asia. *Acta Geologica Sinica (English Edition)*. **88**, 1623-1652.

8. FIGURES

Figure 1. Body Size graphs for (a) Pseudosuchia and (b) Avemetatarsalia. The black points represent omitted taxa due to ambiguity or position in the phylogeny that renders them confounding points to the data: (a) 1, *Sillosuchus*; 2, *Erythrosuchus*; 3, *Machaeroprosopus*; 4, *Smilosuchus*. (b) 1, *Thescelosaurus*; 2, *Kosmoceratops*; 3, *Utahceratops*; 4, *Opisthocoelicaudia* (titanosaur); 5, *Shantungosaurus*; 6, *Alamosaurus* (titanosaur)

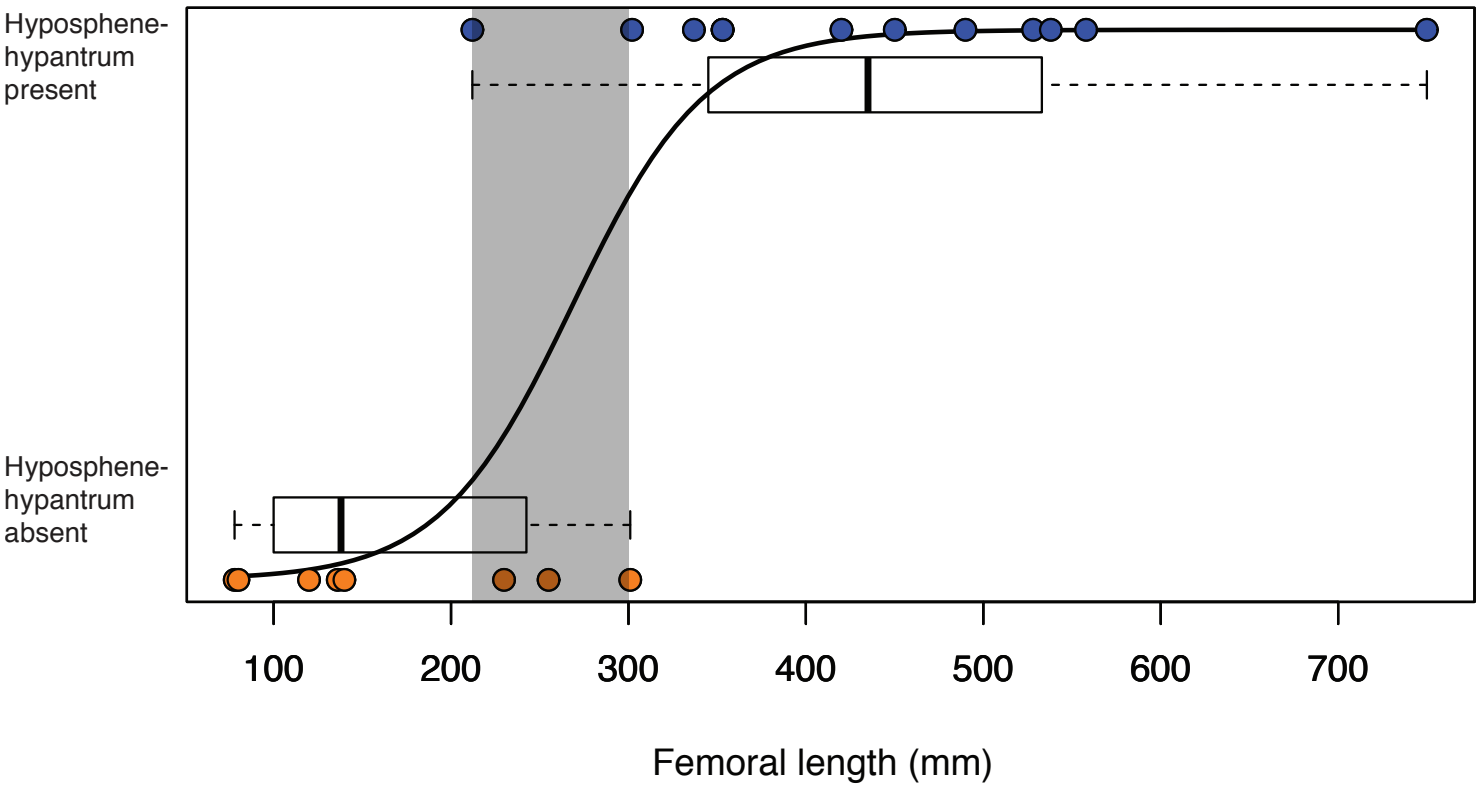
Hyposphene-
hypantrum
present
Hyposphene-
hypantrum
absent
100
200
300
400
500
600
700
Femoral length (mm)

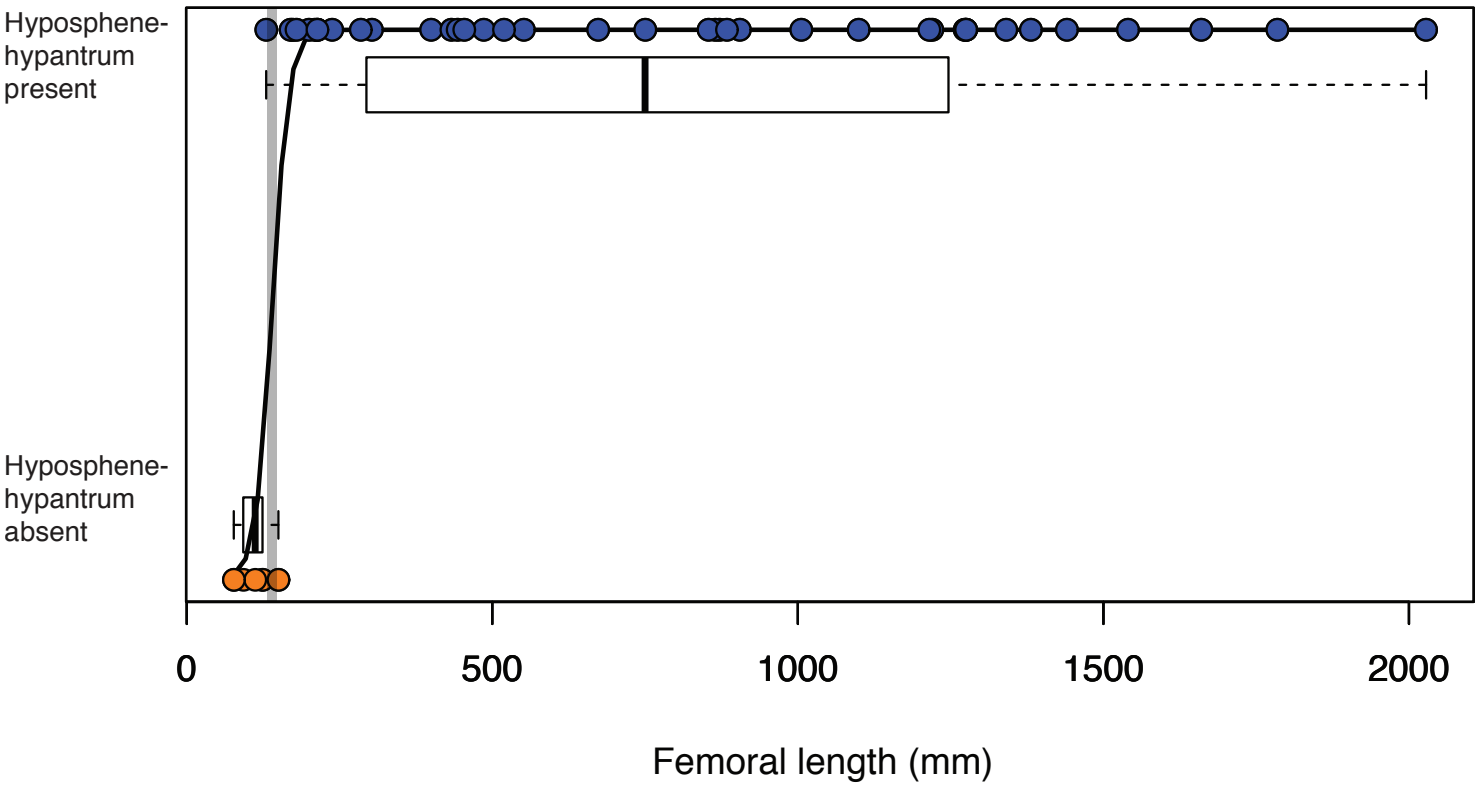
Hyposphene-
hypantrum
present
Hyposphene-
hypantrum
absent
0
500
1000
1500
2000
Femoral length (mm)

Figure 2. Phylogenetic tree of Pseudosuchia (from Erickson and Brochu, 1999; Sereno et al., 2001; Nesbitt, 2011; Irmis et al., 2013) with the presence (blue) and absence (orange) (black = ambiguous) of the hyposphene-hypantrum complex mapped on.

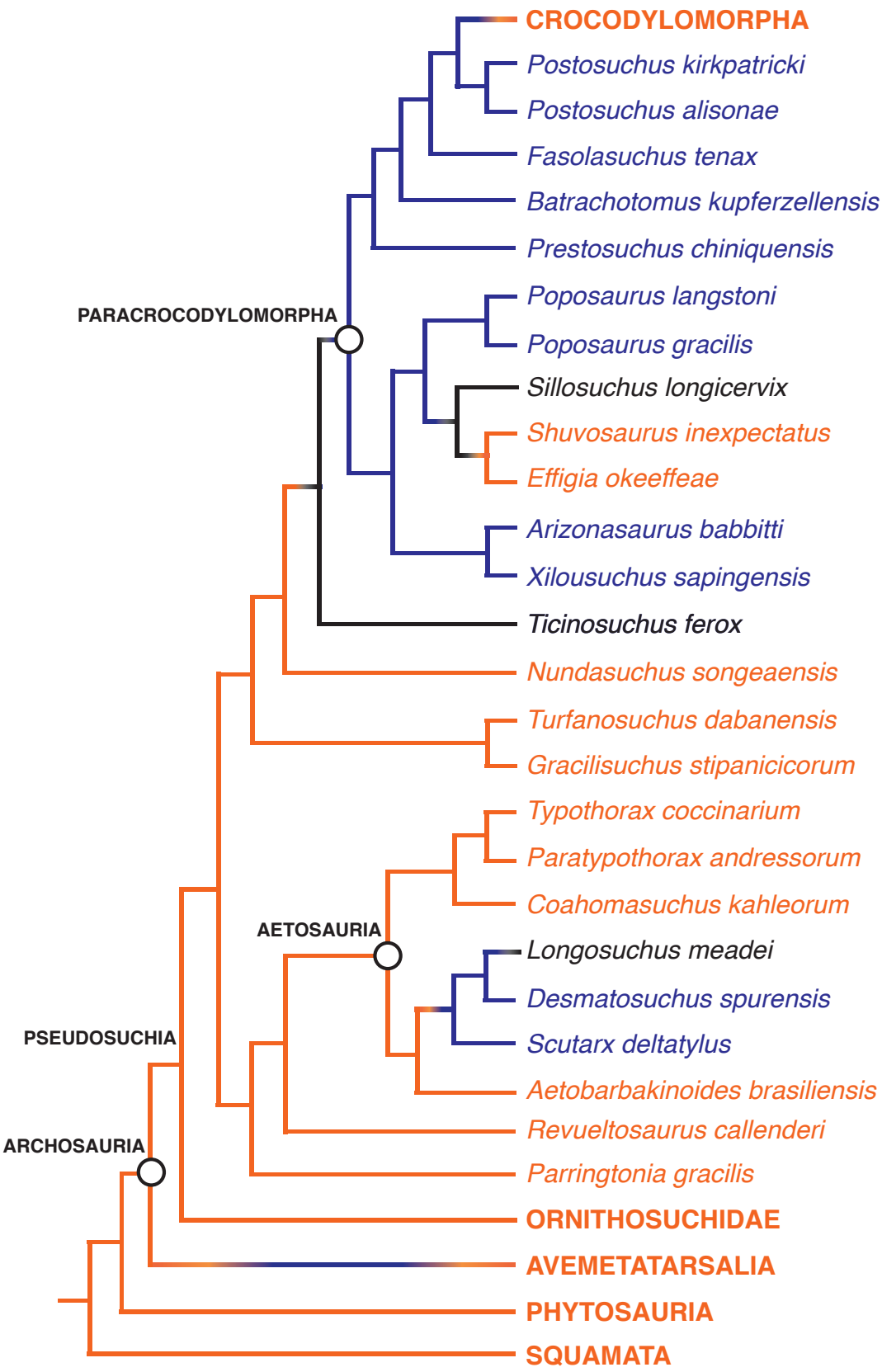
CROCODYLOMORPHA
Postosuchus kirkpatricki
Postosuchus alisonae
Fasolasuchus tenax
Batrachotomus kupferzellensis
Prestosuchus chiniquensis
PARACROCODYLOMORPHA
Poposaurus langstoni
Poposaurus gracilis
Sillosuchus longicervix
Shuvosaurus inexpectatus
Effigia okeeffeae
Arizonasaurus babbitti
Xilousuchus sapingensis
Ticinosuchus ferox
Nundasuchus songeaensis
Turfanosuchus dabanensis
Gracilisuchus stipanicicorum
Typothorax coccinarium
Paratypothorax andressorum
Coahomasuchus kahleorum
AETOSAURIA
Longosuchus meadei
Desmatosuchus spurensis
PSEUDOSUCHIA
Scutarx deltatylus
Aetobarbakinoides brasiliensis
Revueltosaurus callenderi
ARCHOSAURIA
Parringtonia gracilis
ORNITHOSUCHIDAE
AVEMETATARSALIA
PHYTOSAURIA
SQUAMATA

Figure 3. Phylogenetic tree of Avemetatarsalia (from Chiappe et al., 2002; Wilson, 2005; Carrano, 2006; Turner et al., 2007; Butler et al., 2008; Novas et al., 2009; Lee et al., 2014; Nesbitt et al., 2017) with the presence (blue) and absence (orange) of the hyposphene-hypantrum complex mapped on.

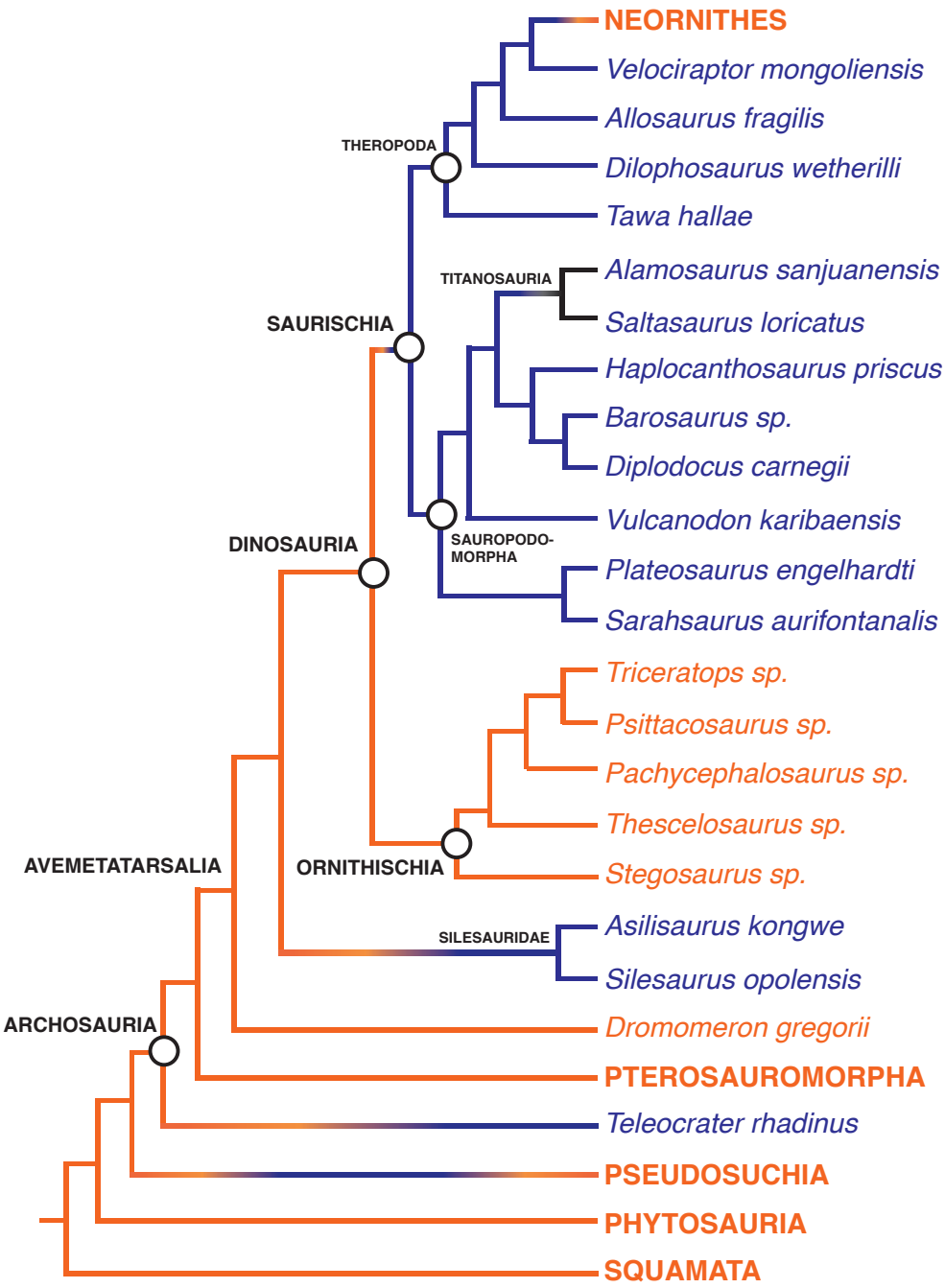
NEORNITHES
Velociraptor mongoliensis
Allosaurus fragilis
THEROPODA
Dilophosaurus wetherilli
Tawa hallae
TITANOSAURIA
Alamosaurus sanjuanensis
Saltasaurus loricatus
SAURISCHIA
Haplocanthosaurus priscus
Barosaurus sp.
Diplodocus carnegii
Vulcanodon karibaensis
SAUROPODO-
MORPHA
DINOSAURIA
Plateosaurus engelhardti
Sarahsaurus aurifontanalis
Triceratops sp.
Psittacosaurus sp.
Pachycephalosaurus sp.
Thescelosaurus sp.
AVEMETATARSALIA
ORNITHISCHIA
Stegosaurus sp.
SILESAURIDAE
Asilisaurus kongwe
Silesaurus opolensis
ARCHOSAURIA
Dromomeron gregorii
PTEROSAUROMORPHA
Teleocrater rhadinus
PSEUDOSUCHIA
PHYTOSAURIA
SQUAMATA

Figure 4. Combined Pseudosuchia and Avemetatarsalia with ancestral state femoral length reconstructions (from Turner and Nesbitt, 2013) illustrated at several major nodes.

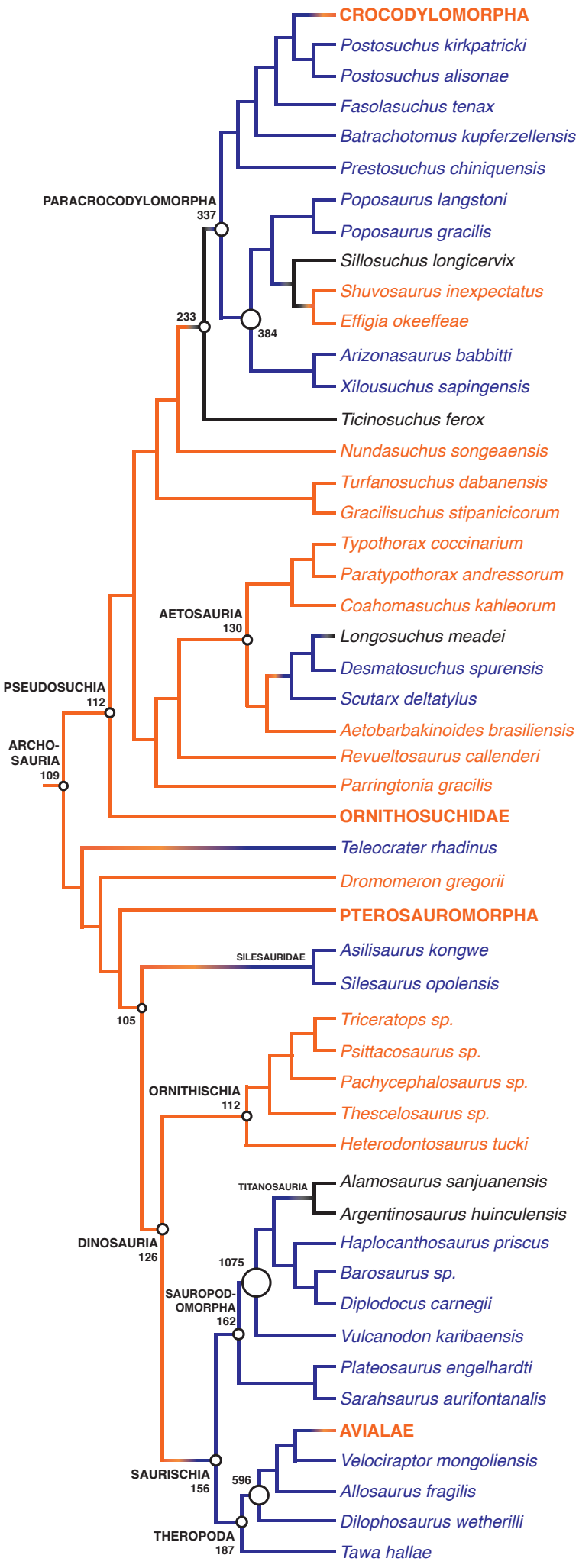
CROCODYLOMORPHA
Postosuchus kirkpatricki
Postosuchus alisonae
Fasolasuchus tenax
Batrachotomus kupferzellensis
Prestosuchus chiniquensis
PARACROCODYLOMORPHA
337
Poposaurus langstoni
Poposaurus gracilis
Sillosuchus longicervix
Shuvosaurus inexpectatus
Effigia okeeffeae
233
384
Arizonasaurus babbitti
Xilousuchus sapingensis
Ticinosuchus ferox
Nundasuchus songeaensis
Turfanosuchus dabanensis
Gracilisuchus stipanicicorum
Typothorax coccinarium
Paratypothorax andressorum
Coahomasuchus kahleorum
AETOSAURIA
130
Longosuchus meadei
Desmatosuchus spurensis
PSEUDOSUCHIA
112
Scutarx deltatylus
Aetobarbakinoides brasiliensis
ARCHO-
SAURIA
109
Revueltosaurus callenderi
Parringtonia gracilis
ORNITHOSUCHIDAE
Teleocrater rhadinus
Dromomeron gregorii
PTEROSAUROMORPHA
SILESAURIDAE
Asilisaurus kongwe
Silesaurus opolensis
105
Triceratops sp.
Psittacosaurus sp.
Pachycephalosaurus sp.
ORNITHISCHIA
112
Thescelosaurus sp.
Heterodontosaurus tucki
TITANOSAURIA
Alamosaurus sanjuanensis
Argentinosaurus huinculensis
DINOSAURIA
126
Haplocanthosaurus priscus
1075
Barosaurus sp.
SAUROPOD-
OMORPHA
162
Diplodocus carnegii
Vulcanodon karibaensis
Plateosaurus engelhardti
Sarahsaurus aurifontanalis
AVIALAE
Velociraptor mongoliensis
SAURISCHIA
156
596
Allosaurus fragilis
Dilophosaurus wetherilli
THEROPODA
187
Tawa hallae

Figure 5. Schematic illustrating the in-person and Photoshop measurements of vertebrae the author took. Measurements “A” and “B” are shown on an *Alligator* vertebra in posterior and ventral oblique views. Measurement “B”/ Measurement “A” = 1.1 (conversion factor).

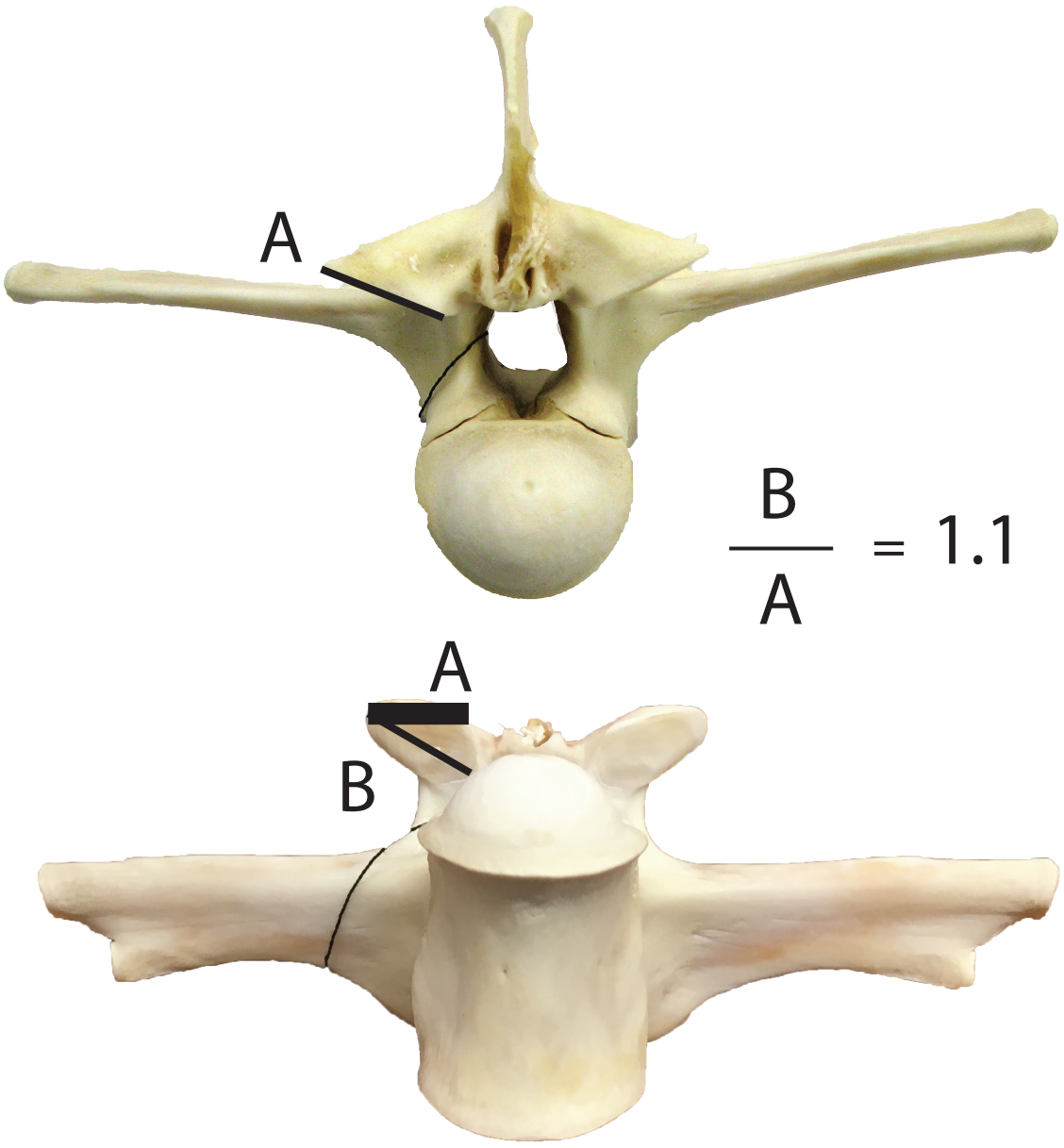
A
B
A
= 1.1
A
B

Figure 6. Graphs representing the relative articulation surface area of archosaur vertebrae. The graphs show (a) how each type of measurement was taken, (b) how the relative articulation surface area is related to body size, (c) the body size relationship when the hyposphene surface is included in the surface area measurement, and (d) several individuals where I had at least 5 trunk vertebrae sampled.

(a)

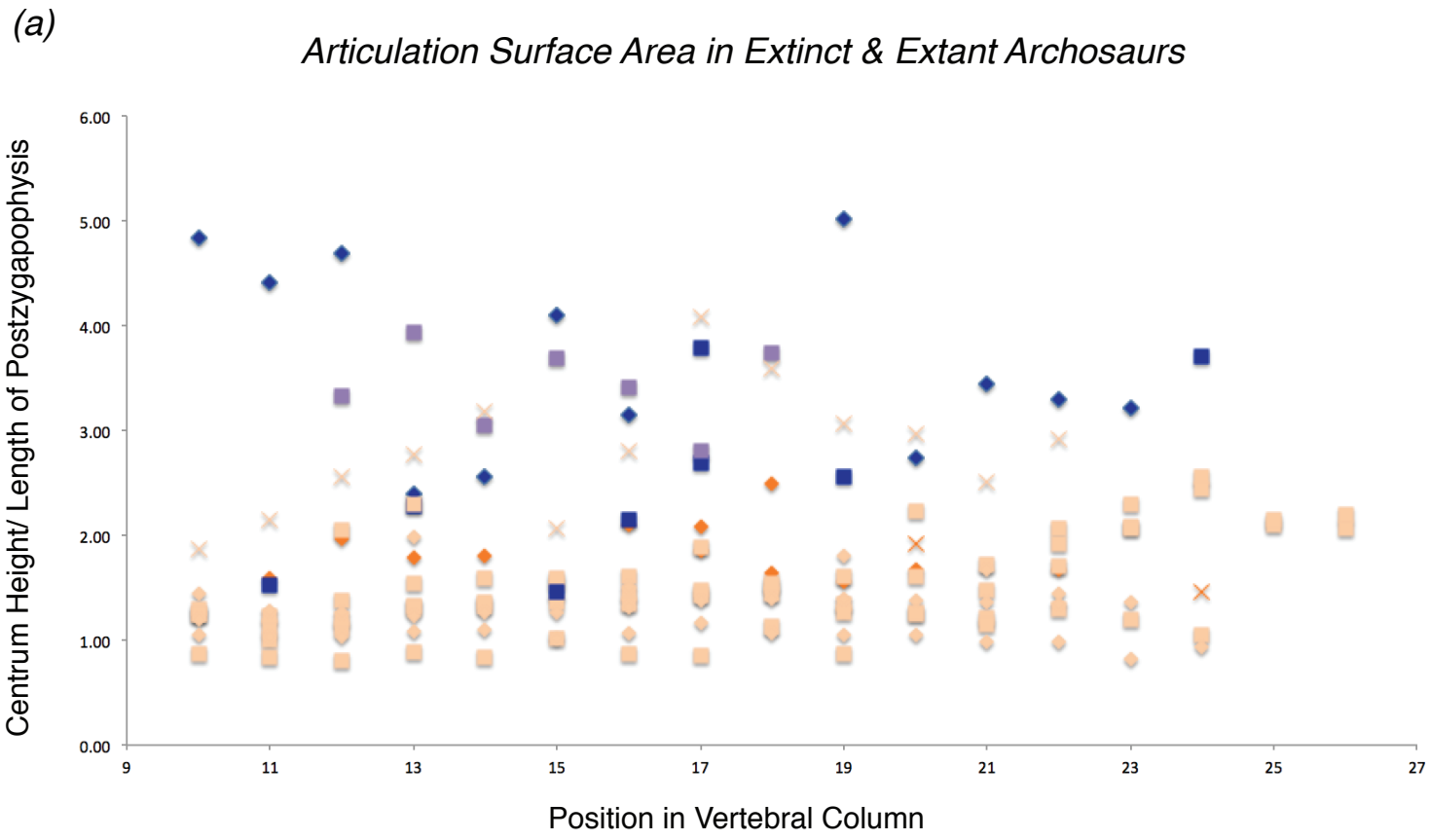

legend

- Avemetatarsalian, hyposphene-hypantrum present, measured in Photoshop
- Avemetatarsalian, hyposphene-hypantrum present, measured in person
- Avemetatarsalian, hyposphene-hypantrum absent, measured in person
- Pseudosuchian, hyposphene-hypantrum present, measured in Photoshop
- Pseudosuchian, hyposphene-hypantrum absent, measured in Photoshop
- Pseudosuchian, hyposphene-hypantrum absent, measured in person
- Outside Archosauria, measured in Photoshop
- Outside Archosauria, measured in person

(b)

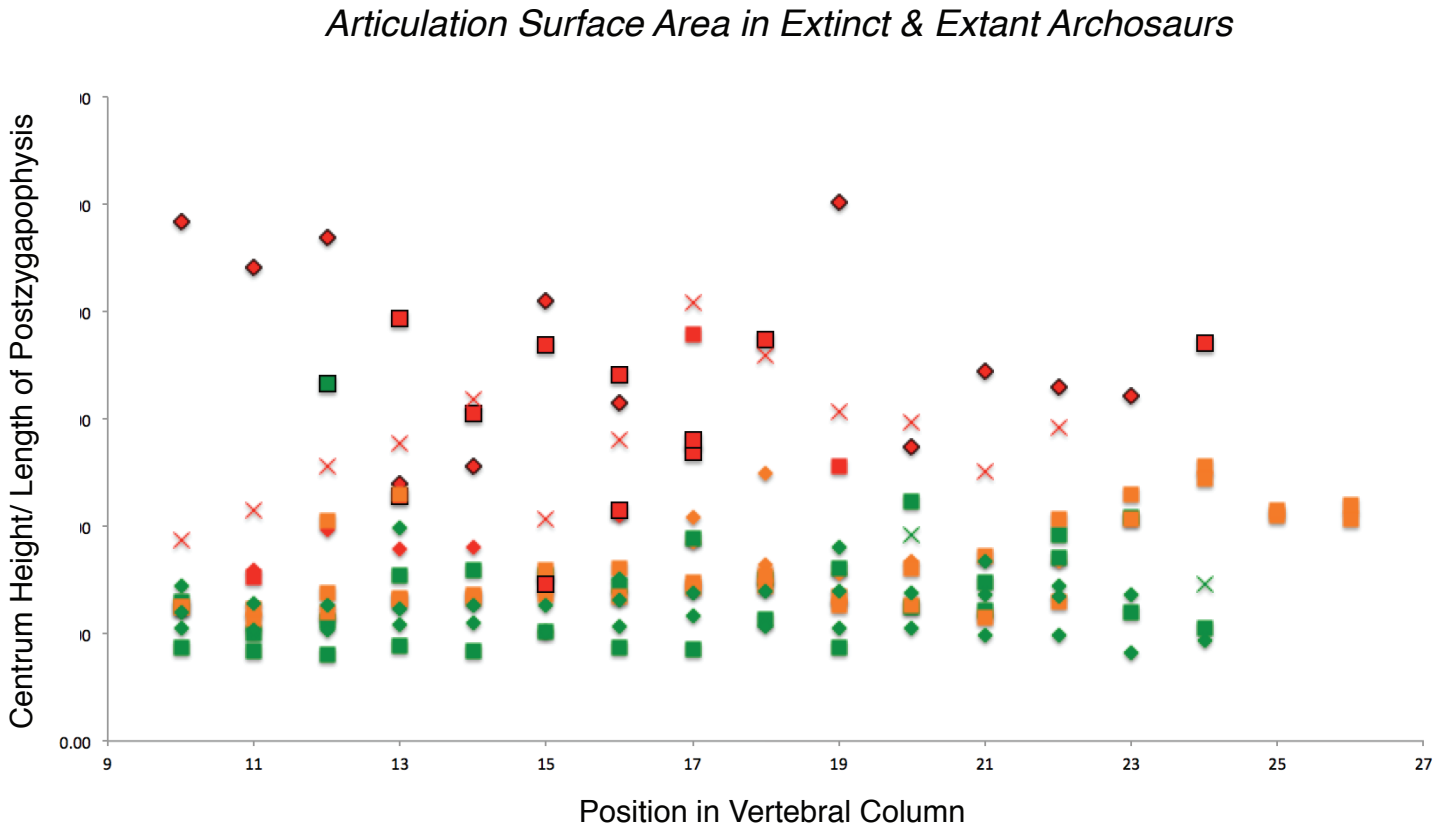

legend

- Avemetatarsalian, femoral length > 400 mm
- Avemetatarsalian, femoral length 300 - 400 mm
- Avemetatarsalian, femoral length < 300 mm
- Pseudosuchian, femoral length > 400 mm
- Pseudosuchian, femoral length 300 - 400 mm
- Pseudosuchian, femoral length < 300 mm
- Outside Archosauria, femoral length > 400 mm
- Outside Archosauria, femoral length < 300 mm

black outline = hyposphene-hypantrum present

(c)

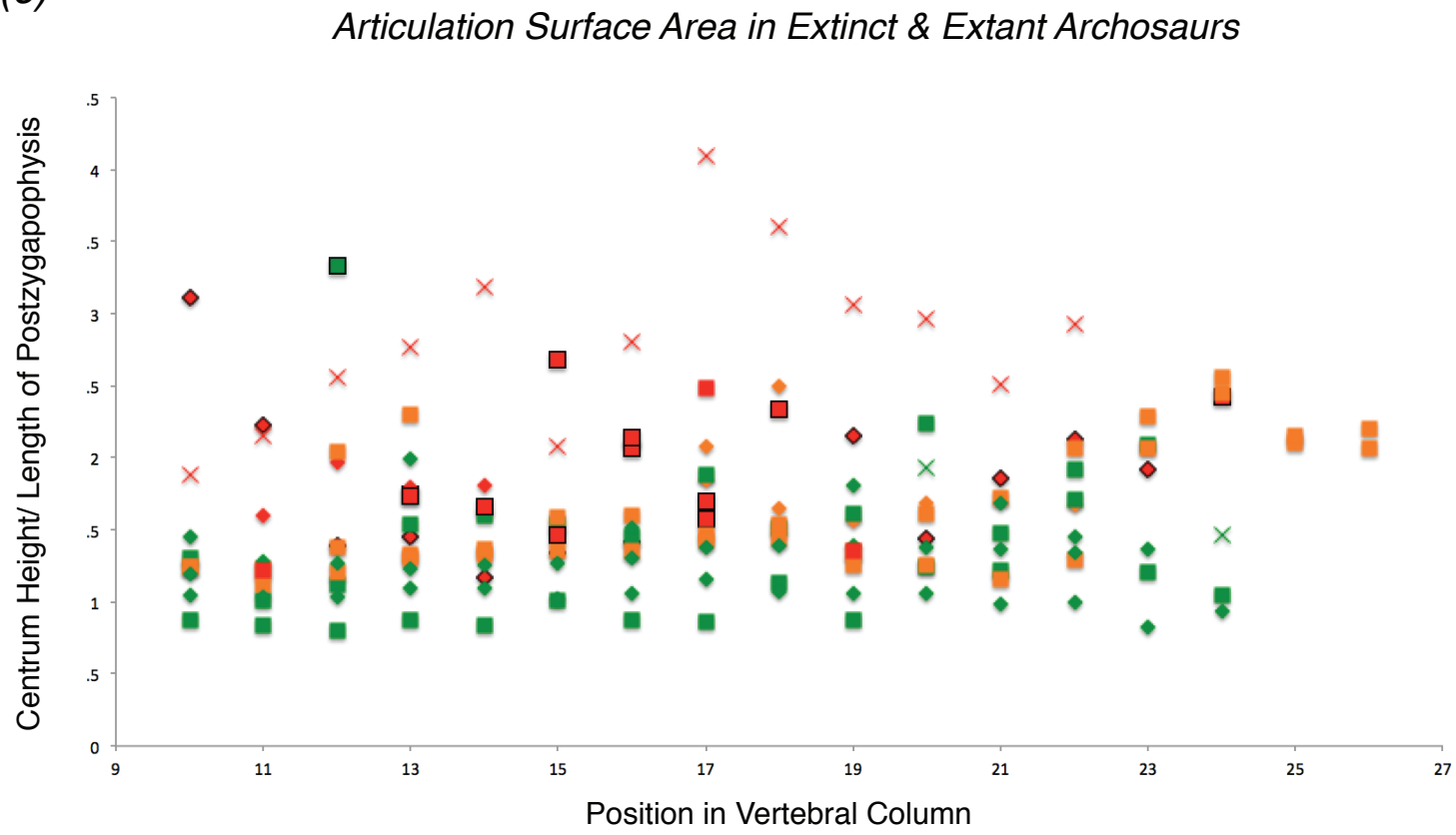

legend

- Avemetatarsalian, femoral length > 400 mm
- Avemetatarsalian, femoral length 300 - 400 mm
- Avemetatarsalian, femoral length < 300 mm
- Pseudosuchian, femoral length > 400 mm
- Pseudosuchian, femoral length 300 - 400 mm
- Pseudosuchian, femoral length < 300 mm
- Outside Archosauria, femoral length > 400 mm
- Outside Archosauria, femoral length < 300 mm

black outline = hyposphene-hypantrum present

(d)

Articulation Surface Area in Extinct & Extant Archosaurs

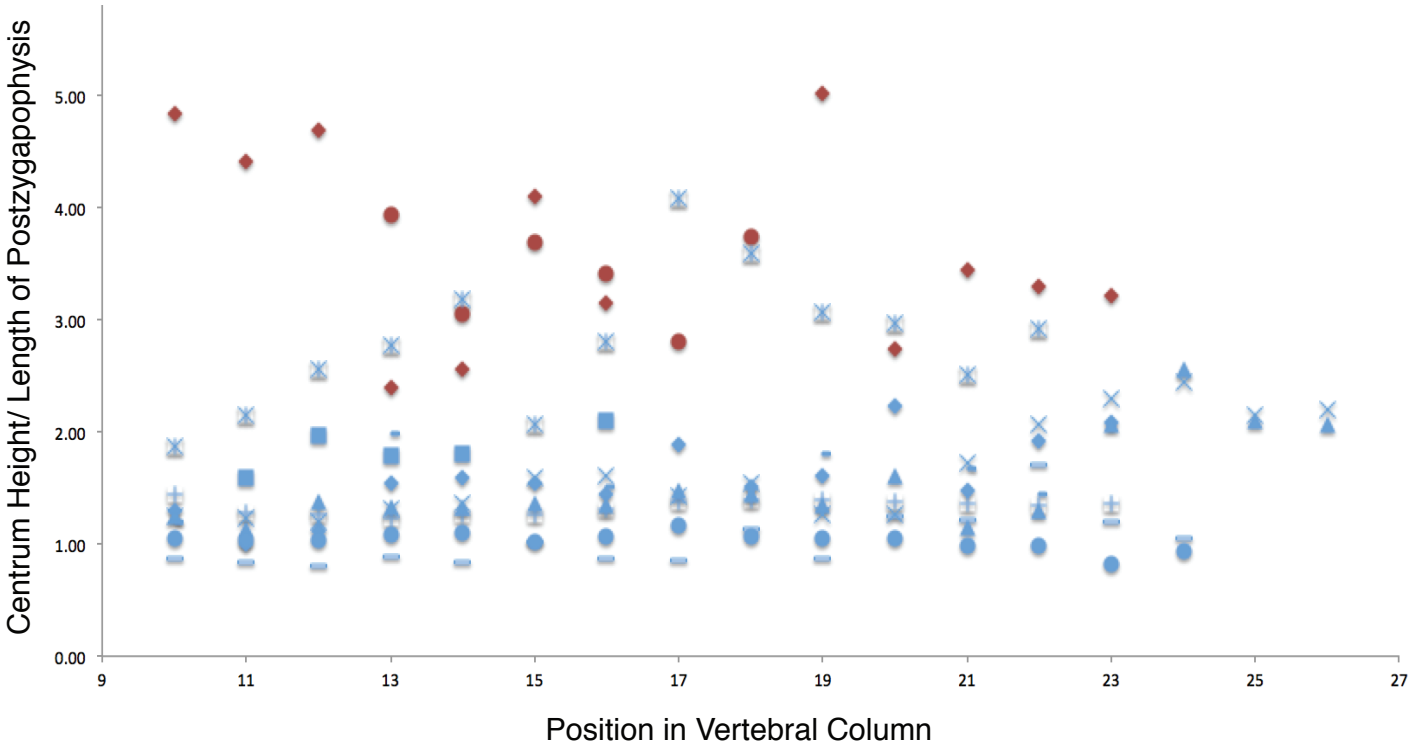

legend

- *Desmatosuchus*
- *Dilophosaurus*
- Kiwi
- Northern Screamer
- Ostrich
- Emu
- Alligator
- Crocodile
- *Deinosuchus*
- *Smilosuchus*
- *Parringtonia*

maroon = hyposphene-hypantrum present
blue = hyposphene-hypantrum absent

Figure 7. Phylogenetic tree showing the loss of the hyposphene-hypantrum in Crocodylomorpha, with ancestral state femoral length reconstructions (from Turner and Nesbitt, 2013) illustrated at several major nodes.

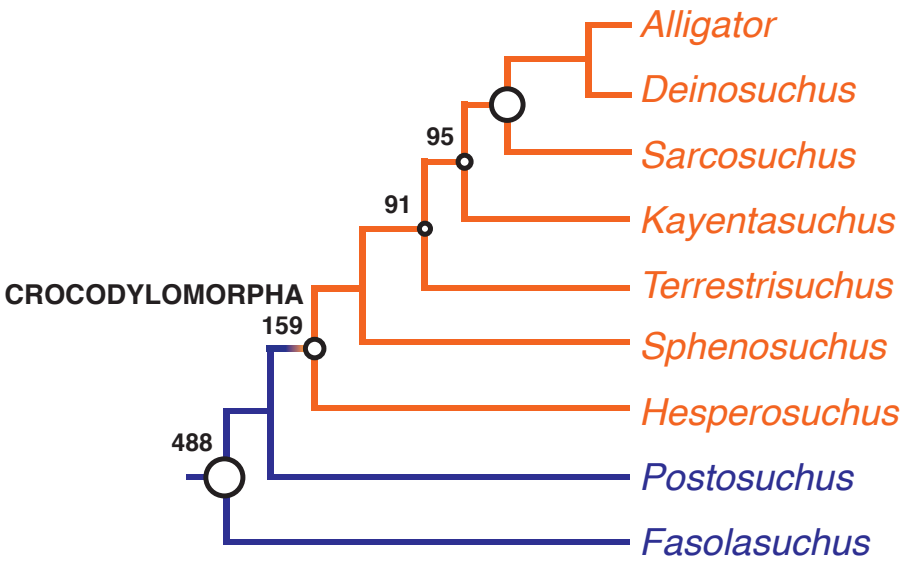
Alligator
Deinosuchus
95
Sarcosuchus
91
Kayentasuchus
Terrestrisuchus
CROCODYLOMORPHA
159
Sphenosuchus
Hesperosuchus
488
Postosuchus
Fasolasuchus

Figure 8. Phylogenetic tree showing the loss of the hyposphene-hypantrum in Neotetanurae theropods, with ancestral state femoral length reconstructions (from Lee et al., 2014) illustrated at several major nodes.

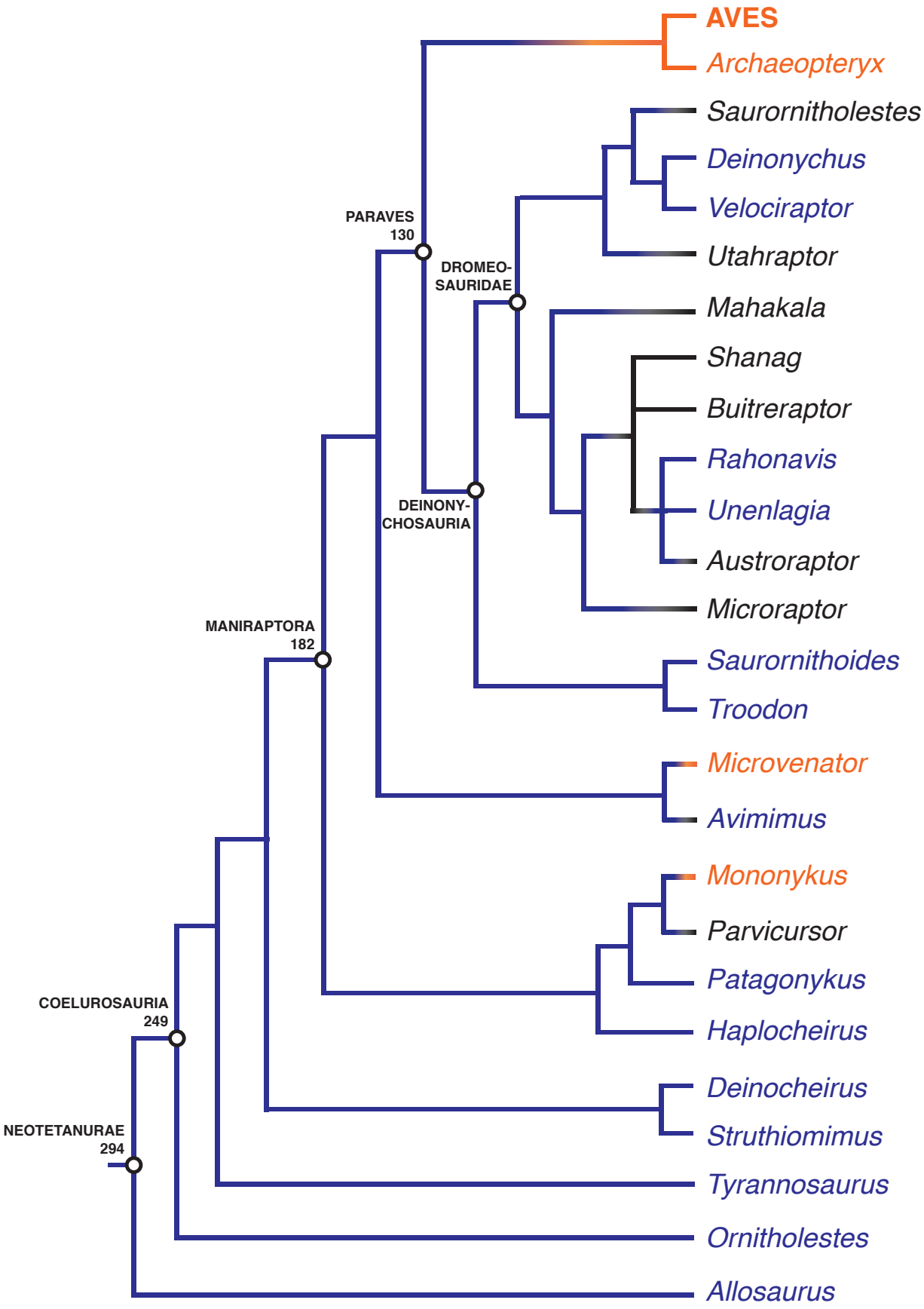
AVES
Archaeopteryx
Saurornitholestes
Deinonychus
Velociraptor
Utahraptor
Mahakala
Shanag
Buitreraptor
Rahonavis
Unenlagia
Austroraptor
Microraptor
Saurornithoides
Troodon
Microvenator
Avimimus
Mononykus
Parvicursor
Patagonykus
Haplocheirus
Deinocheirus
Struthiomimus
Tyrannosaurus
Ornitholestes
Allosaurus
PARAVES
130
DROMEO-
SAURIDAE
DEINONY-
CHOSAURIA
MANIRAPTORA
182
COELUROSAURIA
249
NEOTETANURAE
294

9. TABLES

Table 1. Table including taxon, femoral length, score for presence or absence of the hyposphene-hypantrum articulation, and citation for femoral length. Taxa omitted from our statistical analysis are in grey.

Taxon	Femoral Length (mm)	Hyposphene-hypantrum (1=present, 0=absent)	Source	Major Archosaurian Group
Postosuchus kirkpatricki	528	1	Turner & Nesbitt 2013	Pseudosuchian
Postosuchus alisonae	558	1	Turner & Nesbitt 2013	Pseudosuchian
Fasolasuchus	750	1	Turner & Nesbitt 2013	Pseudosuchian
Batrachotomus	420	1	Turner & Nesbitt 2013	Pseudosuchian
Prestosuchus	538	1	Turner & Nesbitt 2013	Pseudosuchian
Poposaurus langstoni	353	1	Turner & Nesbitt 2013	Pseudosuchian
Poposaurus gracilis	353	1	Turner & Nesbitt 2013	Pseudosuchian
Sillosuchus	440	?	Alcober and Parrish 1997	Pseudosuchian
Shuvosaurus	255	0	Turner & Nesbitt 2013	Pseudosuchian
Effigia	301	0	Turner & Nesbitt 2013	Pseudosuchian
Arizonasaurus	490	1	Turner & Nesbitt 2013	Pseudosuchian
Xilousuchus	302	1	Turner & Nesbitt 2013	Pseudosuchian
Ticinosuchus	240	?	Turner & Nesbitt 2013	Pseudosuchian
Nundasuchus	230	0	measured from NMT RB48	Pseudosuchian
Mandasuchus	212	1	Butler et al. 2017	Pseudosuchian
Turfanosuchus	136	0	Turner & Nesbitt 2013	Pseudosuchian
Gracilisuchus	78	0	Turner & Nesbitt 2013	Pseudosuchian
Longosuchus	337	?	Turner & Nesbitt 2013	Pseudosuchian
Desmatosuchus	450	1	Parker 2008	Pseudosuchian
Aetobarbakinoides	120	0	Desojo et al. 2012	Pseudosuchian
Smilosuchus	545	0	Turner & Nesbitt 2013	Phytosaur
Machaeroprosopus	444	0	Turner & Nesbitt 2013	Phytosaur
Sphenosuchus	140	0	Turner & Nesbitt 2013	Crocodylomorph
Terrestrisuchus	80	0	Turner & Nesbitt 2013	Crocodylomorph

Erythrosuchus	466	0	Turner & Nesbitt 2013	Stem Archosaur
Vancleavea	87	0	Turner & Nesbitt 2013	Stem Archosaur
Euparkeria	65	0	Turner & Nesbitt 2013	Stem Archosaur
Trilophosaurus	250	0	Long and Murry 1995	Stem Archosaur
Teleocrater	170	1	Nesbitt et al. 2017	Avemetatarsalian
Asilisaurus	130	1	Turner & Nesbitt 2013	Avemetatarsalian
Silesaurus	200	1	Turner & Nesbitt 2013	Avemetatarsalian
Hypsilophodon	202	0	Galton 1975	Ornithischian
Psittacosaurus	160	0	Butler et al. 2010	Ornithischian
Heterodontosaurus	112	0	Butler et al. 2010	Ornithischian
Agilisaurus	199	0	Butler et al. 2010	Ornithischian
Lesothosaurus	103	0	Butler et al. 2010	Ornithischian
Scutellosaurus	114	0	Butler et al. 2010	Ornithischian
Stormbergia	202	0	Butler et al. 2010	Ornithischian
Wannanosaurus	92.5	0	Butler et al. 2010	Ornithischian
Stenopelix	144	0	Butler et al. 2010	Ornithischian
Orodromeus	118	0	Butler et al. 2010	Ornithischian
Othneilosaurus	151	0	Butler et al. 2010	Ornithischian
Shantungosaurus	1650	0	Xing et al. 2014	Ornithischian
Zhuchengosaurus	1700	0	Xing et al. 2014	Ornithischian
Huaxiaosaurus	1720	0	Xing et al. 2014	Ornithischian
Edmontosaurus	1250	0	Xing et al. 2014	Ornithischian
Titanoceratops	1020	0	Longrich 2011	Ornithischian
Utahceratops	990	0	Sampson et al. 2010	Ornithischian
Kosmoceratops	800	0	Sampson et al. 2010	Ornithischian
Torosaurus	874	0	Hunt & Lehman 2008	Ornithischian
Plateosaurus	750	1	Turner & Nesbitt 2013	Sauropodomorph

Sarahsaurus	400	1	Marsh 2013	Sauropodomorph
Haplocanthosaurus	1275	1	Mazzetta et al. 2004	Sauropodomorph
Barosaurus	1440	1	McIntosh 2005	Sauropodomorph
Diplodocus	1540	1	measured from CM 94	Sauropodomorph
Vulcanodon	1100	1	Turner & Nesbitt 2013	Sauropodomorph
Apatosaurus	1785	1	Mazzetta et al. 2004	Sauropodomorph
Brachiosaurus	2028	1	Mazzetta et al. 2004	Sauropodomorph
Camarasaurus	1341	1	Mazzetta et al. 2004	Sauropodomorph
Cetiosaurus	1660	1	Mazzetta et al. 2004	Sauropodomorph
Dicraeosaurus	1220	1	Mazzetta et al. 2004	Sauropodomorph
Mamenchisaurus	1275	1	Mazzetta et al. 2004	Sauropodomorph
Omeisaurus	1215	1	Mazzetta et al. 2004	Sauropodomorph
Opisthocoelicaudia	1395	?	Mazzetta et al. 2004	Sauropodomorph (Titanosaur)
Shunosaurus	865	1	Mazzetta et al. 2004	Sauropodomorph
Alamosaurus	1850	?	Fowler & Sullivan 2011	Sauropodomorph (Titanosaur)
Argentinosaurus	2557	?	Mazzetta et al. 2004	Sauropodomorph (Titanosaur)
Tawa	174	1	Turner & Nesbitt 2013	Theropod
Dilophosaurus	552	1	Turner & Nesbitt 2013	Theropod
Albertosaurus	905	1	Christiansen & Farina 2004	Theropod
Tarbosaurus	854	1	Christiansen & Farina 2004	Theropod
Daspletosaurus	1006	1	Christiansen & Farina 2004	Theropod
Gallimimus	673	1	Christiansen & Farina 2004	Theropod
Anserimimus	433	1	Christiansen & Farina 2004	Theropod
Struthiomimus	486	1	Christiansen & Farina 2004	Theropod
Ornithomimus	443	1	Christiansen & Farina 2004	Theropod
Dromiceiominus	454	1	Christiansen & Farina 2004	Theropod
Sinraptor	884	1	Christiansen & Farina 2004	Theropod

Elaphrosaurus	519	1	Christiansen & Farina 2004	Theropod
Ornitholestes	210	1	Christiansen & Farina 2004	Theropod
Saurornitholestes	214	1	Christiansen & Farina 2004	Theropod
Oviraptor	303	1	Christiansen & Farina 2004	Theropod
Tyrannosaurus	1273	1	Christiansen & Farina 2004	Theropod
Allosaurus	872	1	Bybee et al. 2005	Theropod
Velociraptor	238	1	Norell and Mackovicky 1998	Theropod
Microvenator	124	0	Makovicky and Sues 1998	Theropod
Deinocheirus	1381	1	Lee et al. 2014	Theropod
Mononykus	150	0	Chiappe et al. 1992	Theropod
Patagonykus	285	1	Novas 1997	Theropod
Haplocheirus	214	1	Choiniere et al. 2010	Theropod
Avimimus	180	1	Vickers-Rich et al. 2002	Theropod
Deinonychus	344	1	Novas et al. 2009	Theropod
Buitreraptor	77	0	Makovicky et al. 2005	Theropod
Rahonavis	86.9	1	Carrano 2006	Theropod
Deinosuchus	530	0	estimated from Figure 5 in Farlow et al. 2005	Crown Crocodylian
Alligator	250	0	estimated from Figure 5 in Farlow et al. 2005	Crown Crocodylian
Crocodylus	275	0	estimated from Figure 5 in Farlow et al. 2005	Crown Crocodylian
Struthio camelus	334	0	measured from FMNH 3392	Crown Aves

Table 2. Table including vertebral measurements taken in-person.

Taxon	Specimen #	Hyposphene-hypantrum?	Position	Centrum Height (in mm)	Left Post-zygapophysis Long-axis Measured (in mm)	Centrum Height (measured, mm) / Post-zyg (measured, mm)	Left-lateral hyposphene surface (in mm)	Centrum Height (measured, mm) / Post-zyg + hyposphene (both measured, mm)
Alligator mississippiensis	TMM M-12606	no	1	-	-	-	-	-
Alligator mississippiensis	TMM M-12606	no	2	12.6	6.2	2.1	-	-
Alligator mississippiensis	TMM M-12606	no	3	12.8	7.6	1.7	-	-
Alligator mississippiensis	TMM M-12606	no	4	13.6	8.4	1.6	-	-
Alligator mississippiensis	TMM M-12606	no	5	13.8	8.9	1.6	-	-
Alligator mississippiensis	TMM M-12606	no	6	14.5	9.5	1.5	-	-
Alligator mississippiensis	TMM M-12606	no	7	14.5	10.5	1.4	-	-
Alligator mississippiensis	TMM M-12606	no	8	14.3	10.6	1.4	-	-
Alligator mississippiensis	TMM M-12606	no	9	14.0	9.9	1.4	-	-
Alligator mississippiensis	TMM M-12606	no	10	14.3	9.8	1.5	-	-
Alligator mississippiensis	TMM M-12606	no	11	15.3	11.9	1.3	-	-
Alligator mississippiensis	TMM M-12606	no	12	14.9	11.8	1.3	-	-
Alligator mississippiensis	TMM M-12606	no	13	15.4	12.5	1.2	-	-
Alligator mississippiensis	TMM M-12606	no	14	15.1	12.0	1.3	-	-
Alligator mississippiensis	TMM M-12606	no	15	15.0	11.8	1.3	-	-
Alligator mississippiensis	TMM M-12606	no	16	14.9	11.4	1.3	-	-
Alligator	TMM M-	no	17	14.6	10.6	1.4	-	-

mississippiensis	12606							
Alligator mississippiensis	TMM M-12606	no	18	14.7	10.5	1.4	-	-
Alligator mississippiensis	TMM M-12606	no	19	14.7	10.6	1.4	-	-
Alligator mississippiensis	TMM M-12606	no	20	15.1	10.9	1.4	-	-
Alligator mississippiensis	TMM M-12606	no	21	14.7	10.8	1.4	-	-
Alligator mississippiensis	TMM M-12606	no	22	14.6	10.8	1.4	-	-
Alligator mississippiensis	TMM M-12606	no	23	14.5	10.6	1.4	-	-
Crocodylus acutus	USNM 247943	no	1	-	-	-	-	-
Crocodylus acutus	USNM 247943	no	2	23.7	17.1	1.4	-	-
Crocodylus acutus	USNM 247943	no	3	24.7	19.6	1.3	-	-
Crocodylus acutus	USNM 247943	no	4	26.3	21.1	1.3	-	-
Crocodylus acutus	USNM 247943	no	5	25.8	21.6	1.2	-	-
Crocodylus acutus	USNM 247943	no	6	25.3	24.8	1.0	-	-
Crocodylus acutus	USNM 247943	no	7	26.3	26.1	1.0	-	-
Crocodylus acutus	USNM 247943	no	8	26.6	26.7	1.0	-	-
Crocodylus acutus	USNM 247943	no	9	26.0	23.3	1.1	-	-
Crocodylus acutus	USNM 247943	no	10	26.7	25.6	1.1	-	-
Crocodylus acutus	USNM 247943	no	11	28.0	26.9	1.0	-	-
Crocodylus acutus	USNM 247943	no	12	28.6	27.6	1.0	-	-

Crocodylus acutus	USNM 247943	no	13	29.5	27.0	1.1	-	-
Crocodylus acutus	USNM 247943	no	14	30.7	27.8	1.1	-	-
Crocodylus acutus	USNM 247943	no	15	30.5	29.7	1.0	-	-
Crocodylus acutus	USNM 247943	no	16	29.7	28.0	1.1	-	-
Crocodylus acutus	USNM 247943	no	17	28.9	24.9	1.2	-	-
Crocodylus acutus	USNM 247943	no	18	28.0	26.3	1.1	-	-
Crocodylus acutus	USNM 247943	no	19	27.1	25.6	1.1	-	-
Crocodylus acutus	USNM 247943	no	20	26.5	25.1	1.1	-	-
Crocodylus acutus	USNM 247943	no	21	25.5	26.0	1.0	-	-
Crocodylus acutus	USNM 247943	no	22	25.6	25.8	1.0	-	-
Crocodylus acutus	USNM 247943	no	23	22.7	27.4	0.8	-	-
Crocodylus acutus	USNM 247943	no	24	24.2	26.0	0.9	-	-
Dromaius novaehollandiae	NMNH 345221	no	1	5.4	2.4	2.2	-	-
Dromaius novaehollandiae	NMNH 345221	no	2	5.5	8.1	0.7	-	-
Dromaius novaehollandiae	NMNH 345221	no	3	7.2	8.7	0.8	-	-
Dromaius novaehollandiae	NMNH 345221	no	4	9.7	9.9	1.0	-	-
Dromaius novaehollandiae	NMNH 345221	no	5	10.9	10.0	1.1	-	-
Dromaius novaehollandiae	NMNH 345221	no	6	11.0	8.9	1.2	-	-
Dromaius	NMNH	no	7	10.1	7.6	1.3	-	-

novaehollandiae	345221							
Dromaius novaehollandiae	NMNH 345221	no	8	10.7	7.7	1.4	-	-
Dromaius novaehollandiae	NMNH 345221	no	9	12.6	8.2	1.5	-	-
Dromaius novaehollandiae	NMNH 345221	no	10	14.9	11.9	1.3	-	-
Dromaius novaehollandiae	NMNH 345221	no	11	15.8	12.8	1.2	-	-
Dromaius novaehollandiae	NMNH 345221	no	12	17.5	14.5	1.2	-	-
Dromaius novaehollandiae	NMNH 345221	no	13	17.0	13.0	1.3	-	-
Dromaius novaehollandiae	NMNH 345221	no	14	16.8	12.4	1.4	-	-
Dromaius novaehollandiae	NMNH 345221	no	15	20.0	12.6	1.6	-	-
Dromaius novaehollandiae	NMNH 345221	no	16	22.8	14.2	1.6	-	-
Dromaius novaehollandiae	NMNH 345221	no	17	21.1	14.8	1.4	-	-
Dromaius novaehollandiae	NMNH 345221	no	18	23.8	15.5	1.5	-	-
Dromaius novaehollandiae	NMNH 345221	no	19	18.7	14.9	1.3	-	-
Dromaius novaehollandiae	NMNH 345221	no	20	17.4	13.8	1.3	-	-
Dromaius novaehollandiae	NMNH 345221	no	21	20.7	12.1	1.7	-	-
Dromaius novaehollandiae	NMNH 345221	no	22	20.9	10.1	2.1	-	-
Dromaius novaehollandiae	NMNH 345221	no	23	24.7	10.8	2.3	-	-
Dromaius novaehollandiae	NMNH 345221	no	24	27.3	11.2	2.4	-	-
Dromaius novaehollandiae	NMNH 345221	no	25	27.4	12.7	2.2	-	-

Dromaius novaehollandiae	NMNH 345221	no	26	29.2	13.2	2.2	-	-
Apteryx australis	NMNH 500629	no	1	5.2	2.1	2.5	-	-
Apteryx australis	NMNH 500629	no	2	6.2	4.8	1.3	-	-
Apteryx australis	NMNH 500629	no	3	5.6	4.8	1.2	-	-
Apteryx australis	NMNH 500629	no	4	6.5	5.1	1.3	-	-
Apteryx australis	NMNH 500629	no	5	6.5	4.3	1.5	-	-
Apteryx australis	NMNH 500629	no	6	5.5	4.4	1.3	-	-
Apteryx australis	NMNH 500629	no	7	6.9	5.4	1.3	-	-
Apteryx australis	NMNH 500629	no	8	7.5	4.5	1.7	-	-
Apteryx australis	NMNH 500629	no	9	7.2	4.9	1.5	-	-
Apteryx australis	NMNH 500629	no	10	7.4	5.7	1.3	-	-
Apteryx australis	NMNH 500629	no	11	6.1	6.1	1.0	-	-
Apteryx australis	NMNH 500629	no	12	6.3	5.6	1.1	-	-
Apteryx australis	NMNH 500629	no	13	7.3	4.7	1.5	-	-
Apteryx australis	NMNH 500629	no	14	8.1	5.1	1.6	-	-
Apteryx australis	NMNH 500629	no	15	7.4	4.8	1.5	-	-
Apteryx australis	NMNH 500629	no	16	7.9	5.5	1.5	-	-
Apteryx australis	NMNH 500629	no	17	8.2	4.3	1.9	-	-
Apteryx australis	NMNH	no	18	7.2	4.7	1.5	-	-

	500629							
Apteryx australis	NMNH 500629	no	19	7.8	4.8	1.6	-	-
Apteryx australis	NMNH 500629	no	20	9.8	4.4	2.2	-	-
Apteryx australis	NMNH 500629	no	21	8.1	5.5	1.5	-	-
Apteryx australis	NMNH 500629	no	22	10.9	5.7	1.9	-	-
Apteryx australis	NMNH 500629	no	23	9.9	4.7	2.1	-	-
Struthio camelus	NMNH 291160	no	1	0.4	4.7	0.1	-	-
Struthio camelus	NMNH 291160	no	2	20.3	8.9	2.3	-	-
Struthio camelus	NMNH 291160	no	3	10.7	10.3	1.0	-	-
Struthio camelus	NMNH 291160	no	4	12.7	10.8	1.2	-	-
Struthio camelus	NMNH 291160	no	5	14.7	10.6	1.4	-	-
Struthio camelus	NMNH 291160	no	6	17.3	10.7	1.6	-	-
Struthio camelus	NMNH 291160	no	7	19.0	10.9	1.8	-	-
Struthio camelus	NMNH 291160	no	8	14.1	11.2	1.3	-	-
Struthio camelus	NMNH 291160	no	9	16.2	12.3	1.3	-	-
Struthio camelus	NMNH 291160	no	10	19.3	15.5	1.2	-	-
Struthio camelus	NMNH 291160	no	11	19.5	17.3	1.1	-	-
Struthio camelus	NMNH 291160	no	12	23.5	17.0	1.4	-	-
Struthio camelus	NMNH 291160	no	13	23.6	17.7	1.3	-	-

Struthio camelus	NMNH 291160	no	14	23.6	17.7	1.3	-	-
Struthio camelus	NMNH 291160	no	15	24.9	18.4	1.4	-	-
Struthio camelus	NMNH 291160	no	16	25.6	19.0	1.4	-	-
Struthio camelus	NMNH 291160	no	17	27.1	18.4	1.5	-	-
Struthio camelus	NMNH 291160	no	18	28.2	19.5	1.4	-	-
Struthio camelus	NMNH 291160	no	19	24.3	18.0	1.4	-	-
Struthio camelus	NMNH 291160	no	20	27.9	17.4	1.6	-	-
Struthio camelus	NMNH 291160	no	21	21.6	18.8	1.2	-	-
Struthio camelus	NMNH 291160	no	22	19.9	15.4	1.3	-	-
Struthio camelus	NMNH 291160	no	23	28.2	13.6	2.1	-	-
Struthio camelus	NMNH 291160	no	24	32.2	12.6	2.6	-	-
Struthio camelus	NMNH 291160	no	25	31.5	15.0	2.1	-	-
Struthio camelus	NMNH 291160	no	26	34.8	16.8	2.1	-	-
Chauna chavaria	NMNH 18996	no	1	-	-	-	-	-
Chauna chavaria	NMNH 18996	no	2	3.5	4.3	0.8	-	-
Chauna chavaria	NMNH 18996	no	3	5.0	4.2	1.2	-	-
Chauna chavaria	NMNH 18996	no	4	4.6	5.0	0.9	-	-
Chauna chavaria	NMNH 18996	no	5	5.3	4.2	1.3	-	-
Chauna chavaria	NMNH	no	6	5.4	4.8	1.1	-	-

	18996							
Chauna chavaria	NMNH 18996	no	7	4.8	6.4	0.8	-	-
Chauna chavaria	NMNH 18996	no	8	4.4	5.7	0.8	-	-
Chauna chavaria	NMNH 18996	no	9	6.3	6.2	1.0	-	-
Chauna chavaria	NMNH 18996	no	10	6.3	7.2	0.9	-	-
Chauna chavaria	NMNH 18996	no	11	5.7	6.8	0.8	-	-
Chauna chavaria	NMNH 18996	no	12	6.0	7.5	0.8	-	-
Chauna chavaria	NMNH 18996	no	13	6.6	7.5	0.9	-	-
Chauna chavaria	NMNH 18996	no	14	6.4	7.7	0.8	-	-
Chauna chavaria	NMNH 18996	no	15	7.3	7.2	1.0	-	-
Chauna chavaria	NMNH 18996	no	16	6.8	7.8	0.9	-	-
Chauna chavaria	NMNH 18996	no	17	6.5	7.6	0.9	-	-
Chauna chavaria	NMNH 18996	no	18	7.6	6.7	1.1	-	-
Chauna chavaria	NMNH 18996	no	19	5.8	6.7	0.9	-	-
Chauna chavaria	NMNH 18996	no	20	7.5	6.0	1.2	-	-
Chauna chavaria	NMNH 18996	no	21	7.3	6.0	1.2	-	-
Chauna chavaria	NMNH 18996	no	22	8.6	5.0	1.7	-	-
Chauna chavaria	NMNH 18996	no	23	8.0	6.6	1.2	-	-
Chauna chavaria	NMNH 18996	no	24	8.6	8.2	1.1	-	-

Dilophosaurus wetherilli	UCMP 37302	yes	13	59.0	15.0	3.9	19	1.74
Dilophosaurus wetherilli	UCMP 37302	yes	14	55.0	18.0	3.1	15	1.67
Dilophosaurus wetherilli	UCMP 37302	yes	15	59.0	16.0	3.7	6	2.68
Dilophosaurus wetherilli	UCMP 37302	yes	16	58.0	17.0	3.4	11	2.07
Dilophosaurus wetherilli	UCMP 37302	yes	17	56.0	20.0	2.8	13	1.70
Dilophosaurus wetherilli	UCMP 37302	yes	18	56.0	15.0	3.7	9	2.33
Thescelosaurus	UCMP 137113	no	12	45.0	22.0	2.1	-	-
Thescelosaurus	UCMP 137113	no	13	46.0	20.0	2.3	-	-
"Machaeroprosopus" zunii	UCMP 27036	no	10	77.0	41.0	1.9	-	-
"Machaeroprosopus" zunii	UCMP 27036	no	11	84.0	39.0	2.2	-	-
"Machaeroprosopus" zunii	UCMP 27036	no	12	87.0	34.0	2.6	-	-
"Machaeroprosopus" zunii	UCMP 27036	no	13	86.0	31.0	2.8	-	-
"Machaeroprosopus" zunii	UCMP 27036	no	14	86.0	27.0	3.2	-	-
"Machaeroprosopus" zunii	UCMP 27036	no	15	83.0	40.0	2.1	-	-
"Machaeroprosopus" zunii	UCMP 27036	no	16	87.0	31.0	2.8	-	-
"Machaeroprosopus" zunii	UCMP 27036	no	17	90.0	22.0	4.1	-	-
"Machaeroprosopus" zunii	UCMP 27036	no	18	90.0	25.0	3.6	-	-
"Machaeroprosopus" zunii	UCMP 27036	no	19	89.0	29.0	3.1	-	-
"Machaeroprosopus"	UCMP	no	20	89.0	30.0	3.0	-	-

zunii	27036							
"Machaeroprosopus" zunii	UCMP 27036	no	21	83.0	33.0	2.5	-	-
"Machaeroprosopus" zunii	UCMP 27036	no	22	82.0	28.0	2.9	-	-
Parringtonia gracilis	NMT RB426	no	7	8.7	5.1	1.7	-	-
Parringtonia gracilis	NMT RB426	no	8	8.5	6.0	1.4	-	-
Parringtonia gracilis	NMT RB426	no	9	8.9	4.1	2.2	-	-
Parringtonia gracilis	NMT RB426	no	10	8.6	7.2	1.2	-	-
Parringtonia gracilis	NMT RB426	no	13	8.6	4.3	2.0	-	-
Parringtonia gracilis	NMT RB426	no	16	9.1	6.0	1.5	-	-
Parringtonia gracilis	NMT RB426	no	19	9.5	5.3	1.8	-	-
Parringtonia gracilis	NMT RB426	no	21	7.5	4.4	1.7	-	-
Parringtonia gracilis	NMT RB426	no	22	8.5	5.8	1.5	-	-
Asilisaurus kongwe	NMT RB426	yes	12	10	3	3.3	0.1	3.23

Table 3. Table including vertebral measurements taken in Photoshop CC 2015.

Taxon	Specimen #	Hyposphene-hypantrum?	Position	1 cm (10 mm) Measurement from Photo	Centrum Height from Photo	Left Post-zygapophysis from Photo	Left-lateral hyposphene surface from Photo
Plateosaurus	AMNH 2109	yes	24	78.64	1097.2	269.46	155.34
Plateosaurus	AMNH 2108	yes	13	102.66	882.65	351.42	166.92
Allosaurus	AMNH 666	yes	17	49.68	794.43	258.76	221.46
Deinosuchus	TMM 43632-1 (A)	no	11	64.9	783.05	445.44	-
Deinosuchus	TMM 43632-1 (B)	no	12	65.14	940.97	433.75	-
Deinosuchus	TMM 43632-1 (C)	no	13	79.16	842.28	427.29	-
Deinosuchus	TMM 43632-1 (D)	no	14	70.82	806.7	405.89	-
Deinosuchus	TMM 43632-1 (F)	no	16	65.05	793.21	342.86	-
Alamosaurus	TMM 41891-1	no		28.08	585.61	464.51	-
Longosuchus	TMM 31100-448 (A)	no	18	113.7	571.28	207.96	-
Longosuchus	TMM 31100-452 (B)	no	19	112.2	381.25	221.1	-
Trilophosaurus	TMM 31025-140 (24)	no	24	126.29	243.58	151.25	-
Trilophosaurus	TMM 31025-140 (20)	no	20	115.23	194.24	91.6	-
Desmatosuchus	MNA V9300 (D1)	yes	10	91.7	637.55	119.6	72.98
Desmatosuchus	MNA V9300 (D2)	yes	11	93.44	643.68	132.85	143.53
Desmatosuchus	MNA V9300 (D3)	yes	12	88.85	612.74	118.72	310.24
Desmatosuchus	MNA V9300 (D4)	yes	13	85.01	618.47	235.35	168.12
Desmatosuchus	MNA V9300 (D5)	yes	14	90.25	722.24	256.2	333.55
Desmatosuchus	MNA V9300 (D6)	yes	15	86.88	783.38	173.76	391.32
Desmatosuchus	MNA V9300 (D7)	yes	16	94.55	829.64	239.71	322.81
Desmatosuchus	MNA V9300 (D11)	yes	19	83.71	771.98	140.03	205.17
Desmatosuchus	MNA V9300 (D12)	yes	20	77.75	890.85	295.64	290.84
Desmatosuchus	MNA V9300 (D13)	yes	21	64.83	721.29	190.03	178.05
Desmatosuchus	MNA V9300 (D14)	yes	22	49.89	542.48	149.5	90.56
Desmatosuchus	MNA V9300 (D15)	yes	23	63.02	816.44	231.06	172.09
Coahomasuchus	TMM 31100-437	no	17	210.83	353.24	154.11	-
Coahomasuchus	TMM 31100-437 (clump)	no	22	175.3	337.61	182.99	-

Revueltosaurus	PEFO 34561 (DVb)	no	11	255.75	420.36	206.81	-
Revueltosaurus	PEFO 34561 (DVd)	no	13	300.77	442.65	243.98	-
Revueltosaurus	PEFO 34561 (DVf)	no	15	300.08	378.19	265.96	-
Revueltosaurus	PEFO 34561 (DVh)	no	17	286.86	356.5	192.8	-
Haplocanthosaurus	CM 879 (b)	yes	15	56.38	837.41	520.25	130.63
Haplocanthosaurus	CM 879 (a)	yes	16	48.76	843.29	357.77	85.9
Diplodocus	CM 94 (D8)	yes	17	135.27	-	719	415.44
Diplodocus	CM 94 (D2)	yes	11	75.01	-	1055	282.33
Diplodocus	CM 94 (D10)	yes	19	102.74	-	896.27	879.34

Taxon	Specimen #	Centrum Height from Photo (in mm)	Left Post-zygapophysis from Photo (in mm)	Left-lateral hyposphene surface from Photo (in mm)	Conversion Factor
Plateosaurus	AMNH 2109	139.52	34.27	19.75	1.1
Plateosaurus	AMNH 2108	85.98	34.23	11.39	1.1
Allosaurus	AMNH 666	159.91	52.09	44.58	1.1
Deinosuchus	TMM 43632-1 (A)	120.65	68.63	-	1.1
Deinosuchus	TMM 43632-1 (B)	144.45	66.59	-	1.1
Deinosuchus	TMM 43632-1 (C)	106.40	53.98	-	1.1
Deinosuchus	TMM 43632-1 (D)	113.91	57.31	-	1.1
Deinosuchus	TMM 43632-1 (F)	121.94	52.71	-	1.1
Alamosaurus	TMM 41891-1	208.55	165.42	-	1.1
Longosuchus	TMM 31100-448 (A)	50.24	18.29	-	1.1
Longosuchus	TMM 31100-452 (B)	33.98	19.71	-	1.1
Trilophosaurus	TMM 31025-140 (24)	19.29	11.98	-	1.1
Trilophosaurus	TMM 31025-140 (20)	16.86	7.95	-	1.1
Desmatosuchus	MNA V9300 (D1)	69.53	13.04	7.96	1.1
Desmatosuchus	MNA V9300 (D2)	68.89	14.22	15.36	1.1
Desmatosuchus	MNA V9300 (D3)	68.96	13.36	34.92	1.1
Desmatosuchus	MNA V9300 (D4)	72.75	27.68	19.78	1.1

Desmatosuchus	MNA V9300 (D5)	80.03	28.39	36.96	1.1
Desmatosuchus	MNA V9300 (D6)	90.17	20.00	45.04	1.1
Desmatosuchus	MNA V9300 (D7)	87.75	25.35	34.14	1.1
Desmatosuchus	MNA V9300 (D11)	92.22	16.73	24.51	1.1
Desmatosuchus	MNA V9300 (D12)	114.58	38.02	37.41	1.1
Desmatosuchus	MNA V9300 (D13)	111.26	29.31	27.46	1.1
Desmatosuchus	MNA V9300 (D14)	108.74	29.97	18.15	1.1
Desmatosuchus	MNA V9300 (D15)	129.55	36.66	27.31	1.1
Coahomasuchus	TMM 31100-437	16.75	7.31	-	1.1
Coahomasuchus	TMM 31100-437 (clump)	19.26	10.44	-	1.1
Revueltosaurus	PEFO 34561 (DVb)	16.44	8.09	-	1.1
Revueltosaurus	PEFO 34561 (DVd)	14.72	8.11	-	1.1
Revueltosaurus	PEFO 34561 (DVf)	12.60	8.86	-	1.1
Revueltosaurus	PEFO 34561 (DVh)	12.43	6.72	-	1.1
Haplocanthosaurus	CM 879 (b)	148.53	92.28	23.17	1.1
Haplocanthosaurus	CM 879 (a)	172.95	73.37	17.62	1.1
Diplodocus	CM 94 (D8)	222.00	53.15	30.71	1.1
Diplodocus	CM 94 (D2)	235.00	140.65	37.64	1.1
Diplodocus	CM 94 (D10)	245.00	87.24	85.59	1.1

Taxon	Specimen #	Post-zyg measurement from Photo (in mm) x Conversion Factor	Centrum Height (photo, in mm) / Post-zyg (photo, in mm, x CF)	Centrum Height (photo, in mm) / Post-zyg (photo, in mm, x CF) + hyposphene (photo, in mm)
Plateosaurus	AMNH 2109	37.69	3.70	2.43
Plateosaurus	AMNH 2108	37.65	2.28	1.75
Allosaurus	AMNH 666	57.29	2.69	1.57
Deinosuchus	TMM 43632-1 (A)	75.50	1.60	-
Deinosuchus	TMM 43632-1 (B)	73.25	1.97	-
Deinosuchus	TMM 43632-1 (C)	59.38	1.79	-

Deinosuchus	TMM 43632-1 (D)	63.04	1.81	-
Deinosuchus	TMM 43632-1 (F)	57.98	2.10	-
Alamosaurus	TMM 41891-1	181.97	1.15	-
Longosuchus	TMM 31100-448 (A)	20.12	2.50	-
Longosuchus	TMM 31100-452 (B)	21.68	1.57	-
Trilophosaurus	TMM 31025-140 (24)	13.17	1.46	-
Trilophosaurus	TMM 31025-140 (20)	8.74	1.93	-
Desmatosuchus	MNA V9300 (D1)	14.35	4.85	3.12
Desmatosuchus	MNA V9300 (D2)	15.64	4.40	2.22
Desmatosuchus	MNA V9300 (D3)	14.70	4.69	1.39
Desmatosuchus	MNA V9300 (D4)	30.45	2.39	1.45
Desmatosuchus	MNA V9300 (D5)	31.23	2.56	1.17
Desmatosuchus	MNA V9300 (D6)	22.00	4.10	1.34
Desmatosuchus	MNA V9300 (D7)	27.89	3.15	1.41
Desmatosuchus	MNA V9300 (D11)	18.40	5.01	2.15
Desmatosuchus	MNA V9300 (D12)	41.83	2.74	1.45
Desmatosuchus	MNA V9300 (D13)	32.24	3.45	1.86
Desmatosuchus	MNA V9300 (D14)	32.96	3.30	2.13
Desmatosuchus	MNA V9300 (D15)	40.33	3.21	1.92
Coahomasuchus	TMM 31100-437	8.04	2.08	-
Coahomasuchus	TMM 31100-437 (clump)	11.48	1.68	-
Revueltosaurus	PEFO 34561 (DVb)	8.90	1.85	-
Revueltosaurus	PEFO 34561 (DVd)	8.92	1.65	-
Revueltosaurus	PEFO 34561 (DVf)	9.75	1.29	-
Revueltosaurus	PEFO 34561 (DVh)	7.39	1.68	-
Haplocanthosaurus	CM 879 (b)	101.50	1.46	1.19
Haplocanthosaurus	CM 879 (a)	80.71	2.14	1.76
Diplodocus	CM 94 (D8)	58.47	3.80	2.49
Diplodocus	CM 94 (D2)	154.71	1.52	1.22
Diplodocus	CM 94 (D10)	95.96	2.55	1.35